REGULATORY MECHANISMS CONTROLLING *ENGRAILED* GENE EXPRESSION IN THE ZEBRAFISH MYOTOME

ASHISH KUMAR MAURYA
(M.Sc., M.Tech.)

A THESIS SUBMITTED

FOR THE DEGREE OF DOCTOR OF PHILOSOPHY

DEPARTMENT OF BIOLOGICAL SCIENCES

NATIONAL UNIVERSITY OF SINGAPORE

2011

Acknowledgements

Summary

Signaling by secreted proteins of the Hedgehog (Hh) family of morphogens is crucial for the development and patterning of a wide variety of tissue types in metazoans. Different levels and timing of Hh signaling activity have been proposed to specify three distinct cell types in the zebrafish myotome. Two of these, the Medial Fast-twitch Fibres (MFFs) and the slow-twitch Muscle Pioneers (MPs) are characterized by *eng* expression and require the highest levels of Hh signaling for their specification. We have defined a minimal enhancer element of *eng2a* that is sufficient to drive reporter gene expression specifically in MPs and MFFs. Using a tissue culture based screen we identified a number of trans-factors that can regulate the activity of this enhancer. One of the strongest negative regulators identified was Smad5, a transcription factor whose activity is controlled by the BMP signaling pathway. Using an antibody specific to activated/phosphorylated Smads, we found a strict negative correlation between nuclear accumulation of pSmad and *eng2a* expression in myotomal cells and show that abrogation of pSmad accumulation results in activation of *eng2a*, even when Hh signaling is attenuated. Conversely, we show that driving nuclear accumulation of pSmad suppresses the induction of *eng* expression even when Hh pathway activity is maximal. We also demonstrate that the nuclear accumulation of pSmads is depleted by maximal Hh pathway activation. Using a Bimolecular Fluorescence Complementation assay, we show that a synthetic form of the Gli2 repressor can interact with Smad1 specifically in the nuclei of myotomal cells in the developing embryo and that this interaction depends upon BMP signaling activity. Our results demonstrate that the *eng2a* promoter integrates repressive and activating signals from the BMP and Hh pathways respectively, to limit its

expression to the MPs and MFFs; we suggest a novel basis for cross talk between the Hh and BMP pathways, whereby BMP mediated repression of Hh target genes is promoted by a direct interaction between Smads and truncated Glis, an interaction that is abrogated by Hh induced depletion of the latter.

Table of Contents

List of Publications

Maurya, A. K., Tan, H., Souren, M., Xingang, W., Wittbrodt, J. and Ingham, P. W. (2011).

Integration of Hedgehog and BMP signaling by the *engrailed2a* gene in the zebrafish myotome.

Development 138:755-765; doi:10.1242/dev.062521

List of Abbreviations

μl	micro-litres
BAC	Bacterial Artificial Chromosome
BHK21	Baby Hamster Kidney cells
bHLH	basic Helix-Loop-Helix
BiFC	Bi-Fluorescence Complementation
BMP	Bone Morphogentic Protein
BMPr	BMP Receptor
bp	base-pairs
ca-	constitutively active-
ChIP	Chromatin Immuno-Precipitation
Ci	Cubitus interruptus
CNE	Conserved Non-coding Element
Cos2	Costal2
d	days post fertilization
DCNE	Downstream CNE
dn-	dominant negative-
dpa	Days post amputation
eCFP	enhanced Cyan Fluorescent Protein
eGFP	enhanced Green Fluorescent Protein
En	Engrailed
Eng	Engrailed

FRT	Flippase Recognition Target
Fu	Fused
h	Hours Post Fertilization
Hh	Hedgehog
HRP	Horse Radish Peroxidase
IFT	Intra-Flagellar Transport
kb	kilo base pairs
MCS	Multiple Cloning Site
ME	Muscle Enhancer
Mef2	Myocyte enhancer factor 2
MFF	Medial Fast Fibers
MHB	Mid-Hindbrain Boundary
MO	Morpholino
MP	Muscle Pioneer
MRF	Myogenic Regulatory Factors
nl	nano litres
PBS	Phosphate Buffer Saline
PFA	Paraformaldehyde
PKA	Protein kinase A
PolyA	Poly Adenylation signal
Ptc	Patched
Smo	Smoothened
ss	somite stage

SSF	Superficial Slow Fibers
Sufu	Suppressor of Fused
Tg	Trangenic
tRFP	turbo Red Fluorescent Protein
UAS	Upstream Activating Sequences
UCNE	Upstream CNE
Vc	Venus N-terminal fragment
Vn	Venus C-terminal fragment
ZnFn	Zinc-Finger

List of Figures

Chapter 1: Introduction

1.1. Hedgehog signaling

The *Hedgehog* (Hh) gene was originally identified through its segment polarity mutant phenotype in *Drosophila* (section 7.3; Nusslein-Volhard and Wieschaus, 1980). Segment polarity mutants were one of the four phenotypic classes identified in a large scale screen designed to identify all the genes required to direct the segmentation of the *Drosophila* embryo. Segment polarity mutants have the correct number of segments but display defects in the patterning of each segment. In *Hh* mutants, the posterior 'naked' cuticle in each segment is replaced by the anteriorly restricted denticles, thereby displaying a continuous lawn of denticles and hence the name Hedgehog (Figure 1.1) (Nusslein-Volhard and Wieschaus, 1980). Genetic analysis suggested that Hh acts as a signal to maintain the expression of another segment polarity gene, *wg,* which is expressed in neighbouring cells in each segment (Ingham, 1991). Molecular cloning of the *hh* gene revealed that it encodes a secreted glycoprotein involved in intercellular signaling (Lee et al., 1992; Mohler and Vani, 1992; Tabata et al., 1992). A number of genes homologous to *Drosophila hh* were identified in vertebrates. The realization of their importance in vertebrate development came from the finding that they confer polarizing activity to three major tissue organizing centers namely the notochord, floorplate and the zone of polarizing activity (Echelard et al., 1993; Krauss et al., 1993; Riddle et al., 1993; Roelink et al., 1994), the inductive activities of which were well known from classical embryological manipulations (reviewed in Brockes, 1991; Fietz et al., 1994; Ruiz i Altaba and Jessell, 1993). Since this discovery Hh signaling has been implicated as

having crucial functions in proliferation, patterning, morphogenesis and maintenance of a vast number of tissue types in animals (reviewed in Ingham and McMahon, 2001). Aberrations in the signaling pathway have been causally linked to many forms of cancer, especially basal cell carcinoma, medulloblastoma, rhabdomyosarcoma (reviewed in di Magliano and Hebrok, 2003). Recent studies in animal models and human clinical trials have demonstrated the efficacy of perturbing Hh signaling pathway in the treatment of some of these cancers (di Magliano and Hebrok, 2003; Rudin et al., 2009; Von Hoff et al., 2009; Yauch et al., 2009). Interestingly, forward genetic screens and genome wide association studies have linked some negative regulators of Hh signaling pathway to variations in body sizes in zebrafish (Koudijs et al., 2005) and to variations in height in humans (Lettre et al., 2008; Weedon et al., 2008). Thus, an understanding of the mechanisms of Hh signaling is of direct relevance to human development and disease.

1.2. Patterning in response to graded Hh signaling

The roles of Hh signaling have been well studied in a number of contexts. Here I will discuss the two contexts in which its roles in cell fate specification through differential target gene activation are best characterized, namely the wing imaginal disc of the fly and the vertebrate neural tube (Figure 1.2).
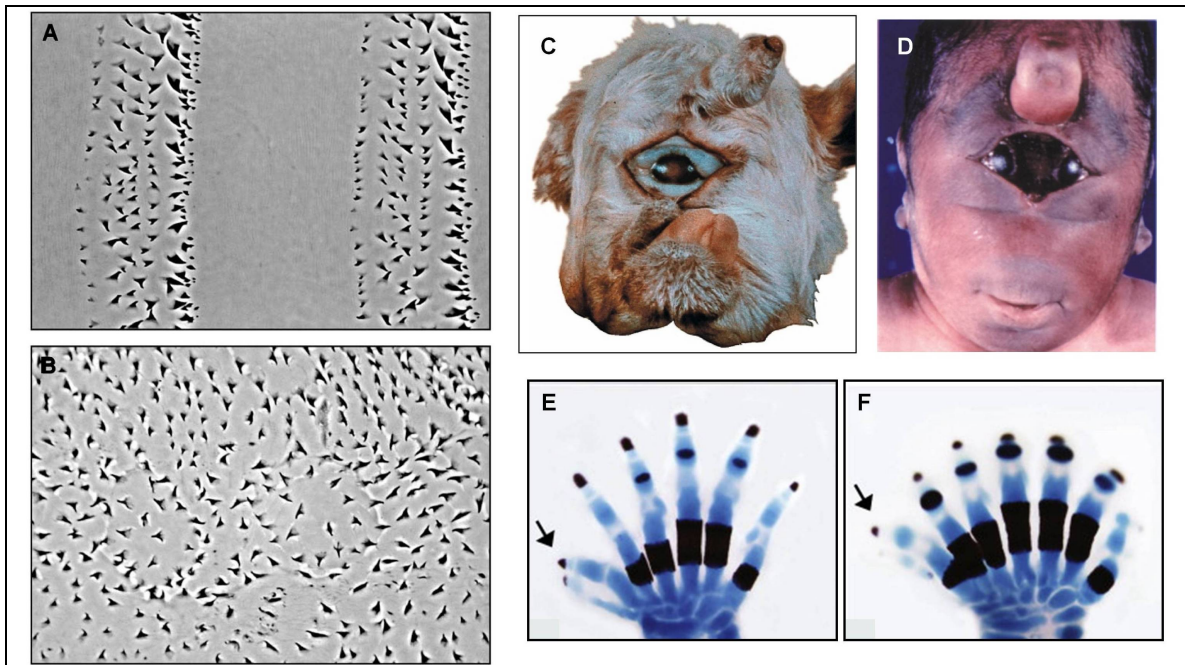
Figure 1.1: Perturbations in the Hh signaling pathway lead to severe phenotypic consequences in *Drosophila* and in vertebrates.

A, B – Cuticle preparations of a wildtype (A) and a *hh* (B) mutant *Drosophila* larvae showing disrupted segment polarity (with permission from Alexandre, 2008).

C – Inhibition of Hh pathway by the plant alkaloid cyclopamine during gestation results in the cyclopic birth defect in a lamb (with permission from James et al., 2004).

D – Still born human fetus showing facial defects characteristic of disruptions in the Hh signaling pathway (with permission from Wilkie and Morriss-Kay, 2001).

E, F – Limb phenotypes, ectopic digits in mice caused by the loss of Gli3 (E) and Kif7 (F) activity, components of the mammalian Hh pathway (image courtesy C.C. Hui).
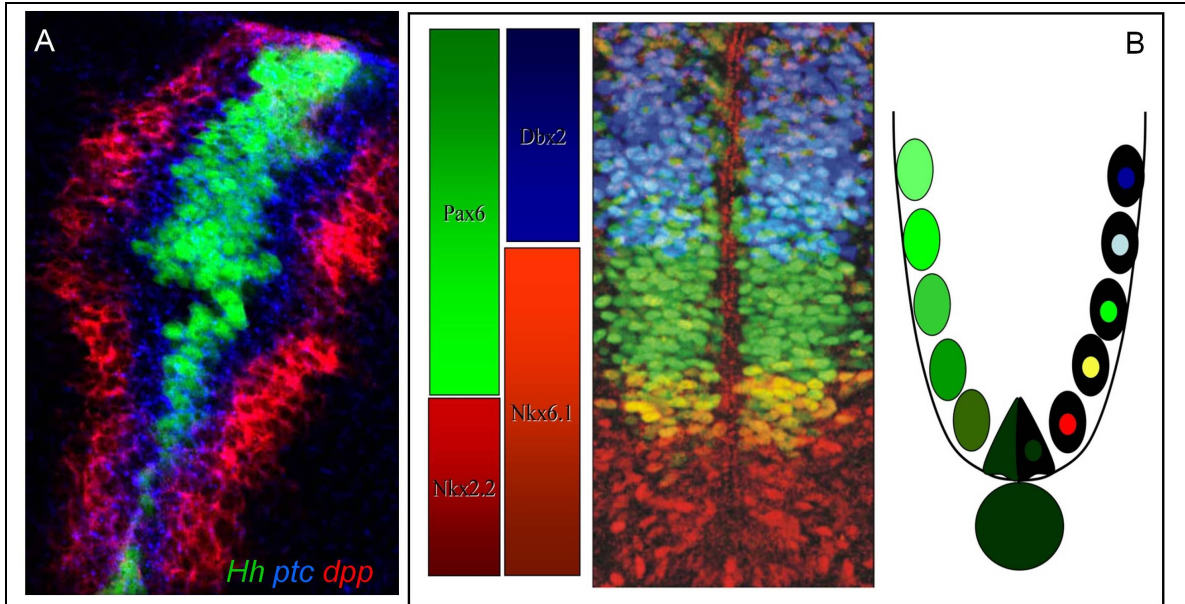
Figure 1.2: Hh acts as a morphogen to ellicit a graded response in *Drosophila* wing imaginal discs and in the vertebrate neural tube.

A – Ectopic expression of a stripe of Hh in the anterior wing disc results in graded response as inferred by *ptc* (blue) transcription and a threshold response as displayed by *dpp* (red), a few cell diameters away from the source of Hh. *ptc* extends up to 10-12 cell diameters, *dpp* signal is masking the blue color (António Jacinto, unpublished).

B – Neuronal specification by graded Shh sets up at least five distinct cell types in the chick neural tube, shown are boundaries marked by transcription factors delineating distinct thresholds to Shh signaling activity in a cross section of the chick neural tube (left panels). Schematic (right panel) showing the inferred Hh pathway activity (green) in the ventral half of the neural tube. A - Image courtesy P.W. Ingham; B – modified from Briscoe et al., 2000.

Imaginal discs are sheets of undifferentiated epithelial cells organized in the form of discs in the larvae of holometabolous insects. Individual imaginal discs give rise to appendages like antenna, eyes, legs, wings, halteres and genitalia during metamorphosis. Part of the mesothoracic imaginal disc gives rise to the adult wing and is divided into two lineage-restricted compartments, anterior and posterior (Garcia-Bellido et al., 1976). Cells in the posterior compartment express both the homeodomain protein Engrailed (En) as well as Hh (Lee et al., 1992; Mohler and Vani, 1992; Tabata et al., 1992); the latter is secreted by posterior compartment cells and spreads into the anterior compartment, forming a steep gradient that induces differential target gene expression in response, thereby acting as a morphogen. Within the anterior compartment, Hh target genes like *patched* (*ptc*, which encodes the Hh receptor, see later) is induced in a graded manner (Figure 1.2) and can be detected up to 10 cell diameters from the boundary. *en* expression is induced by the highest levels of Hh abutting the antero-posterior border in a narrow stripe, whereas *collier* and *dpp* are activated further away from the boundary in response to lower levels of Hh (Figure 1.2) (Mullor et al., 1997; Strigini and Cohen, 1997). Dpp is a long range morphogen belonging to the same class as the vertebrate BMP ligands, which acts to pattern the wing disc downstream of Hh signaling. The response of cells to the Dpp signal is also modulated by Hh pathway activity. Cells at the antero-posterior boundary that receive the highest levels of Hh signals show attenuated response to Dpp, when assayed by activated Mad, transcription factor that mediates Dpp signaling (Tanimoto et al., 2000). This has been attributed to transcriptional down-regulation of the Dpp receptor Tkv in response to high threshold Hh pathway activity (Tanimoto et al., 2000).

The morphogen-like properties of Hh have also been extensively studied in the context of the developing vertebrate neural tube. Shh secreted by two axial midline structures, the notochord and the floorplate, induce and specifiy at least 5 distinct classes of neuronal progenitors (namely p0, p1, p2, pMN, and p3 domains, p stands for progenitor domain) in the ventral half of the neural tube (Figure 1.2) (Briscoe et al., 2000). Shh is necessary and sufficient for the generation of these ventral cells types (Chiang et al., 1996; Marti et al., 1995; Roelink et al., 1995). Direct visualization of Shh showed that it spreads across these neuronal progenitors (Gritli-Linde et al., 2001) and expression of the target gene *Ptc1* displays a graded pattern along the ventral half of the neural tube (Goodrich et al., 1996; Marigo and Tabin, 1996). Cell autonomous perturbations in the Hh pathway also suggest a direct requirement for Shh in specifying these neuronal subtypes (Briscoe et al., 2001; Hynes et al., 2000). Further evidence for such graded patterning comes from chick explant cultures of naïve neural plate cells exposed to varying concentrations of Shh. These experiments showed that the Shh concentration thresholds required for specification of the neuronal progenitors correlated with their distance from the Shh producing cells within an embryo. Increasing thresholds of Shh were required for progressively ventrally located progenitors (Briscoe and Ericson, 1999). Therefore, similar to the *Drosophila* wing imaginal disc, Shh acts as a direct and long range morphogen in the vertebrate neural tube (Briscoe and Ericson, 1999).

1.3. Antagonism between the Hh and BMP signaling pathway

In the developing vertebrate neural tube, BMPs from the lateral non-neural ectoderm and roofplate (dorsal most cells along the entire length of the forming neural tube) specify

dorsal neuronal cell types (Basler et al., 1993; Lee et al., 2000; Lee et al., 1998; Liem et al., 1997; Liem et al., 1995). In at least some cases BMP has been shown to act in opposition to Hh signaling. BMPs can suppress Shh induced ventral cell fates (Barth et al., 1999; Basler et al., 1993; Liem et al., 2000; Liem et al., 1995; Mekki-Dauriac et al., 2002) Secreted BMP inhibitors can potentiate the ability of Shh to induce ventral cell fates *in vivo* (Patten and Placzek, 2002) and BMP inhibitors are expressed by the notochord (Liem et al., 2000; McMahon et al., 1998). Conversely, ectopic Shh can suppress BMP-induced dorsal cell fates (Roelink et al., 1994) and Shh limits the ventral expansion of dorsal cell fates (Liem et al., 1995).

In the context of the neural tube, ectopic Shh can suppress BMP-induced dorsal cell fates (Roelink et al., 1994) and Shh limits the ventral expansion of dorsal cell fates (Liem et al., 1995). Secreted BMP inhibitors can potentiate the ability of Shh to induce ventral cell fates *in vivo* (Patten and Placzek, 2002) and BMP inhibitors are expressed by the notochord (Liem et al., 2000; McMahon et al., 1998). Conversely, BMPs can suppress Shh induced ventral cell fates (Barth et al., 1999; Basler et al., 1993; Liem et al., 2000; Liem et al., 1995; Mekki-Dauriac et al., 2002).

Similar antagonism is also seen in neural stem cells within the embryonic forebrain, where Shh can suppress BMP induced proliferation of progenitor cells and differentiation into astroglial cells in primary cultures (Zhu et al., 1999). Later during the development of the cerebellum, BMP2 has been shown to suppress the mitogenic response of Shh on granule cell precursors and induces differentiation of these cells (Rios et al., 2004). This

antagonism is not limited to the development of the nervous system. In a recent study the induction of the zebrafish hematopoetic stem cells in the floor of the dorsal aorta was shown to be positively regulated by BMPs and this induction is antagonized by Hh signals from the dorsal side (Wilkinson et al., 2009). Another example of this antagonism in non-neural tissues is in the specification of the pancreas, where Hh promotes β-cell differentiation by restricting the repressive effects of BMPs (Tehrani and Lin, 2011). What remains unclear and requires further analysis is at what level the two pathways interact? Are the signaling components of one pathway directly interacting and influencing the outcomes of the other pathway or, are the two pathways controlling the transcription of each other's signaling components?

1.4. Biogenesis of the extracellular Hh gradient

1.4.1. Regulation of Hh production, maturation, secretion and distribution

The *hh* gene product is a 45 kD peptide whose C-terminal half catalyzes a self splicing reaction to produce a 19 kD N-terminal signaling fragment, also referred to as Hh-N (Bumcrot et al., 1995; Lee et al., 1994). This N-terminal fragment retains all signaling activity, whereas no other function (other than the self splicing reaction) has been attributed to the C-terminal fragment. Execution of this autocleavage reaction results in a cholesterol moiety being added to the C-terminus of Hh-N (Porter et al., 1996). Acyltransferases then add a palmitoyl group at the N-terminus of Hh-N (Chamoun et al., 2001). The N-terminal palmitoylation in the secreting cells is essential for its signaling

activity and was shown to be critical for the removal of a short peptide at the N-terminus of Hh. This short N-terminal fragment when left unremoved can block binding of Hh to its receptor (Ohlig et al., 2011). Addition of the C-terminal cholesterol moiety results in membrane retention of the ligand (Bumcrot et al., 1995; Lee et al., 1994; Porter et al., 1995), a property consistent with a role for the protein in juxtacrine signaling but apparently at odds with its role as a morphogen. Hh still needs to be dispersed in a gradient and this appears in sharp contrast with its membrane bound nature. Insights into this process come from *Drosophila* mutants in the *dispatched* gene (Burke et al., 1999). *dispatched* mutant flies fail to secrete Hh and accumulate Hh in producing cells (Burke et al., 1999). Dispatched is a 12-pass transmembrane protein and has been suggested to control vesicle trafficking and apico-basal sorting of the Hh ligand. Therefore, Dispatched functions by releasing membrane bound Hh (Burke et al., 1999).

1.5. Interpreting the extracellular Hh gradient

1.5.1. Hh signal transduction components

Cells need to be able to sense and transduce different levels of extracellular Hh into distinct and tissue specific transcriptional responses. A large part of the signaling pathway used by cells to transduce the Hh signal was elucidated using fly genetics. The Hh pathway components (Figure 1.3) in flies include its receptor, Patched (Ptc) - a twelve pass transmembrane protein (Hooper and Scott, 1989; Ingham et al., 1991; Nakano et al., 1989); two related transmembrane co-receptors Intereference Hedgehog (Ihog) and Brother of Ihog (Boi) (Yao et al., 2006); Smoothened (Smo) – a seven pass

transmembrane protein (Alcedo et al., 1996; van den Heuvel and Ingham, 1996) and a central transducing component of the pathway; a set of intracellular transducing proteins Costal2 (a motor/scaffolding protein, Cos2) (Forbes et al., 1993; Wang et al., 2000b), Fused (Fu, a serine threonine kinase) (Alves et al., 1998; Forbes et al., 1993; Therond et al., 1999), Suppressor of Fused (Sufu, a cytoplasmic tether for Cubitus interruptus (Ci) and acts as a negative regulator of the pathway) (Methot and Basler, 2000; Preat, 1992); a set of kinases (PKA, GSK3B and CKI) that modulate Ci processing and finally the transcription factor Ci that mediates all transcriptional responses of the pathway (Alexandre et al., 1996; Forbes et al., 1993).
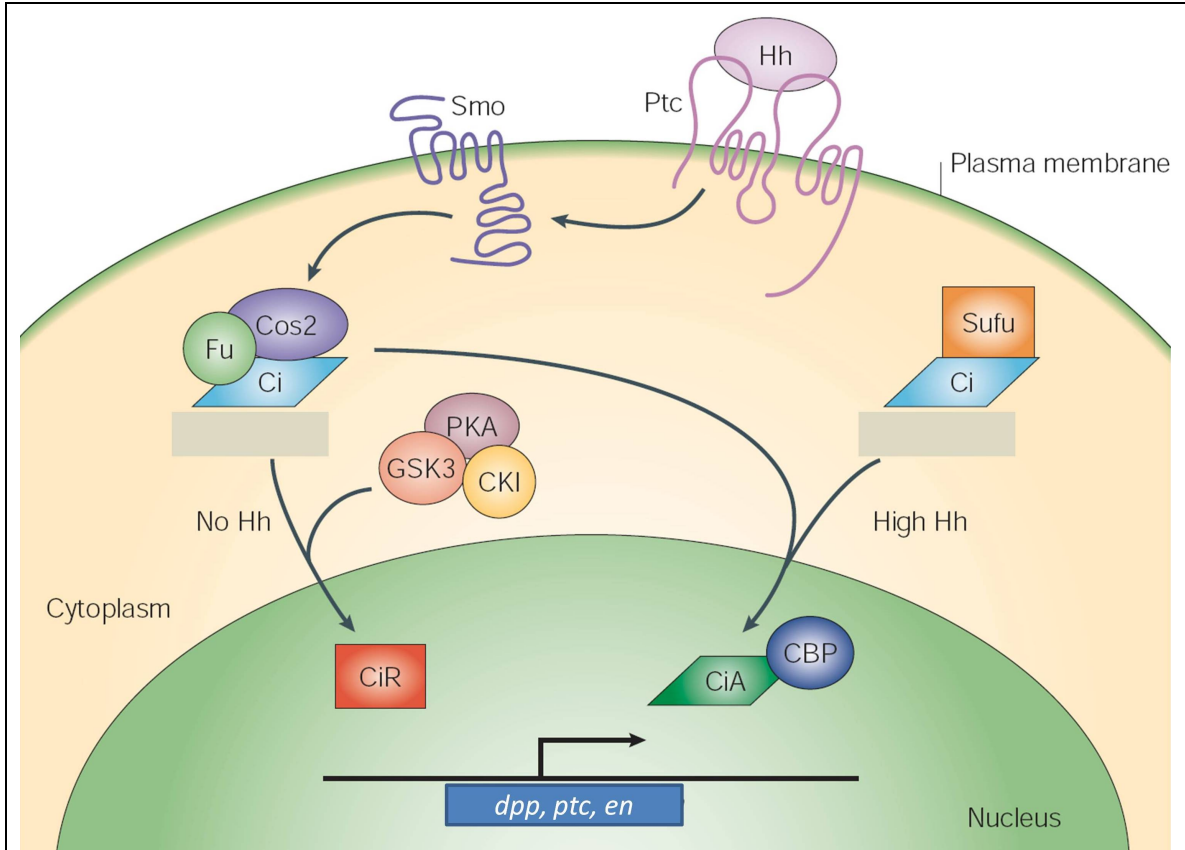
Figure 1.3: Schematic summarizing mechanisms of Hh signal transduction in *Drosophila*, modified from Hooper and Scott, 2005.

In a cell that is not exposed to the Hh ligand, Ptc, the Hh receptor, potently and catalytically inhibits Smo (Taipale et al., 2002). Inhibition of Smo results in the phosphorylation of Ci (Price and Kalderon, 1999), directing it to proteolytic processing to a shorter N-terminal repressor form (Aza-Blanc et al., 1997). This repressor form inhibits Hh responsive target genes. When a cell is exposed to Hh, the ligand binds to the co-receptors, Ihog and Boi, which facilitate its binding to Ptc (Yao et al., 2006). Binding of Hh inactivates Ptc (Ingham et al., 1991; Stone et al., 1996) resulting in the activation of Smo and the accumulation of full length activator forms of Ci (Aza-Blanc et al., 1997), which activates the repressed target genes (Alexandre et al., 1996; Muller and Basler, 2000). The level of Hh a cell receives is thought to control the ratio between Ci-activator (Ci^A) and repressor (Ci^R), resulting in activation of different target genes in different cells. Of the few *bona fide* transcriptional Hh targets that have been characterized in detail, all have been found to have sequences similar or identical to the Ci/Gli (Gli are vertebrate orthologs of Ci) consensus binding site upstream of their promoters (Agren et al., 2004; Alexandre et al., 1996; Dai et al., 1999; Gustafsson et al., 2002; Laner-Plamberger et al., 2009; Sasaki et al., 1997; Winklmayr et al., 2010). Genome-wide Chromatin Immuno-precipitation (ChIP) screens, however, have identified hundreds of putative Gli/Hh targets, a significant proportion of which are not associated with Gli consensus binding sites (Vokes et al., 2007; Vokes et al., 2008)

In addition to being the receptor, Ptc has been attributed with two distinct roles in signaling: (1) It acts as a negative feedback loop whose expression is induced by pathway activity, antagonizing pathway activity and (2) it acts to sequester and limit the spread of

Hh proteins close to the source (Chen and Struhl, 1996). How the Hh-Ptc complex communicates to Smo remains unknown. What is known is that Ptc does not directly interact with Smo to suppress its activity (Johnson et al., 2000). It has been suggested that Ptc regulates Smo through a small molecule lipid intermediate (Khaliullina et al., 2009). A possible candidate for such a lipid is phosphatidylinositol-4 phosphate, which can modulate the activity of Smo and its levels can be modulated by Ptc (Yavari et al., 2010). Smo communicates to the intracellular transducers through its C-terminal tail. A conformational switch resulting from the neutralization of positively charged residues by phosphorylation of the C-terminal tail of Smo is thought to be essential for downstream signaling events (Zhao et al., 2007).

The current model for signaling downstream of Smo invokes Cos2, which acts as a scaffold for kinases (like PKA, GSK3 and CK1) that phosphorylate Ci (Figure 1.3) (Robbins et al., 1997; Sisson et al., 1997; Zhang et al., 2005). When activated, Smo releases Ci from the phosphorylating scaffold. This leads to the accumulation of full length form of Ci which translocates to the nucleus to activate Hh target genes. The Ci^A is distinct from the full length form, as expression of the constitutive full length form cannot recapitulate the highest levels of Hh activity (Methot and Basler, 1999; Wang et al., 2000b). The biochemical nature of this Ci activator and its biogenesis are also not understood. Based on these mechanisms and other experimental evidence, three different Hh sensing cellular states are thought to exist in the fly wing imaginal disc, (1)- No Hh, high Ci^R production, (2) – low Hh, lower Ci^R and full length Ci, (3) – High Hh, no Ci^R but high Ci^A (Hooper and Scott, 2005).

1.5.2. Vertebrate Hh signaling components

The core Hh pathway is largely conserved between insects and vertebrates, although there are some significant differences. In some cases, multiple orthologs exist for a single *Drosophila* pathway component, whereas in other cases only one ortholog exists. All vertebrates examined so far, including teleosts, have a single *smo* gene which is essential for the transduction of all responses to Hh signaling. Mammals have three Hh genes while teleosts, such as zebrafish, have four or five. Several of these have been shown to function through two *Ptc* orthologs (*Ptc1* and *Ptc2*). Three *ci* orthologs, *Gli1*, *Gli2* and *Gli3* exist in mammals and a fourth *gli2* co-ortholog exists in zebrafish (Ke et al., 2005).

Ptc1, one of two vertebrate orthologs of *Drosophila ptc,* is expressed in close proximity to Hh expression domains and serves as a good indicator for cells responding to Hh (Concordet et al., 1996; Goodrich et al., 1996; Hepker et al., 1997; Marigo et al., 1996b). Expression of *Ptc2* is less dependent on Hh signaling and more diffuse than *Ptc1* (Carpenter, 1998; Lewis et al., 1999a; Motoyama et al., 1998). Removal of *Ptc1* results in strong de-repression of the pathway in mammals, less so in zebrafish (Goodrich et al., 1997; Wolff et al., 2003) whereas, removing *Ptc2* results in milder phenotypes in mammals (Nieuwenhuis et al., 2006). Simultaneous removal of both *ptc1* and *ptc2* results in much stronger Hh pathway de-repression than that resulting from inactivation of either one alone in zebrafish embryos (Koudijs et al., 2008; Wolff et al., 2003).

Kif7, the vertebrate orthologue of Cos2, has conserved roles in Hh signal transduction in

zebrafish and mammals, where it binds Gli and acts as a negative regulator of the pathway (Cheung et al., 2009; Endoh-Yamagami et al., 2009; Ingham and McMahon, 2009; Liem et al., 2009; Tay et al., 2005). In zebrafish embryos, removal of Kif7 along with another conserved member of the signaling pathway, Sufu (whose *Drosophila* ortholog is involved in cytoplasmic sequestration of Ci) results in hyper-activation of the pathway downstream of Smo. Kif7 has now been shown to have conserved roles in the mammalian Hh signaling pathway, where it is involved in the production of both activator and repressor forms of Gli2 and Gli3 (Cheung et al., 2009; Endoh-Yamagami et al., 2009; Liem et al., 2009).

Gli1 encodes a constitutive transcriptional activator (Lee et al., 1997; Marigo et al., 1996a). In mice, its inactivation has no developmental phenotypes (Park et al., 2000) whereas in zebrafish, *gli1* mutations are lethal (Chandrasekhar et al., 1999; Karlstrom et al., 2003). Over-expression of *Gli1* can induce transcription of Hh target genes in the absence of Hh pathway activity (Hynes et al., 1997; Ruiz i Altaba, 1998; Ruiz i Altaba, 1999; Sasaki et al., 1997). *Gli1* is itself an Hh target gene and its expression is indicative of pathway activity (Lee et al., 1997) and therefore is considered a downstream feed forward component of the Hh pathway.

Gli2 appears to function like *Drosophila* Ci, functioning as an activator or a repressor in response to Hh signaling (Aza-Blanc et al., 2000; Karlstrom et al., 2003; Mullor et al., 2001; Regl et al., 2002; Ruiz i Altaba, 1998; Sasaki et al., 1997). Sinilarly, Gli3 functions as both an activator and a repressor; its processing into the repressor form is inhibited by

Hh pathway activity (Wang et al., 2000a). In mice, the *Gli3* mutant phenotype suggests that it acts predominantly as a repressor (Hui and Joyner, 1993; Persson et al., 2002), and the defects can be rescued by the simultaneous removal of either *Shh* or *Smo* (Litingtung and Chiang, 2000; Rallu et al., 2002; Wijgerde et al., 2002).

Several novel components and modulators of the core Hh signaling pathway have been identified by forward genetic screens in vertebrates. Interestingly, many of these new genes link Hh signaling to the primary cilia, a cellular organelle long thought of as a vestige from our protozoan past. The strongest links between cilia and Hh signaling come from mouse mutants of the Intra-Flagellar Transport proteins (IFT) (Eggenschwiler and Anderson, 2007; Huangfu et al., 2003). IFT proteins function to transport cargo within cilia and are also required for their formation. Several of the mouse IFT mutants display strong disruptions in the Hh signaling pathway (reviewed by Goetz and Anderson, 2010). Pathway components including Ptc, Smo, Gli and Sufu have been shown to be enriched in the cilia of mammalian cells (Corbit et al., 2005; Haycraft et al., 2005; Rohatgi et al., 2007). In the context of Hh signaling, plasma membrane seems to have taken the role of primary cilium in *Drosophila*. Somatic cells in *Drosophila* do not possess a primary cilium and translocation of Smo to the plasma membrane and Ptc away from the membrane into vesicles has been found to be critical for downstream signaling (Denef et al., 2000). However, in mammalian cells upon reception of Shh, Ptc1 is driven away from the cilia and Smo translocates into the cilia (Rohatgi et al., 2007).

By contrast with mouse, zebrafish IFT mutants do not display any Hh related phenotypes, leading to the suggestion that the involvement of primary cilium is a feature specific to

mammalian Hh signaling. However, recent studies have shown that upon simultaneous removal of both the maternal and zygotic contribution, a zebrafish *polaris* (IFT88) mutant displays a Hh pathway phenotypes (Huang and Schier, 2009). The involvement of cilia in the transduction of Hh in the zebrafish has been confirmed by the finding that *dzip1* mutants, which show Hh related muscle and neuronal specification phenotypes (Sekimizu et al., 2004; Wolff et al., 2004) have recently been shown to lack primary cilia (Glazer et al., 2010; Kim et al., 2010; Tay et al., 2010). Therefore the central role of cilia as the site of Hh signal transduction is conserved amongst all vertebrates.

1.5.3. Integrating Hh signaling response by controlling Ci/Gli activity

The molecular basis of the Hh morphogen activity is still not fully understood. It is thought that varying levels of extracellular Hh activity are translated into different intracellular levels of the activator and repressor forms of the Ci/Gli (Ericson et al., 1997; Ruiz i Altaba, 1998; Sasaki et al., 1997; Stamataki et al., 2005). A two fold increase in Hh concentration can be mimicked by a similar fold change in the concentration of Gli activators inside cells (Stamataki et al., 2005).

The activation of differential target gene expression in response to different thresholds of Hh pathway activity also remains poorly understood, for example, how certain target genes like *ptc* seem to be expressed at levels that are directly proportional to pathway activity (Alexandre et al., 1996; Wolff et al., 2003), whereas others like *dpp* respond to concentration thresholds of the ligand (Ingham and Fietz, 1995; Muller and Basler, 2000). Apart from these two distinct modes of regulation, how are distinct thresholds

interpreted? Is it the strength and/or the number of Ci binding sites that directly govern this threshold, or do other factors help in setting up these boundaries? In the *Drosophila* wing imaginal disc, *dpp* is activated intermediate levels of signaling activity and is repressed both in the absence of Hh signaling and in cells exposed to the highest levels of Hh (Muller and Basler, 2000); by contrast, *en* is activated only by the highest levels of pathway activity (Mullor et al., 1997; Strigini and Cohen, 1997). In some cases it has been proposed that it is not the number or strength of Ci binding sites that determine differential gene expression in response to differential Hh threshold, but the ratio of Ci^A vs. Ci^R in the responding cells (Muller and Basler, 2000).

In addition to concentration dependent target gene regulation there also exists much less understood temporal integration of Hh signaling. Explant cultures of the chick neural tube cultured in Shh conditioned media, show how cells first express the most dorsal markers and over time switch off dorsal markers and sequentially adopt more ventral fates (Ericson et al., 1997). More evidence for such temporal integration of pathway activity comes from over-expression of different versions of Gli activators in the neural tube: a potent form of Gli can induce an ectopic ventral cell type in 12 h compared to 72 h for a Gli with dampened activity (Stamataki et al., 2005). How the Hh signal strength is integrated temporally by the transducing machinery remains unclear.

1.6. Hh signaling and control of cell fates within the zebrafish myotome

In the gastulating vertebrate embryo part of the mesoderm forms the somites. Somites are

transient structures and can be identified as clusters of mesodermal cells lying on both sides of the midline (notochord and the neural tube). They are the most prominent segmented structures post gastrulation. They give rise to muscles, bones, cartilage and tendons along the trunk and tail of the vertebrate embryo. In the zebrafish embryo, most of the somitic cells are fated to become muscle and the myotome begins to differentiate prior to any of the other somitic tissue types.

Lineage tracing experiments in zebrafish have shown that cells that will form muscles occupy the marginal zone before the onset of gastrulation. Myogenesis in zebrafish is thought to begin at about 70% epiboly when *myoD,* a bHLH transcription factor that acts as a master regulator of muscle cell formation (Devoto et al., 1996; Weinberg et al., 1996), is first seen to be expressed in myogenic precursors, initially in the tail bud and adaxial cells and slightly later in the lateral fast muscle progenitors in the somites (Devoto et al., 1996; Lewis et al., 1999b). Adaxial cells are a morphologically distinct monolayer of mesodermally derived cells positioned next to the forming notochord in a bud stage zebrafish embryo (Figure 1.4) (Devoto et al., 1996; Hirsinger et al., 2004).

Skeletal muscle fibers can be broadly classified into two types, slow-twitch and fast-twitch. Slow-twitch fibers are specialized for continuous and prolonged activity and are largely powered by oxidative metabolism; they appear red in color due to the large number of mitochondria they possess. Fast-twitch fibers, on the other hand, are used for short bursts of activity, powered mainly by anaerobic metabolism. Muscle tissue usually has a mix of the two fiber types and their ratio can be altered in response to physiological

input.

Cell lineage studies in zebrafish have shown that adaxial cells give rise to mono-nucleated slow-twitch fibers (Figure 1.4) (Devoto et al., 1996). The loss of this cell type from the embryonic zebrafish myotome results in U-shaped somites as opposed to the characteristic chevron shape seen in wild type embryos. Most of these U-shaped somite mutants identified in the screen performed at the Max Planck Institute in Tübingen (van Eeden et al., 1996b) were later shown to dirupt genes encoding components of the Hh signaling pathway (Chen et al., 2001; Karlstrom et al., 1999; Nakano et al., 2004; Schauerte et al., 1998; Varga et al., 2001).

Figure 1.4: Schematic displaying the chain of events leading to specification and patterning of muscle cell types within the zebrafish embryonic myotome in response to Hh pathway activity. Schematic shows cross sections of the myotome (Wolff et al., 2003).
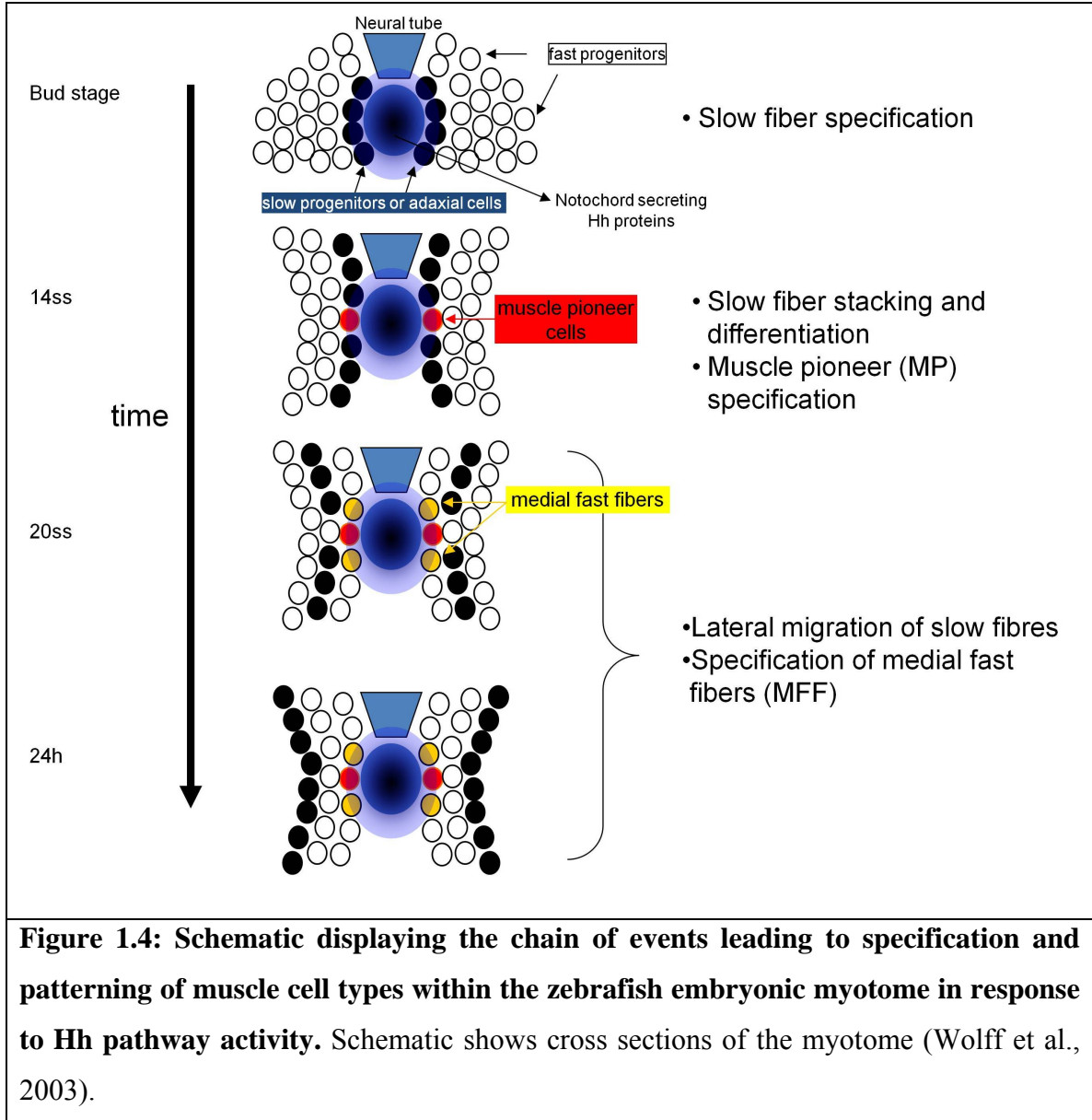
These mutants imply that, exposure of adaxial cells to Hh from the forming notochord allocates them to the slow-twitch myogenic lineage. Consistent with this, ectopic expression of *shh* results in conversion of the entire myotome to the slow-twitch myogenic fate (Blagden et al., 1997). The remaining myogenic progenitors differentiate later into fast-twitch myofibers (Figure 1.4) (Blagden et al., 1997; Currie and Ingham, 1996; Devoto et al., 1996). Hh induces expression of the transcription factor Prdm1a in adaxial cells, the activity of which is both necessary and sufficient to drive the slow-twitch fiber differentiation program (Baxendale et al., 2004; Roy et al., 2001). After the induction of adaxial cells to the slow fiber fate, they elongate to span the width of the somite, displacing each other dorso-ventrally, and then migrate laterally to the surface of the myotome, through the dividing fast muscle progenitors (Figure 1.4) (Devoto et al., 1996). This migration is thought to induce a wave of differentiation within the fast muscle progenitors (Henry and Amacher, 2004). These newly differentiating cells will form multi-nucleated fast-twitch muscle fibers.

A small population (2-6 out of about 20 adaxial cells in each hemisegment) of the slow fibers do not migrate, remain medially located close to the notochord (Figure 1.4) (Currie and Ingham, 1996). This subpopulation of slow fibers differentiates into the Muscle Pioneers (MPs), so called because they are the earliest fibers to differentiate within the embryo (Hatta et al., 1991). The MPs later get incorporated into the horizontal myoseptum, which divides the somite into the dorsal and the ventral halves. MPs can be identified by their expression of *engrailed* genes (*eng1a*, *eng1b* and *eng2a*) (Ekker et al., 1992; Hatta et al., 1991; Roy et al., 2001; Thisse et al., 2001) as well as by the expression

of *wnt11* (Philipp et al., 2008; Thisse et al., 2001) and *sfrp2* (Tendeng and Houart, 2006). The origins and functions of MP within the adaxial cells are not very well understood.

Previous studies have suggested that the specification of MP fate requires a higher level of Hh signaling activity than that required for the rest of the slow-twitch fibers: embryos mutant for *shh* (*syu*), *scube2* (*you*) and *disp* (*con*), in which the activation of the Hh pathway is attenuated but not eliminated, form some slow fibers but lack MPs (Hollway et al., 2006; Kawakami et al., 2005; Lewis et al., 1999b; Nakano et al., 2004; Woods and Talbot, 2005). Conversely, increased activation of the Hh pathway, through the over-expression of *shh*, the inhibition of PKA or the inactivation of Shh receptors *ptc1* and *ptc2*, can force adaxial cells and indeed other myoblasts to differentiate into MPs (Currie and Ingham, 1996; Hammerschmidt et al., 1996; Hollway et al., 2006; Wolff et al., 2003).

After the radial migration of adaxial cells, some myoblasts committed to the fast-twitch lineage also come into close apposition with the notochord. These similarly respond to high Hh signaling by activating transcription ofeng genes, but unlike adaxial cells, differentiate into multinucleated fast-twitch fibers, the MFFs, for medial fast fibers (Figure 1.4) (Wolff et al., 2003). Expansion of the MFF population occurs in embryos homozygous for loss of function mutations of the *dzip1* gene or following morpholino mediated knock-down of the *Su(fu)* gene (Wolff et al., 2003; Wolff et al., 2004).

Pharmacological inhibition of the Hh pathway using cyclopamine results in a graded response in zebrafish muscle cell fate specification (Figure 1.5) (Wolff et al., 2003).

Exposure to lower concentrations (15 µM) results in loss of MP only, higher doses (20 µM) results in loss of both MP and MFF fibers whereas at 30 µM concentration the specification of all slow fibers along with MPs and MFFs is blocked (Figure 1.5) (Wolff et al., 2003). Therefore, Hh signaling controls at least two distinct decisions in the myotome, (1) - it regulates the early binary, slow vs. fast fiber type cell fate decision and (2) – higher or prolonged exposure to its activity induces two distinct cell types within each of the lineages, the MPs - a sub-set of the slow-twitch fibers and the MFFs - a subset of medially located fast twitch fibers adjacent to the notochord (Figure 1.4) (Roy et al., 2001; Wolff et al., 2003).
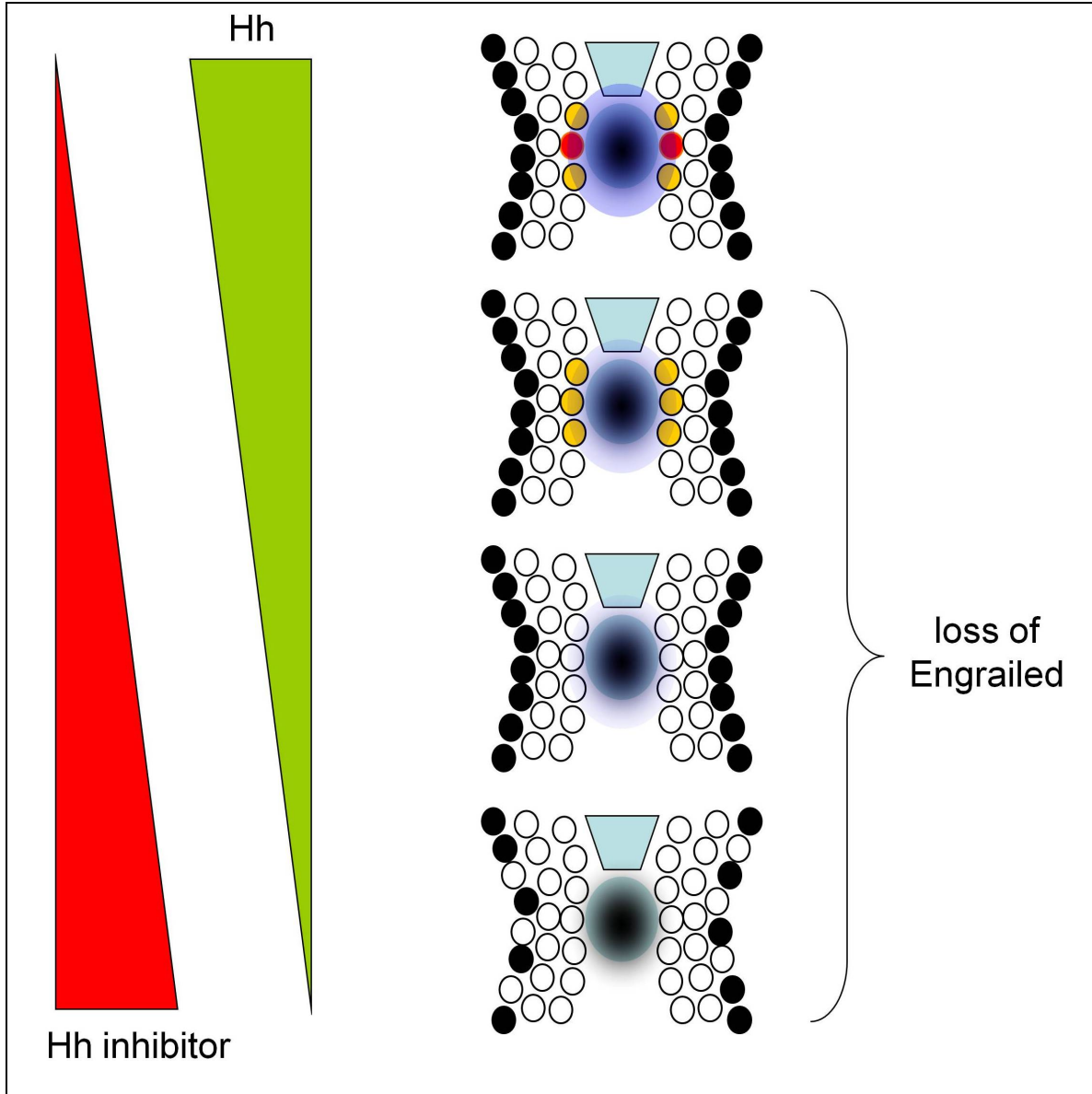
Figure 1.5: Schematic of cross section of zebrafish embryonic myotome showing the consequences of perturbation of Hh signaling pathway using increasing concentrations of cyclopamine. See also Figure 1.4 to identify the cell populations, adapted from (Ingham and Kim, 2005).

Chapter 2: Specific Aims

In order to investigate how high levels of Hh signaling induces distinct cell types within the slow and the fast muscle compartment, I have focused on regulatory mechanisms controlling the earliest and best known marker gene expression in these cell types (MP, MFFs), i.e. *eng*. I chose *eng2a* out of the three *eng* genes expressed in the myotome because of its simpler expression patterns (MHB, MPs and MFFs in early embryos), compared to *eng1a*, *eng1b* that are additionally expressed in the pectoral fin bud and in neurons of the spinal cord.

2.1. Generation of Hh signaling reporters and comparison of Hh response within individual adaxial cells

Do MP and MFF progenitors receive higher levels of Hh signals or are they predisposed to respond to Hh in response to other signals? Visualizing Hh signaling within these cells during their specification could help resolve these questions. Towards this end, I have generated transcriptional reporters for the *ptc* genes to visualize and quantify Hh signaling in live zebrafish embryos. Support for such an approach comes from Hh signaling in the *Drosophila* wing imaginal disc. Cells responding to higher thresholds of Hh are consistently marked by higher levels of *ptc* transcription (Ingham and Fietz, 1995).

2.2. Identification and characterization of cis-regulatory elements of the eng2a gene

To identify regulatory mechanisms controlling the induction of Eng by Hh, I have identified minimal *cis*-regulatory elements around the *eng2a* gene. Although this element displays Hh responsive activity *in vitro* and *in vivo*, it does not contain any obvious Gli consensus binding sites within its sequence.

2.3. Identification of trans-regulatory factors controlling eng expression

Having identified the *cis*-regulatory elements, my next aim was to identify the trans-acting factors that mediate its regulation. I chose to take an unbiased approach, using a cell culture based trans-regulatory screen (Souren et al., 2009). The regulatory potential of some of these factors was tested in zebrafish embryos.

2.4. Functional characterization of identified regulators

Using gain- and loss-of-function experiments in the zebrafish embryonic myotome I have characterized the roles of some of the regulatory factors identified in the screen (BMP-Smad signaling and myogenic factor - Mef2).

Chapter 3: Materials and Methods

3.1. Zebrafish strains and husbandry

Adult fish were maintained on a 14h light/ 10h dark cycle at 28°C in the AVA
(Singapore) certificated IMCB zebrafish facility. All experiments were subject to
A*STAR IACUC approval. Mutant strains of zebrafish were maintained as heterozygote
and homozygote embryos were obtained by inter-crossing the heterozygote adults.
Mutant strains used are *disp1*^{tf18b} (Nakano et al., 2004; van Eeden et al., 1996a), *ptc1*^{hu1602}
and *ptc2*^{tj222} double heterozygotes (Koudijs et al., 2008), *dzip1*^{ts294e} (Brand et al., 1996;
Wolff et al., 2004), *smo*^{b641} (Varga et al., 2001) and *yot*^{ty119} (Karlstrom et al., 1999). The
actin:GAL4 line was generated by Scheer and Campos-Ortega (1999). The
Tg(PACprdm1:gfp)^{i106} and the *Tg(Smhc:eGFP)* lines were generated by Elworthy et al
(2008).

3.2. RNA in-situ hybridizations were done according to the protocol in (Thisse et al., 2001)

Gene	Clone name	Promoter, enzyme used	Reference
ptc1	PWI-39	T3, XbaI	(Concordet et al., 1996)
sfrp2	Zf-sfrp2-pCR4-TOPO	T3, NotI	(Tendeng and Houart, 2006)
smad1	pCS2-smad1	T3, BamHI	(Dick et al., 1999)
smad5	Zf smad5-11/1	T7, BamHI	(Dick et al., 1999)

3.3. Whole mount immuno-histochemistry

Primary antibodies used

Epitope/antibody name	Animal developed in	Dilution used for staining	Provider
pSmad	rabbit	1 in 150	Cell Signaling
4D9 (Eng)	mouse	1 in 50-200	DHSB (Patel et al., 1989)
F59 (Slow Myosin Heavy Chain)	mouse	1 in 50	DHSB (Devoto et al., 1996)
Prox1	rabbit	1 in 1000	(Glasgow and Tomarev, 1998)
GFP	rabbit-488	1 in 500	Invitrogen
mCherry	mouse	I in 500	Living Colors, Clonetech
tRFP	rabbit	1 in 500	Evrogen
N-Smad1,5,8	rabbit	1 in 200	Santa Cruz Biotechnology
Mef2	rabbit	1 in 500	Santa Cruz Biotechnology (Hinits and Hughes, 2007)
HA-tag	rabbit	1 in 500	Santa Cruz Biotechnology
F310 (Fast Myosin Heavy Chain)	mouse	1 in 50	DSHB
turboFP635	rabbit	1 in 500	Evrogen

Secondary antibodies used

Epitope/antibody name	Dilution used for staining	Provider
Goat anti-mouse IgG-405	1 in 750	Molecular Probes, Invitrogen
Goat anti-mouse IgG-488	1 in 750	Molecular Probes, Invitrogen
Goat anti-mouse IgG-546	1 in 750	Molecular Probes, Invitrogen
Goat anti-mouse IgG-633	1 in 750	Molecular Probes, Invitrogen
Goat anti-mouse IgG-HRP	1 in 750	Molecular Probes, Invitrogen
Goat anti-rabbit IgG-488	1 in 750	Molecular Probes, Invitrogen
Goat anti-rabbit IgG-568	1 in 750	Molecular Probes, Invitrogen
Goat anti-rabbit IgG-488	1 in 750	Molecular Probes, Invitrogen
Goat anti-rabbit IgG-HRP	1 in 750	Molecular Probes, Invitrogen

Embryos were fixed in 4% PFA either for 3 h at room temperature or overnight at 4°C. They were then washed in PBTX (PBS+0.1% tritonX100) twice, followed by a 5 min wash in 50% methanol in PBTX and finally stored in pure methanol at -20 from 2 h to several months. To continue, embryos were rehydrated using a 50% methanol in PBTX wash, followed by several washes in PBTX alone. Embryos were then incubated in PBDT (PBS, 1% BSA fraction V, 1% DMSO, 0.5% tritonX100) for 1 h. The primary antibody at the appropriate dilution was added to PBDT and then applied to the embryos for 2 h at room temperature or overnight at 4°C. Embryos were then washed for 30 min at least twice in PBDT. The secondary antibody, diluted in PBDT, was applied to embryos for 2 h at room temperature or overnight at 4°C. Embryos were then washed several times in PBDT and put in 80% glycerol in PBS and imaged. If the secondary antibody conjugated to HRP (horseradish peroxidase) was used, an additional step of deactivating

endogenous peroxidases after rehydration from methanol was employed by incubating embryos in 3% hydrogen peroxide for 10 mins. For staining embryos were incubated in SIGMA*FAST*™ DAB solution until desired staining was obtained. Embryos were then transferred to 80% glycerol in PBS after 2 washes in PBTX.

3.4. Microinjections

Morpholinos were made to 3 nmol/μl stock solution and were injected at concentrations ranging from 0.4 to 1.5 nmol/μl.

Morpholinos designed in this study

bmpr1ba E1-I1   GTAAAATGTTGACACTCACCCAAGT

sfrp2 ATG   TAGGCACGCATCTTTACTTCAGTTG

mpp7 ATG   CTCATACAGACCCATCTCACTGCCG

Gadd45b ATG   ATAGTGGTAATCCACAAGTCTCCGG

smyd2a ATG   ATCGCTATTGACCTGCTGCTCGCGT

smyd2b ATG   TGCCTTCATCATACACACAAATCAG

Previously described morpholinos

smad1 ATG (obtained from Karuna Sampath)   (McReynolds et al., 2007)

AGGAAAAGAGTGAGGTGACATTCAT

smad5 ATG (obtained from Karuna Sampath)   (McReynolds et al., 2007)

ACATGGAGGTCATAGTGCTGGGCTG

gli2a ATG (obtained from Gene Tools)   (Wolff et al., 2003)

GAGGTGGGACTTGTGGTCTCCATGA

gli3 ATG (obtained from Rolf Karlstrom)   (Tyurina et al., 2005)

GACAGGATACTCGTTGTTGTGAAAC

bmp4 (obtained from Karuna Sampath)   (Leung et al., 2005)

GTCTCGACAGAAAATAAAGCATGGG

mef2d/c ATG (obtained from Gene Tools)   (Hinits and Hughes, 2007)

GAATCTGGATCTTTTTCCTCCCCAT

Capped RNA for over-expression by microinjection was prepared by using the mMessage kits from Ambion according to manufacturer's instructions. For making Shh RNA, a plasmid containg the full length coding sequence of Shh (Krauss et al., 1993) was digested with EcoRI, purified and transcribed using the SP6 promoter. For dnPKA RNA, the plasmid was digested with NotI and transcribed using the SP6 promoter (Hammerschmidt et al., 1996).

DNA constructs

Tol2 DNA constructs were injected at a concentration of 25 ng/µl along with 25 ng/µl Tol2 RNA (Balciunas et al., 2006). DNA Constructs without Tol2 arms were injected at 100 ng/µl. In each case a drop size of 1-5 nl was injected.

3.5. DNA constructs generated

Homologous recombination in bacteria to produce recombinant DNA constructs

Homologous recombination for manipulating plasmid and BAC DNA was performed using the SW105 strain (Warming et al., 2005). The SW105 strain when grown at 32 ˚C shows suppressed homologous recombination, whereas when heat shocked at 42 ˚C for 15 min can recombine homologous strands of DNA in the presence of double strand breaks. SW105 cells containing the plasmid or BAC to be modified were induced for recombination and made electro-competent. A linear fragment of DNA containing a reporter gene alongside an antibiotic marker gene (Kanamycin and Ampicillin) was PCR amplified with oligonucleotides that harbor 55 bp of homology at their 5' end. The homology arms on the oligonucleotides were designed to flank the desired insertion site on the plasmid or BAC (Figure 3.1). This PCR fragment was electroporated into the SW105 containing the plasmid or BAC. The correct recombinants were obtained by selection of the antibiotic marker gene on the linear amplified DNA cassette (Figure 3.1).
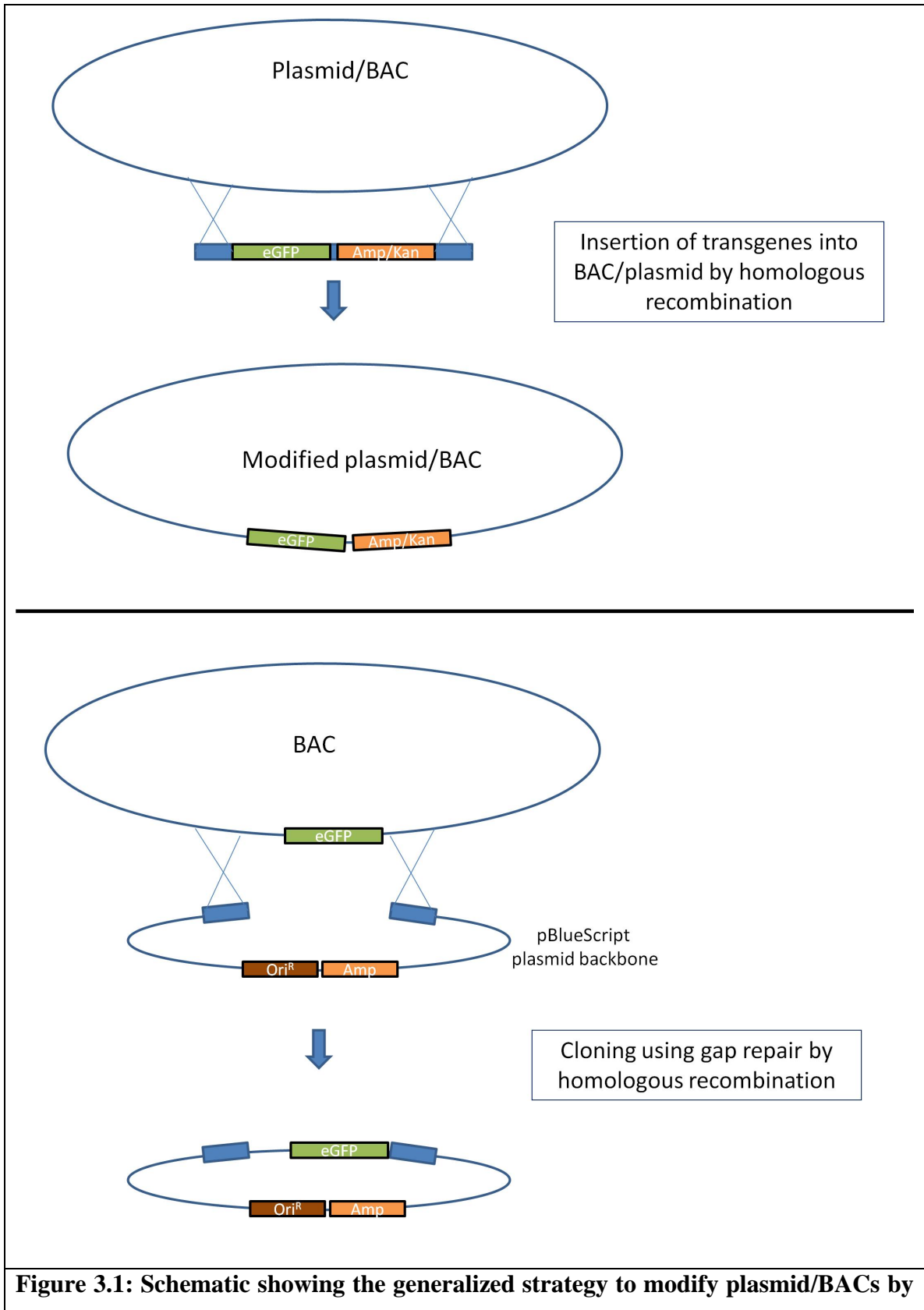
Figure 3.1: Schematic showing the generalized strategy to modify plasmid/BACs by

homologous recombination in bacteria.

Top panel – Shows the design of targeting construct for insertion of reporter genes into BACs and Plasmids. Bottom panel – Shows design of targeting construct to clone fragments from a BAC into a plasmid by gap repair by homologous recombination in bacteria.

Targeting **construct** **(pEGFP-FRT-amp-FRT,** **pECFP-FRT-amp-FRT,**
pmCherry-FRT-amp-FRT) for inserting reporter genes into BACs by homologous
recombination in bacteria

The above mentioned constructs combine the reporter gene and an ampicillin resistance
gene flanked by FRT sites (Figure 3.2). Ampicillin resistance open reading frame was
amplified from pBlueScript and an EM7 promoter added to the 5' end embedded in the 5'
oligonucleotide. This PCR product was further amplified using oligonucleotides
containing homology arms for insertion into pEGFP-N1 plasmid (Kanamycin resistance
only, Clonetech) using homologous recombination in SW105 bacteria (Lee et al., 2001).
The ampicillin resistance gene was inserted at the 3' end of the poly-adenylation signal
for eGFP (Figure 3.2). The exact same strategy was used to make pECFP-FRT-amp-FRT
targeting cassette (Figure 3.2). For generating the same cassette with mCherry, the
pEGFP-FRT-amp-FRT plasmid was amplified such that the backbone was amplified
including the polyA and FRT-amp-FRT, excluding the eGFP sequence. Unique
restriction sites were added at the 5' ends of the oligonucleotides. The coding sequence of
mCherry was PCR amplified and cloned into the same sites of the amplified plasmid
backbone.
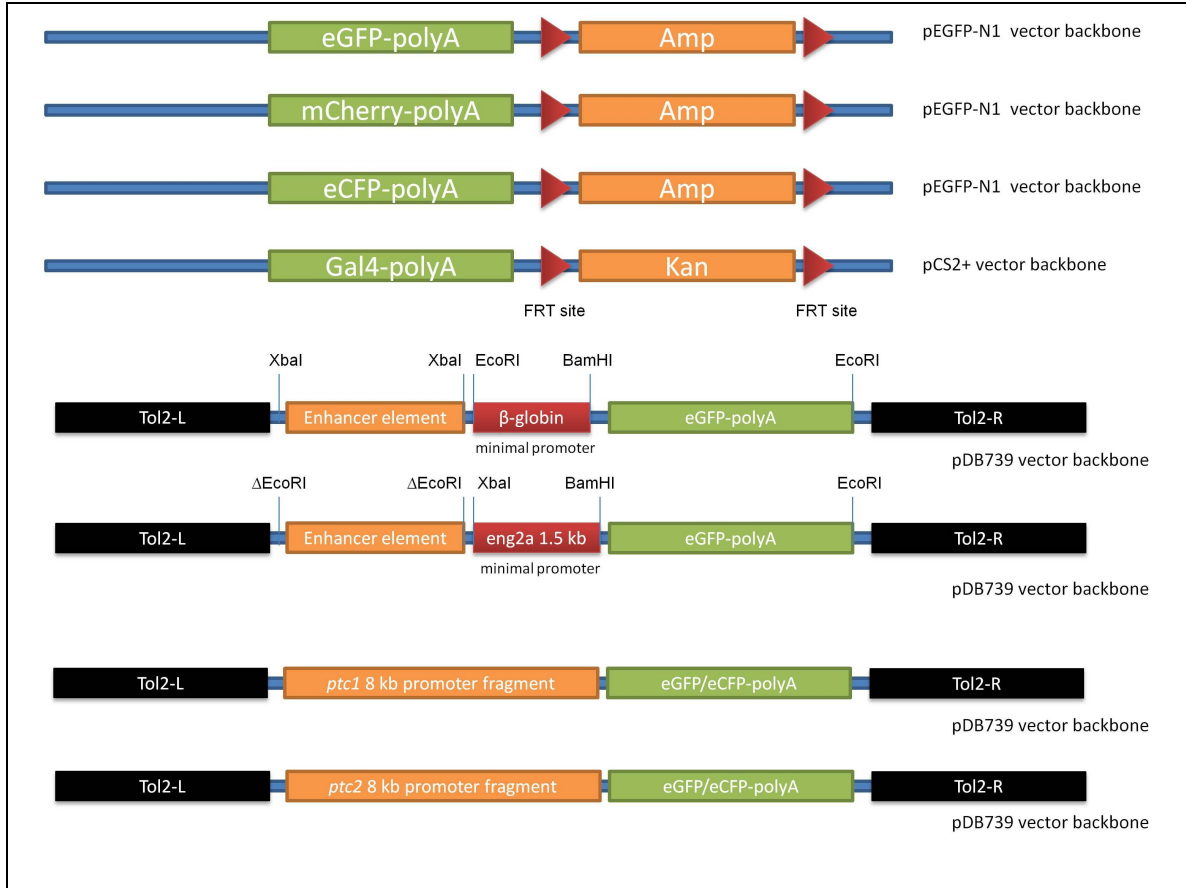
Figure 3.2: **Schematic showing the targeting cassettes used for homologous recombination (top half) and Tol2 based constructs used to assay regulatory potential of putative enhancer fragments (bottom half).**

BAC and promoter constructs

The eGFP-FRT-amp-FRT cassette was amplified using oligonucleotides containing homology arms to the *eng2a* gene locus. The homology arms were designed to insert eGFP in frame after the first codon of *eng2a* and no deletion of the BAC would be predicted to occur. The ampicillin resistance gene was excised by culturing the BAC in 0.1% arabinose for an hour and isolating clones negative for ampicillin resistance (Lee et al., 2001).

The 4, 8 and 12 kilo base pairs (kb) promoter constructs were made again by using homologous recombination in bacteria by gap repair (Figure 3.1) (Lee et al., 2001). The origin of replication along with the ampicillin resistance gene was amplified using oligonucleotides with homology arms to the *eng2a* locus. The homology arms were oriented such that the recombination event will result in the promoter and eGFP of the modified BAC being cloned into the pBlueScript backbone. This could then be selected for by screening for ampicillin resistance.

The 10 kb-eGFP construct was made by cutting the 12 kb promoter construct by ScaI and cloning the large fragment into blunt ended EcoRI of miniTol2 vector (Urasaki et al., 2006). An *eng2a*:Gal4-VP16 BAC transgene was construted in a similar way by homologous recombination in bacteria. An 8 kb-*eng2a*:Gal4 construct was generated by cloning the 8 kb promoter fragment along with the Gal4 transgene from the BAC into a pBluescript minimal backbone using homologous recombination by gap repair (Lee et al., 2001). The 8 kb *ptc1* and *ptc2* promoter constructs were generated using a similar strategy as the 4, 8 and 12 kb *eng2a* eGFP constructs (Figure 3.1 and 3.2). Starting from a

BAC the reporter gene along with the promoter was directly cloned into a Tol2 plasmid using homologous recombination.

Shorter Tol2 constructs

βg-eGFP-Tol2: β-globin-eGFP-polyA was excised from βg-Egfp-SP72 (obtained from Marc Ekker's lab) using EcoRI and cloned into the same site of pDB739 (plasmid containing the mini Tol2 arms originally made by Steve Ekker was obtained from V. Korzh). Clones were sequenced and those which had M13F primer binding sites close to the β-globin promoter were kept and named βg-eGFP-Tol2 (Figure 3.2).

1.5 kb *eng2a* promoter constructs: The 1.5 kb promoter fragment was amplified with oligonucleotides for XbaI and BamHI adaptors. The PCR product was digested with XbaI and BamHI and cloned into the same site of βg-eGFP-Tol2, replacing the β-globin minimal promoter (Figure 3.2). Fragments whose activity was to be tested were PCR amplified with EcoRV adaptors, cut using EcoRV and cloned into blunted XbaI site of the 1.5 kb-*eng2a*-promoter construct (Figure 3.2). Orientation of the inserted fragments was determined by sequencing.

UAS bi-cistronic constructs (Figure 3.3)

turboFP635: tRFP was cut using BamHI and AflII (includes the polyA signal) from the pturboFP635-N1 plasmid (Avrogen), its ends blunted and cloned into blunted EcoRI digested UAS-Tol2. The plasmid obtained was called UAS-tRFP.

UAS-MCS: The multiple cloning site along with the polyA signal of pCS2+ was cut using BamHI and NotI, blunted and cloned into the blunt EcoRI site of UAS-Tol2.

UAS-MCS-UAS-tRFP: UAS-tRFP was cut using HindIII and SpeI, blunted and cloned into blunted SpeI site of UAS-MCS (Figure 3.3).
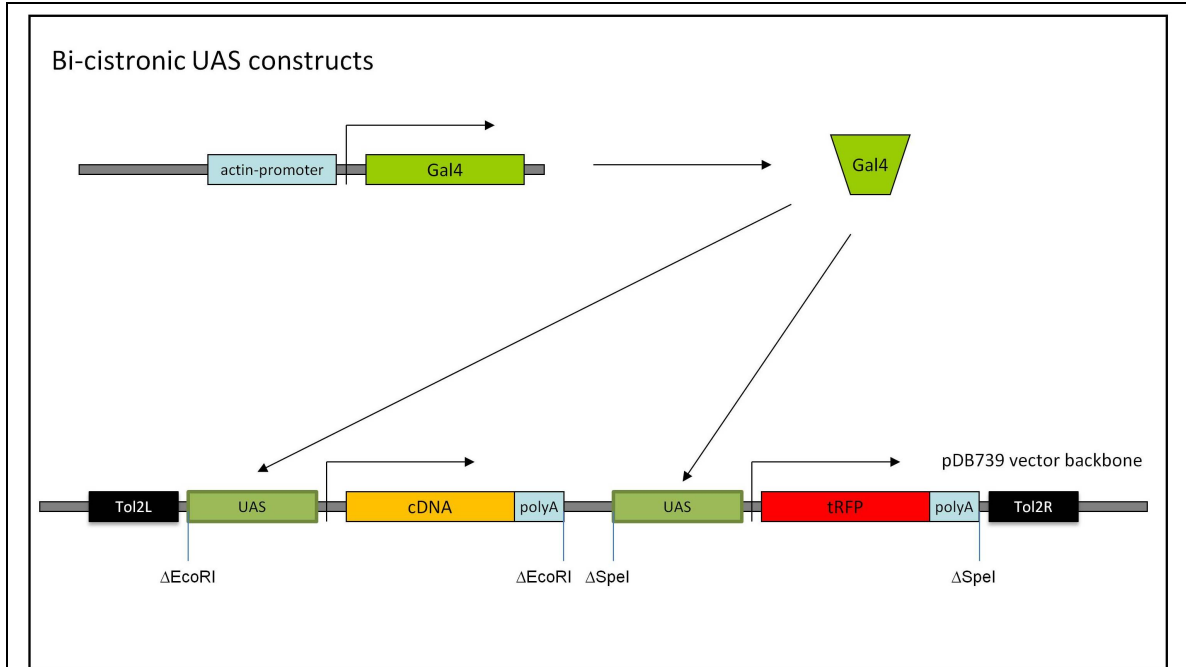
Figure 3.3: Schematic showing the construction and design of a Gal4-UAS based expression system to target expression of cDNAs in myotomal cells. The expression of the transgene can be visualized by expression of tRFP from another UAS promoter on the same transgene.

dorsalin-1: The plasmid pKB502 (Basler et al., 1993) containing a myc tagged *dorsalin-1* cDNA was digested with HindIII and BamHI, blunted and the *dorsalin-1* cDNA was cloned into the blunted NcoI site of UAS-Tol2 vector, producing the UAS-*dorsalin-1* construct. UAS-tRFP was then digested using HindIII and SpeI, blunted and cloned into the blunted NotI site of UAS-*dorsalin-1* to obtain UAS-*dorsalin-1*-UAS-tRFP-Tol2 construct.

caALK3 (constitutively active BMP receptor): The mouse *caAlk3* cDNA (Wieser et al., 1995) was cut using EcoRI and NotI, blunted and cloned into the blunt EcoRI site of UAS-Tol2. The UAS-tRFP was then cut using HindIII and SpeI, blunted and cloned into blunted SpeI site of the UAS-caALK3-Tol2 plasmid.

dnBMPr: The *dnBMPr* (SP64T) cDNA (Suzuki et al., 1994) was cut using HindIII and EcoRI, followed by a strategy similar to that used for *caALK*.

xsmad7: The flag tagged *xenopus-smad7* cDNA was cut using EcoRI and NotI, blunted and cloned into blunt NcoI site of UAS-Tol2. Then UAS-tRFP was cut using HindIII and SpeI, blunted and cloned into blunted NotI site of UAS-*xsmad7*. The cDNA was obtained from Claire Ann Canning (IMB, Singapore) and originally constructed by Birgit Andree (IMB, Singapore).

msmad6: A flag tagged mouse *Smad6* expression clone was obtained from Steve Harvey, originally constructed by (Imamura, 1997).

shh: An expression plasmid containing the full length *shh* (Krauss et al., 1993) was digested with HindIII and XbaI, blunted and cloned into the blunt EcoRI site of UAS-MCS-UAS-tRFP.

dnPKA: The *dnPKA* cDNA (Concordet et al., 1996) was cut using HindIII and XbaI, blunted using T4 Polymerase and cloned into a blunted EcoRI site of UAS-MCS-UAS-tRFP plasmid.

midkine-a – An expression plasmid, pCS2P-*mdka*, was obtained from Christoph Winkler (Schafer et al., 2005). The cDNA was cut using HindIII and NotI, its ends blunted and cloned into the blunt EcoRI site of UAS-Tol2. The UAS:tRFP cassette was cloned into this plasmid as for the UAS:*caALK3* construct.

sfrp2: A plasmid containing the full length zebrafish *sfrp2* was obtained from Corinne Houart (Tendeng and Houart, 2006). The cDNA was cut using EcoRI and cloned into the same site of *UAS-MCS-UAS-tRFP*.

gli1: An expression plasmid, His-*gli1*-pcDNA3.1 (Karlstrom et al., 2003), was obtained from Sudipto Roy. The cDNA was cut using NheI and XbaI, ends blunted and cloned into the blunted EcoRI site of *UAS-MCS-UAS-tRFP*.

mShh-CD4F: An expression plasmid was obtained from Henk Roelink (Incardona et al., 2000). The cDNA was cut using SacII, HindIII, blunted and cloned into the blunt EcoRI site of *UAS-MCS-UAS-tRFP*.

BiFC constructs

The coding sequences for Gli2aR (truncated), Smad1, and Smad5 were individually PCR amplified from cDNA prepared from 22 h embryos with oligonucleotides that contained restriction enzyme sites at their 5' end. The PCR products were purified and digested with the corresponding restriction enzymes, purified again and cloned into the Vn-pCS2+, Vc-pCS2+ (Vn and Vc being half fragments encoding the venus used for the bifluorescence complementation assay) constructs, obtained from Steve Harvey (Harvey and Smith, 2009). The Vn, Vc fusion constructs were blunt cloned into UAS-Tol2 vector at the blunted EcoRI site and using a strategy similar to the bi-cistronic UAS constructs (*caALK3*), the two UAS, Vn, Vc fusion transgenes were cloned into a single plasmid (Figure 3.4).
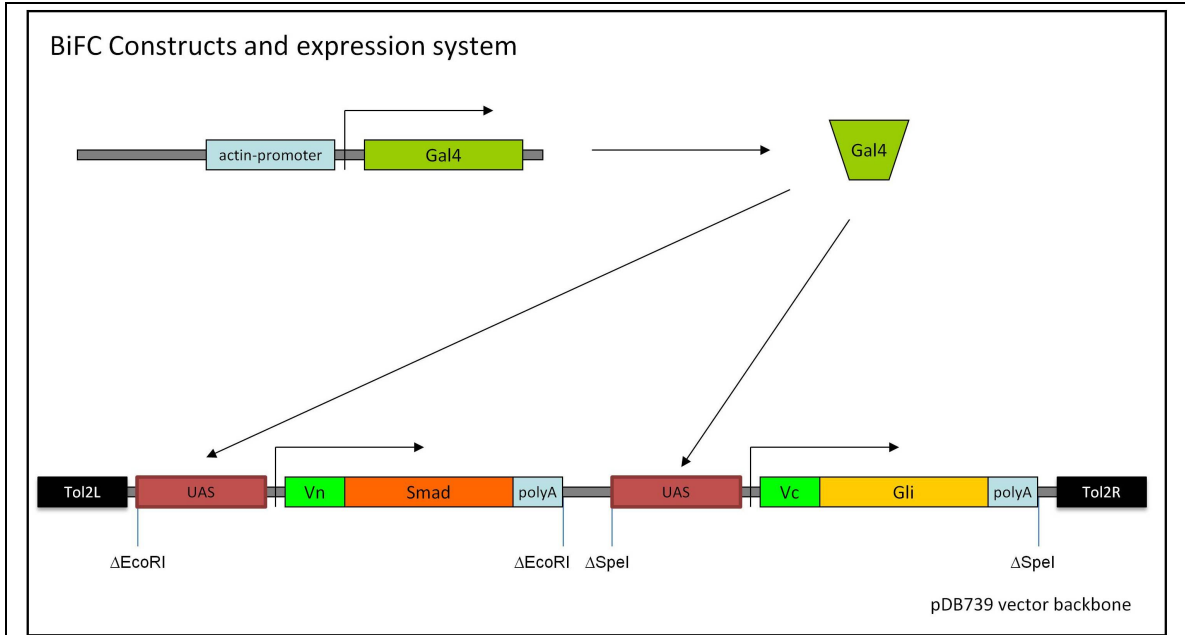
Figure 3.4: Schematic showing the design and expression system used to assay interaction between two proteins using BiFC.

BiFC constructs generated

The placement of Vn, Vc fragments in the following construct names reflects their location on the protein of interest. For example, Vn-Smad1 means that Vn was fused at the N-terminus of Smad1.

Vn-Smad1-pCS2+

Vc-Smad1-pCS2+

UAS:Vn-Smad1

UAS:Vc-Smad1

Gli2aR-Vc-pCS2+

Gli2aR-Vn-pCS2+

Vc-Gli2aR-pCS2+

Vn-Gli2aR-pCS2+

UAS:Gli2aR-Vc

UAS:Gli2aR-Vn

UAS:Vn-Gli2aR

UAS: ΔZnFn-Gli2aR-Vc

Gli2-FL-Vn-pCS2+

Gli2a-FL-Vc-pCS2+

UAS:Gli2-FL-Vn

UAS:Gli2a-FL-Vc

Vn-Gli1-pCS2+

Vc-Gli1-pCS2+

UAS:Vn-Gli1

UAS:Vc-Gli1

Gli3R-Vn-pCS2+

Gli3R-Vc-pCS2+

UAS:Gli3R-Vn

UAS:Gli3R-Vc

Vn-Smad5-pCS2+

Vc-Smad5-pCS2+

Vn-Sufu-pCS2+

Vc-Sufu-pCS2+

UAS:Vn-Sufu

UAS:Vc-Sufu

UAS:Vc-Smad4

Bi-cistronic UAS contructs

UAS:Vn-Gli2aR=UAS:Vc-Smad1

UAS:Gli2aR-Vc=UAS:Vn-Smad1

UAS:Vn-Gli2aR=UAS:Vc-Smad4

UAS:Vn-Smad1=UAS:Vc-Smad4

UAS:Gli2a-Vc=UAS:Vn-Smad1

UAS:Gli2a-Vn=UAS:Vc-Smad1

UAS:Vc-Smad1=UAS:Vn-Gli1

UAS:Vn-Smad1=UAS:Vc-Gli1

UAS:Vn-Smad1=UAS:Vc-Smad4

UAS:Vn-Gli1=UAS:Vc-Sufu

UAS:Gli2aR-Vn=UAS:Vc-Sufu

UAS:Gli2a-Vc=UAS:Vn-Sufu

UAS:Gli2a-Vn=UAS:Vc-Sufu

UAS:Gli2aR-Vc=UAS:Vn-Sufu

UAS:Vn-Smad1=UAS:Vc-Sufu

UAS:Vc-Smad1=UAS:Vn-Sufu

UAS: ΔZnFn-Gli2aR-Vc=UAS:Vn-Smad1

UAS: ΔZnFn-Gli2aR-Vc=UAS:Vn-Sufu

3.9. Transgenic lines

Transgenic lines obtained and maintained in this study were as follows, *Tg(eng2a:eGFP)*, *Tg(HA-ptc1:eGFP)*, *Tg(HA-ptc1:eCFP)*, *Tg(eng2a:mCherry)*, *Tg(eng2a:GAL4)*. Transgenic lines for several UAS expression constructs were generated but almost all of

these got severely silenced in the subsequent generations (*shha*, *dnPKA*, *caALK3*, *mSmad6*, *xsmad7*, *dnBMPr*, *mdka*, *smad1*).

3.10. Trans-regulation Screen

A 2 kb regulatory element (-8 to -6 kb upstream of the *eng2a* start codon) along with a 1.5 kb promoter fragment of *eng2a* was cut using BglII and BamHI from the 12 kb-*eng2a*-eGFP reporter construct (Figure 4.1 A, transgene -8-6 kb), blunted using T4 polymerase and cloned into the EcoRV site of pGL4.10 (Promega, USA). Trans-regulation screening was carried out as previously described (Souren et al., 2009) using a set of 1152 full-length medaka cDNAs selected on the basis of the annotation of the orthologous zebrafish genes. Briefly, BHK21 (Baby Hamster Kidney fibroblasts) cells were co-transfected with three different plasmids (Figure 3.5), (1) - *eng2a*-ME:firefly luciferase, (2) - CMV:medaka cDNA and (3) - CMV:Renilla luciferase. Transfected cells were cultured for two days and assayed for dual luciferase activity. A CMV:renilla luciferase was used as a viability and transfection control. Potential regulators were ranked by their ability to alter the expression of *eng2a*-ME:luciferase normalized against the Renilla luciferase activity. Raw firefly luciferase luminescence values were normalized against an internal Renilla luciferase control and against the average value of each 96-well plate. The cut-off value for repressors was 0.33 and 3-fold activation for activators.
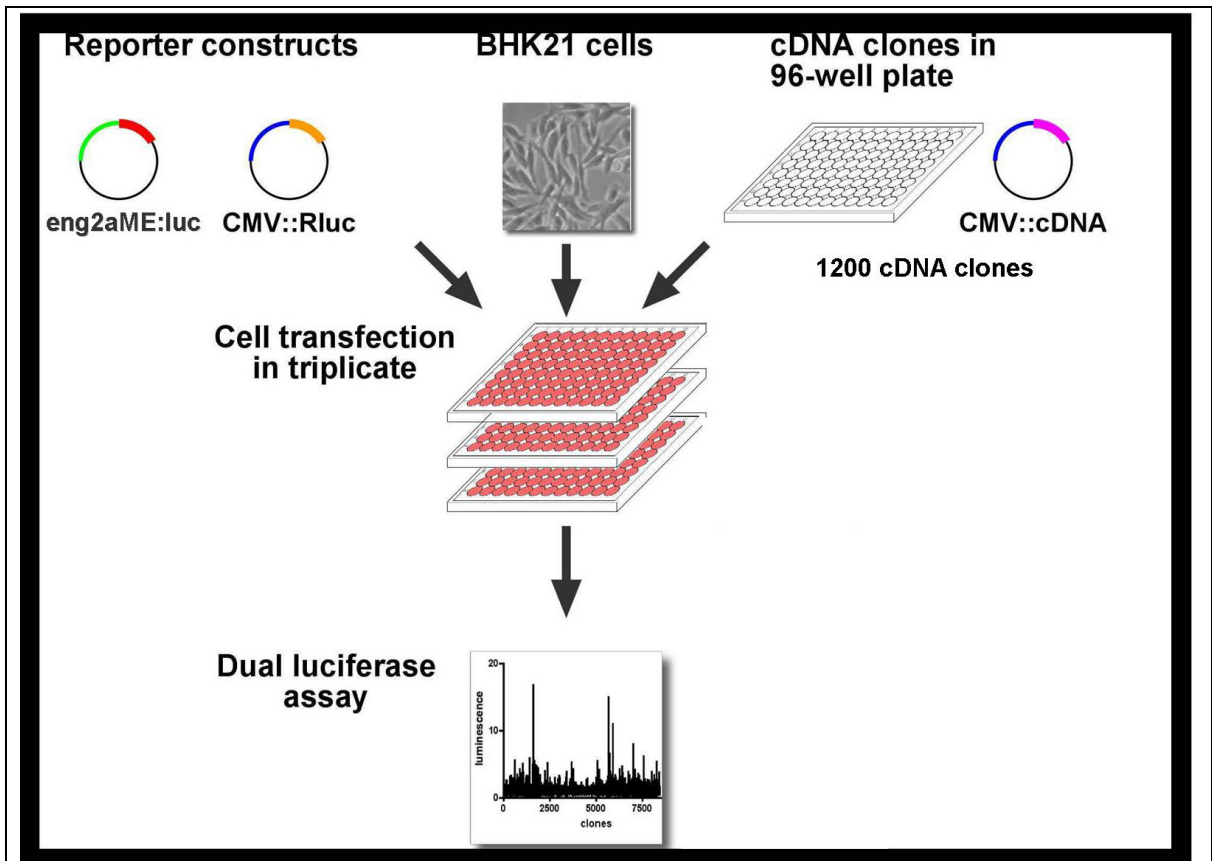
Figure 3.5: Schematic displaying the strategy and methodology of a tissue culture based trans-regulation screening used to identify trans-factors regulating *eng2a* ME activity.

3.11. Image analysis

Specimens were imaged with a 60x oil immersion objective on an Olympus Fluoview confocal microscope. Images were acquired using Olympus FV10-ASW software and analyzed using ImageJ software (http://rsbweb.nih.gov/ij/). Control and experimental specimens were imaged under identical conditions. Unless otherwise stated, images shown represent merged stacks of 8-12 parasagittal optical sections derived from the trunk region closest to the embryonic yolk extension. Selected images were exported and assembled using Microsoft PowerPoint.

Chapter 4: Results - Identification and analysis of *cis*-regulatory elements of *eng*

4.1. Cis-*regulatory analysis of the* eng2a *gene locus*

To identify *cis*-regulatory sequences of the *eng2a* gene, I isolated three BACs (CH211-150E22, DKEY-251D18 and DKEY-182G13) containing the entire *eng2a* gene and several kb of upstream and downstream sequences. The BACs were identified based on the BAC-end sequence reads mapped onto the zebrafish genome sequence (Mar 2006 assembly, danRer4) on the UCSC genome browser and obtained from ImaGenes. The BACs were verified for the correct insert by PCR and sequencing. These BACs were modified using homologous recombination in bacteria (Lee et al., 2001) to insert reporter genes (eGFP, mCherry or Gal4-VP16) in-frame into the *eng2a* gene after the first codon (Figure 3.1 and 3.2). Embryos injected with the modified BACs closely recapitulated endogenous pattern of *eng2a* expression in the MHB, MPs and MFFs (data not shown). I next wanted to narrow down this regulatory activity to shorter regions within the BAC. Therefore, I made several reporter constructs containing differing lengths of the *eng2a* promoter (1.5, 4, 8, 10 and 12 kb upstream of *eng2a* ATG driving eGFP, all of which are derived from the CH211-150E22 BAC) and tested their activities in transgenic zebrafish embryos (Figure 4.1).
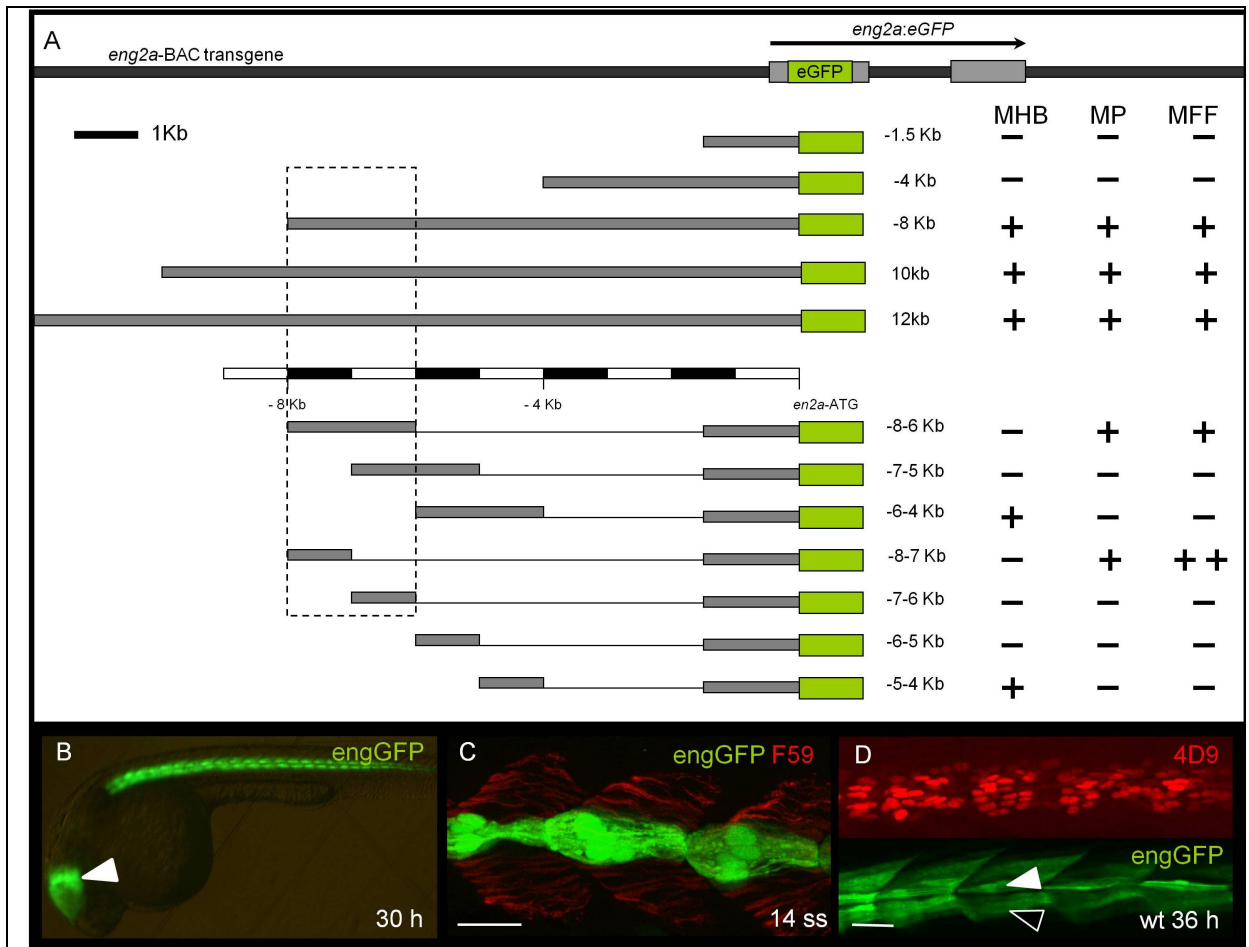
Figure 4.1: *Cis*-**regulatory analysis of the zebrafish *eng2a* gene, promoter deletion constructs and their activity.**

A – *eng2a* BAC transgene, derived promoter deletion constructs and summary of their activity in stable transgenic embryos (MHB - mid-hindbrain boundary, MP - muscle pioneers, MFF - medial fast fibers).

B – A 30 h *Tg(eng2a:eGFP)[i233]*, transgenic for the 10 kb promoter construct, displaying eGFP expression in the MHB (arrow) and the myotome.

C – A 14 ss *Tg(eng2a:eGFP)[i233]* embryo marked for mAb F59, marking slow-twitch muscle fibers and eGFP marking a subset of these slow fibers, the MPs.

D – A 36 h *Tg(eng2a:eGFP)[i233]* embryo stained with mAb 4D9, marking endogenous Eng in MP, MFF nuclei. Cells marked by eGFP and 4D9 overlap precisely. White arrow points to MP and black arrow is showing a MFF. Scale bars are 25 microns.

The 1.5 and 4 kb fragments displayed no detectable activity in embryos, whereas the 8, 10, and 12 kb fragments drove robust expression within all the three major domains of expression (MHB, MPs and MFFs; Figure 4.1). I generated several transgenic zebrafish lines with all but one of these constructs (1.5 kb - 5, 8 kb - 4, 10 kb - 5, 12 kb - 2 lines). The transgenic lines bearing these constructs established that *cis*-elements driving *eng2a* gene expression in the MHB, MP and MFFs must lie in the 4 kb region from -8 to -4 kb upstream of the *eng2a* start codon.

I have also made the 4, 8, 10 and 12 kb promoter constructs with mCherry as the reporter gene and another 8 kb promoter construct driving GAL4-VP16 (GAL4) trans-activator. I obtained several lines with the 10 kb promoter fragment driving mCherry, the line with strongest expression was selected and maintained. In this line mCherry marks the MHB, MPs and MFFs. The GAL4-UAS system is adapted from yeast, where the Gal4 trans-activator protein binds to UAS sequences in the genome and transcribes downstream sequences. This system has been extensively used by fly geneticists to express cDNAs ectopically (Fischer et al., 1988), including reporter genes and has successfully been used in zebrafish embryos (Scheer and Campos-Ortega, 1999). I have generated a stable transgenic zebrafish line with this construct that when combined with a *UAS:kaede* transgenic line (Hatta et al., 2006) clearly marks a subset of Eng^{+} cells. For unknown reasons this line displays mosaic expression and this mosaicism varies between different individuals, although the level of Kaede expression is fairly high in the positive cells. I intended to study the role of MP, MFF cells during embryonic and larval stages. One

approach would be to ablate these cell types using the *UAS:nfsB-mCherry* transgenic line (Pisharath, 2007; Pisharath and Parsons, 2009) under the control of *eng2a:GAL4*. The Nitroreductase (nfsB) enzyme from *E.coli* converts pro-drugs like metronidazole (met) cytotoxic. Therefore by controlling the availability of met one can control the cytotoxicity of the transgene temporally. I discontinued working on this largely due to the mosaic nature of the transgenic expression from the GAL4 line, which would result in ablation of only a subset of Eng$^+$ fibers, confounding interpretations. Nonetheless this line can be used to ectopically mis-express cDNAs within Eng$^+$ cells in a mosaic manner.

4.2. Identifying minimal enhancer elements of the eng2a gene

To map this enhancer activity more precisely within the -8 to -4 kb region, I made a number of constructs carrying fragments of varying lengths from the -8 to -4 kb region upstream of the *eng2a* 1.5 kb "minimal" promoter driving eGFP (Figure 4.1). This 1.5 kb promoter fragment by itself displays little or no activity in transgenic embryos. I found inferring enhancer activity by transient transgenic expression to be misleading. Several constructs drove expression in and around the medial regions of the somite in transient transgenics, but when I obtained stable transgenics many of these constructs failed to show activity in the MP, MFFs. Therefore regulatory activity of all fragments reported here is based on stable transgenic lines, with more than 4 distinct lines displaying common patterns of expression (Figure 4.1).

As a first set of dissection of the region, I divided it into three overlapping 2 kb fragments: -8-6, -7-5 and -6-4 kb (Figure 4.1). Transgenic lines show that the MP, MFF

activity resides in the -8-6 kb fragment and the MHB activity is displayed by the -6-4 kb fragment. The -8-6 kb fragment displays activity that is qualitatively similar to that of the larger promoter constructs (8, 10 and 12 kb promoter constructs) within the myotome (Figure 4.1 A, D and 4.2 B). I also divided the 4 kb region into non-overlapping 1 kb fragments and tested their activity in transgenic embryos. The MP, MFF activity was retained in the -8-7 kb fragment, but this fragment displayed much higher levels of activity in the MFFs comparatively and the activity extended further to non Eng$^+$ fast fibers. The -5-4 kb fragment displayed activity specific to the MHB region.

A

2 kb muscle enhancer (ME)

Construct	MHB	MP	MFF
-8-7.7 kb	−	−	−
-7.8-7.6 kb	−	−	−
-7.6-7.4 kb	−	−	−
-7.4-7.2 kb	−	+	+ +
-7.2-7 kb	−	−	−
-7.8-6.9 kb	−	+	+ +
-7.8-6.45 kb	−	+	+
-7.6-6.9 kb	−	+	+ +
-7.6-6.45 kb	−	+	+
-7.4-6.9 kb	−	+	+ +
-7.4-6.45 kb	−	+	+
-7.2-6.9 kb	−	−	−
-7.2-6.45 kb	−	−	−
-7.4-6 kb	−	+	+
-7.2-6 kb	−	+	−
-5.3-4.5 kb (UCNE)	+	−	−

Minimal MP, MFF enhancer

B ME-eGFP 24 h

C UCNE-eGFP 24 h

Figure 4.2: Fine mapping of the minimal enhancer elements of the *eng2a* gene

A – Shown are transgenes generated to map the minimal enhancer elements, their activity in transgenic embryos is summarized. The dotted box marks the *eng2a* muscle enhancer.

57

B – A 24 h transgenic embryo displaying the activity of the *eng2a* ME (marked by dotted box in A). No MHB specific expression is seen with this construct.

C- A 24 h transgenic embryo displaying the activity of UCNE (upstream conserved non-coding element) in the MHB region. No muscle specific expression is seen with this construct.

To map the muscle specific, de-repressed activity of the -8-7 kb fragment, I divided it into 5 fragments of about 200-250 bp size, with about 25 bp overlap between adjacent fragments. Transgenic lines made from these constructs showed that the muscle activity mapped to a 230 bp fragment (stretching from -7436 to -7205 bp upstream of the *eng2a* ATG). Transgenic lines made with the 230 bp construct showed eGFP expression in the MPs and de-repressed expression in the MFFs, closely matching the activity of the entire -8-7 kb fragment (Figure 4.2). The endogenous *eng2a* gene is expressed more strongly in the MPs than MFFs. This ectopic activity also seen with the -8-7 kb construct suggests that these fragments may be missing silencer elements or repressor sites that are present in the larger -8-6 kb region (also see Figure 8.10).

I next wanted to identify shorter fragments that would mimic the activity of the -8-6 kb fragment. Any sequences within the first kb (-8-7) displayed de-repressed activity and the second kb (-7-6) did not show any activity by itself. This suggested that the complete element must exist on the boundary between the first and the second kb of the -8-6 kb region. I next made several constructs that contained varying lengths within the -8-6 kb region (Figure 4.2) all flanking the -7 kb boundary region and tested them in stable transgenic embryos. Constructs that include the 230 bp de-repressed muscle enhancer and about 100 bp into the 7-6 region displayed activity similar to that of the 230 bp enhancer (Figure 4.2). Constructs that carry 350 bp from the -7-6 region recapitulate endogenous *eng2a* like activity, which is restricted to MPs and MFFs (Figure 4.2). Therefore the silencer element must lie within the 250 bp from -6.9 to -6.65 kb upstream of the *eng2a*

start codon. Another fragment stretching from -7229 to -6020 bp and lacking the 230 bp (de-repressed minimal element) displays weak activity specifically within the MPs.

In summary, the *eng2a* muscle enhancer has at least two components to its architecture, (1) - a smaller enhancer element that has Hh induced activating ability but is missing some repressor elements and, (2) - a distinct adjacent fragment that contains repressive elements but also retains some Hh induced activating ability that can target expression just to the MPs. I note that the location of these elements is distinct from that of the previously identified mandibular muscle enhancer adjacent to the MHB enhancer of the mouse *En2* gene (Degenhardt et al., 2002; Logan et al., 1993) and the analogous axial muscle enhancer identified upstream of the Amphioxus *en* gene (Beaster-Jones et al., 2007). From now on, for consistency, the fragment stretching from -8 to -6 kb upstream of the *eng2a* gene will be referred to as the *eng2a* "muscle enhancer" (ME), as it recapitulates the endogenous expression of *eng* in the muscle.

4.3. Analysis of conserved elements around the eng2a *gene*

In addition to the analysis of the promoter region of *eng2a*, I tested the regulatory potential of conserved non-coding elements (CNE) around the *eng2a* gene. The elements chosen were more than 50 bp and had more than 50% nucleotide similarity between the zebrafish, mouse and human genomes. I found one such stretch of sequence upstream, one in the intron and three downstream of the *eng2a* gene (1285 bp stretch – 6773 bp downstream; 2000 bp stretch – 14190 bp downstream and 732 bp stretch – 29595 bp downstream of the *eng2a* start codon). To test the regulatory potential of these conserved

elements they were coupled to minimal promoters (β-globin and/or 1.5 kb endogenous *eng2a* promoter fragment) and tested in stable transgenic zebrafish embryos (Figure 3.2). The upstream CNE displayed MHB specific activity starting during segmentation stages (section 4.2, Figure 4.2 C). The most proximal downstream CNE also displayed strong MHB specific activity. The other two downstream CNEs and the intronic CNE displayed no specific pattern of activity within transgenic embryos. The intronic and the most proximal CNE did display activity specific to MPs in transient transgenic embryos, but not in transgenic embryos (data not shown).

4.4. eng2a *transgenics and their response to Hh signaling*

I next characterized the *Tg(eng2a:eGFP)^{i233}* transgenic line (made from the 10 kb promoter construct, Figure 4.1) in response to perturbations in Hh signaling. This line was chosen for this analysis mainly because of its high level of reporter gene expression (Figure 4.1). I activated the pathway by microinjection of mRNA encoding either the Shh protein or a dominant negative form of the regulatory sub-unit of PKA (Currie and Ingham, 1996; Hammerschmidt et al., 1996). Injection of Shh or dnPKA RNA at one cell stage into *Tg(eng2a:eGFP)^{i233}* embryos led to a large increase in the number of eGFP positive MPs, whereas, exposure to 30 µM cyclopamine resulted in almost complete absence of eGFP expression from the embryonic myotome (Figure 4.3) as previously described for the endogenous Eng protein (Wolff et al., 2003). The effect of cyclopamine on eGFP expression depended upon the timing of exposure. Earlier exposure (0 h until 4 ss) resulted in loss of MP specific expression only (Figure 4.3), whereas later exposure (14 ss onwards) resulted in the loss of MFF specific expression alone (data not shown)

(Wolff et al., 2003). No discernable effect on eGFP expression in the MHB was seen irrespective of the timing of cyclopamine exposure. The eGFP staining of the myotome in these experiments precisely matched the cells whose nuclei were marked by the 4D9 antibody (Figure 4.3), which recognizes the products of all four *eng* genes in zebrafish (Ekker et al., 1992; Hatta et al., 1991; Patel et al., 1989).
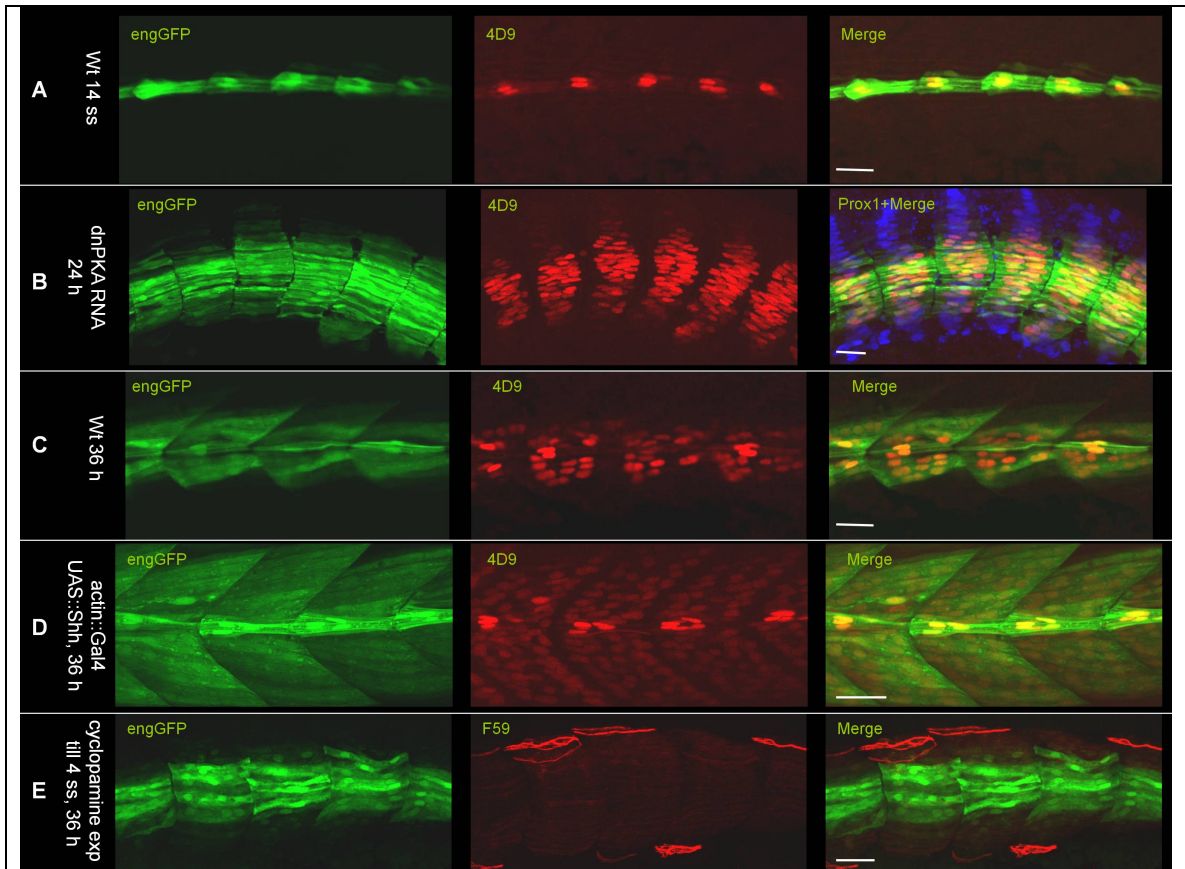
Figure 4.3: *eng2a cis*-**regulatory elements faithfully recapitulate the response of Eng to perturbations in the Hh pathway activity**

A – Parasagittal optical sections of a 14 ss *Tg(eng2a:eGFP)^{i233}* embryo showing eGFP marking MP.

B – Parasagittal optical sections of a 24 h *Tg(eng2a:eGFP)^{i233}* embryo injected with dnPKA RNA to up-regulate Hh signaling, showing a large increase in the number of MP, marked by eGFP and 4D9. Prox1 antibody marks all slow fibers.

C – Parasagittal optical sections of a 36 h *Tg(eng2a:eGFP)^{i233}* embryo showing eGFP expression in mono-nucleate MPs and multi-nucleate MFFs, eGFP precisely marks the cells labeled by 4D9.

D – Parasagittal optical sections of a 36 h *Tg(eng2a:eGFP)^{i233}, Tg(actin:GAL4)* embryo injected with *UAS:Shh* displaying an expansion of MFF, evident from the expansion of 4D9, eGFP expressing multinucleate fibers.

E – Parasagittal optical sections of a 36 h *Tg(eng2a:eGFP)^{i233}* embryo exposed to 30 µM

cyclopamine until 4 ss, displaying a loss of MP, evident from the loss of eGFP expressing cells in the slow compartment marked by F59. Expression of eGFP in MFFs is preserved. Scale bars are 25 microns.

These experiments show that the *eng2a:eGFP* transgene faithfully recapitulates the response of the endogenous gene to Hh pathway activity and its perturbations (Currie and Ingham, 1996; Wolff et al., 2003). I next induced ectopic transient expression of Shh in the myotome using the Gal4-UAS binary mis-expression system, *actin:Gal4* (Scheer and Campos-Ortega, 1999) driving *UAS:Shh-UAS:tRFP*. The *actin:Gal4* driver marks the progenitor cells of all skeletal muscles in the embryo. Expression of the *UAS:Shh* within a few cells of the myotome resulted in conversion of almost the entire fast fiber population into *eng* positive MFFs, a phenotype resembling that of *dzip1* mutants (see section 8.1). Therefore, Shh controls *eng* transcription in both slow and fast muscle lineages (Wolff et al., 2003) and by controlling the timing of *shh* over-expression we were able to either expand the MP (by *shh* RNA injections) or the MFF (*UAS:Shh, actin:Gal4*) populations at the expense of other fiber types.

I also crossed the *Tg(eng2a:eGFP)^{i136}* line into several mutants with disruptions in the Hh signaling pathway, including *dispatched1(disp1), dzip1, ptc1-ptc2* double mutants, and *smo*. The transgene faithfully recapitulated the myotomal expression of *eng* genes in these mutants and in wildtype embryos (data not shown; Chen et al., 2001; Nakano et al., 2004; Varga et al., 2001; Wolff et al., 2003; Wolff et al., 2004). Therefore, from here onwards I have used either 4d9 or eGFP staining from *Tg(eng2a:eGFP)^{i136}* interchangeably to label MPs and MFFs.

Chapter 5: Results - Quantification of Hh signaling in live embryos during muscle cell fate specification

5.1. Observing Hh signaling in live zebrafish embryos – Positional bias in adaxial cells?

Our understanding of the specification of cell fates within the zebrafish myotome comes largely from studies dealing with Hh signaling. Although Hh is critically required for their specification, we still do not understand how the same signal specifies some cells to the migratory slow muscle lineage but other cells from the same progenitor pool to the non-migratory MPs. It remains unclear if this difference in specification (MP vs. Slow) is entirely due to differences in the levels of Hh signaling (Aanstad et al., 2009; Wolff et al., 2003) or whether other cues help to delineate the two cell types.

To investigate whether a subset of the adaxial cells receive more Hh signaling than others, I analyzed transcription of Hh target genes *ptc1* and *ptc2* using reporter transgenes in live zebrafish embryos. Transcription of *ptc* genes is directly controlled by Hh signaling in a non-tissue specific manner and therefore serves as readout for the amount of Hh signal a cell is receiving at any particular time (Alexandre et al., 1996; Concordet et al., 1996). The Ptc protein is thought to turn over quickly within vertebrate cells (Rohatgi et al., 2007). A fluorescent protein on the other hand does not undergo such rapid turnover and should remain stable for several hours (Corish and Tyler-Smith, 1999). Therefore such a reporter would reveal the total amount of Hh signaling a cell has received integrated over several hours. Adaxial cells that receive high levels of Hh

signaling would be predicted to become muscle pioneers and fast fibers with high levels of Hh signaling would be predicted to form the MFFs.

For these experiments, I isolated BACs containing the *ptc1* gene and the *ptc2* gene loci (*ptc1*: CH211-226H23; *ptc2*: CH211-74E1, DKEY-262N24). Using homologous recombination in bacteria, I inserted eGFP and eCFP reporter genes in frame after the start codon of *ptc1* and *ptc2*. I then made shorter constructs carrying 8 kb promoter fragment along with the reporter genes from the modified BACs and made several transgenic zebrafish lines with them (Figure 3.1 and 3.2). The 8 kb-ptc1-eGFP and 8 kb-ptc1-eCFP transgenic lines faithfully mimic the endogenous expression pattern of the *ptc1* gene, i.e. ventral neural tube, adaxial cells, developing fin rays, and branchial arches among other regions (Figure 5.1). More than 10 lines were generated for both transgenes (*ptc1:HA-eGFP* and *ptc1:HA-eCFP*); a large number of these transgenics displayed suppressed expression of the reporter gene. For further experiments, I focused on single lines that displayed high levels of reporter gene activity.
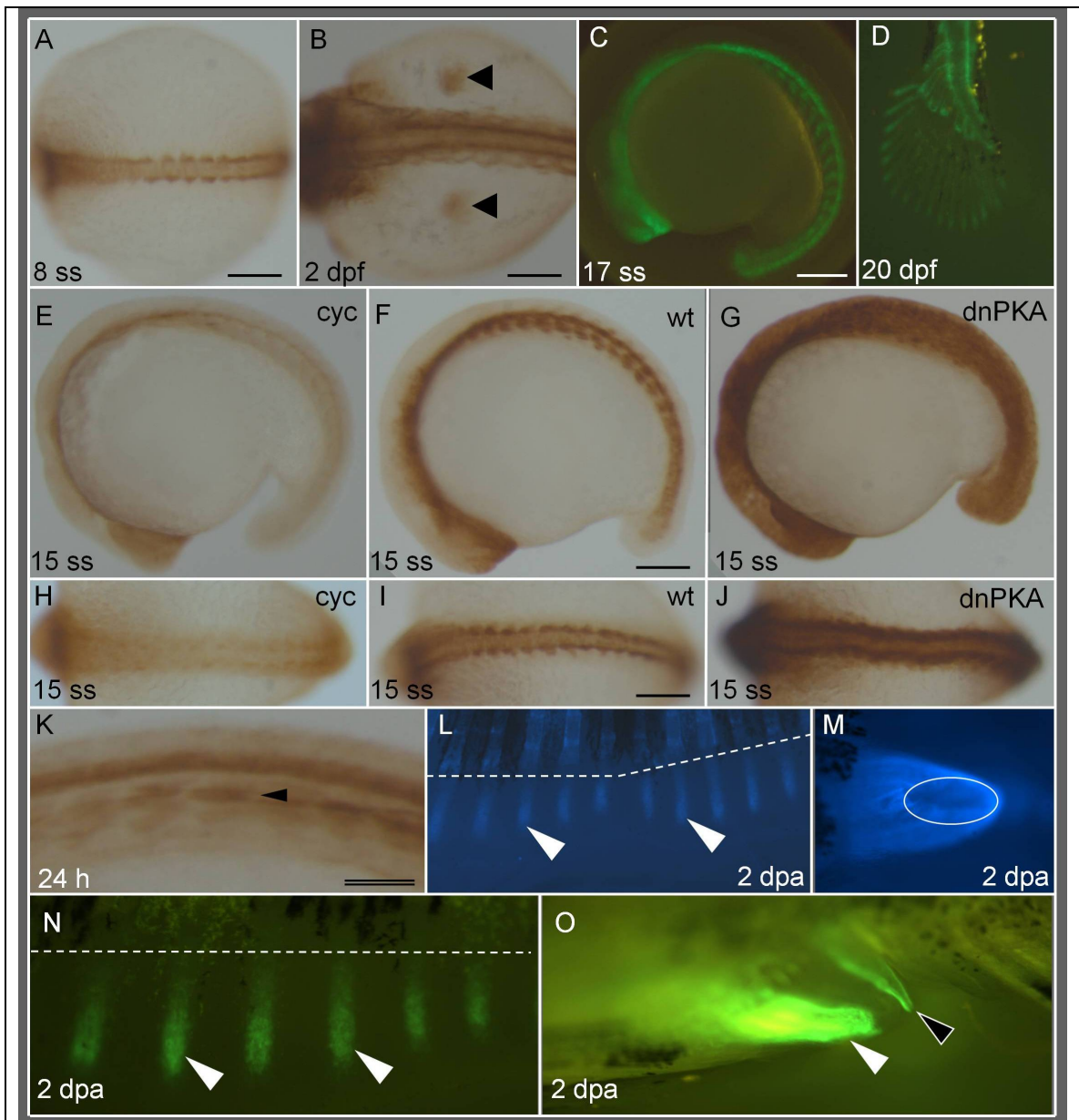
Figure 5.1: *ptc1* **reporter transgenics and their response to variations in Hh activity and during regeneration upon injury**

A – Dorsal view of an 8 ss *Tg(ptc1:HA-eCFP)* embryo marked with an antibody against the HA-tag, displaying reporter expression in adaxial cells and in the neural tube.

B – Dorsal view of a similarly stained 2 d *Tg(ptc1:HA-eCFP)* embryo, showing reporter expression in the midline and in the developing pectoral fins (arrows).

C – Lateral view of a live 17 ss *Tg(ptc1:HA-eGFP)* embryo clearly displaying strong

expression around the midline - adaxial cells, ventral neural tube and in the forebrain.

D – Lateral view of a live 20 d *Tg(ptc1:HA-eGFP)* embryo displaying expression in the growing caudal fin, at the base and at the tips of forming fin rays. Expression also seen in the hypochord and ventral neural tube.

E, H – Lateral and dorsal view of a 15 ss *Tg(ptc1:HA-eCFP)* embryo exposed to 30 μM cyclopamine, marked with HA antibody. Compare the reduction of ptc reporter activity to wt embryos in F, I and in embryos injected with dnPKA RNA at similar stages.

F, I – Similarly stained and staged *Tg(ptc1:HA-eCFP)* wt embryos displaying normal *ptc1* reporter activity.

G, J – Similarly stained and staged *Tg(ptc1:HA-eCFP)* embryos injected with dnPKA RNA to up-regulate Hh pathway activity.

K – Lateral view of a 24 h *Tg(ptc1:HA-eCFP)* embryo stained for HA, showing stronger reporter expression in MPs (arrow) compared to the rest of the fibers.

L – Caudal fin of a live *Tg(ptc1:HA-eCFP)* adult after 2 days post amputation (dpa). The dotted line shows the amputation site and eCFP is seen marking a restricted population of cells in the forming fin rays, marked by white arrows.

M – Ventral view of a similarly regenerating fish, showing eCFP expression in the gut around the anal opening (shown by white ellipse). This gut specific expression was seen only in regenerating animals and marked many regions along the length of the entire gut (data not shown).

N – Caudal fin of a live *Tg(ptc1:HA-eGFP)* adult after 2 days post amputation (dpa). The dotted line shows the amputation site and eGFP is seen marking a restricted population of cells in the forming fin rays (marked by white arrow), similar to the response of the *Tg(ptc1:HA-eCFP)* line.

O – Lateral view of a similarly regenerating fish, showing eGFP expression in the gut around the anal opening (white arrow) and in the urinary tract (black arrow), similar to the response of the *Tg(ptc1:HA-eCFP)* line. Scale bar is 150 microns (single line) and 50 microns (double line)

Constructs with 8 kb promoter fragment of *ptc2* gene driving eGFP or eCFP displayed activity in the skeletal muscles and the nervous system in transient transgenics. Around 150 embryos injected with the 8 kb-ptc2-eCFP construct were raised and tested for transmission of the transgene under a fluorescent dissecting microscope, but none displayed detectable levels of reporter genes in their progeny. I suspect that there were several transgenic lines that were obtained but none that displayed visible reporter gene expression; however, this was not verified by genomic DNA analysis. Therefore, I focused on the transgenics generated for the 8 kb-ptc1-eGFP and eCFP constructs.

5.2. ptc *reporter transgenics recapitulate* ptc *expression pattern and report Hh pathway activity*

I next wanted to assess the sensitivity of the *ptc*-reporters to perturbations in Hh pathway activity. Activation of the Hh pathway by injection of *dnPKA* RNA resulted in widespread activation of the *ptc1* reporters, whereas incubating these embryos in 30 μM cyclopamine significantly reduced transgenic expression (Figure 5.1 E-J). At the onset of *eng* expression in 14 ss embryos, I did not observe significant variation in eGFP levels amongst the adaxial cells (Figure 5.1 C, F, data not shown), although at later stages (24 h) higher levels of reporter gene activity was observed in MP (Figure 5.1 K) and MFFs (data not shown; Wolff et al., 2003), in comparison to the surrounding fibers. These results suggest that Eng$^+$ slow as well as fast fibers do receive higher levels of Hh signals. This does not rule out if high Hh is the cause for these cells becoming Eng$^+$ or do these cells receive more Hh as a consequence of other event.

Apart from the somites, *ptc1* reporter lines displayed transgenic expression in several other developing tissues that are known to respond to Hh signals. Expression marked the ventral neural tube, hypochord, dorsal aorta, developing fins (15 d), branchial arches, amongst other areas. Hh signaling is also critical in patterning regenerating zebrafish fins (Figure 5.1). I investigated whether the reporters are activated in regenerating fins. Two days after amputation of half of the caudal fin in adult zebrafish, both *ptc1* reporter lines displayed similar expression in a restricted population of cells in the regenerate (Figure 5.1 L, N). Surprisingly, I also observed reporter gene expression in the digestive and urinary tract after fin amputation (Figure 5.1 M, O). The internal organ specific expression was not observed in uninjured animals or after 10 days of fin amputation. The internal organ specific expression may be a stress response; although how is it conveyed to this distant location from the regenerate is not clear.

Chapter 6: Results - Screen to identify *trans*-factors controlling *eng2a* ME activity

6.1. Functional conservation despite divergent sequence

Conservation of non-coding sequences between distantly related vertebrate genomes has been shown to be a strong predictor for identifying *cis*-regulatory elements (Aparicio et al., 1995; Bejerano et al., 2006; Nobrega et al., 2003; Woolfe et al., 2005). A large number of these conserved non-coding elements displayed association with genes involved in vertebrate embryonic development (Woolfe et al., 2005). The rationale behind such an approach is that sequences that have remained unchanged between animals that have diverged for about 400 million years (teleosts and mammals) must be under strong positive selection and therefore functional (Aparicio et al., 1995).

The only conserved element within the -8-4 kb region upstream of the *eng2a* ATG between zebrafish and mammals is the MHB enhancer, whereas the ME is not conserved at the sequence level (shown graphically in Figure 6.1). I next investigated whether the regulatory mechanisms controlling *eng2a* expression within the myotome are conserved between an evolutionary distant teleost, medaka (diverged 150 million years ago from zebrafish) (Wittbrodt et al., 2002). For this, I tested the 8 kb *eng2a* promoter construct in medaka embryos for activity in MP/MFF like cells.
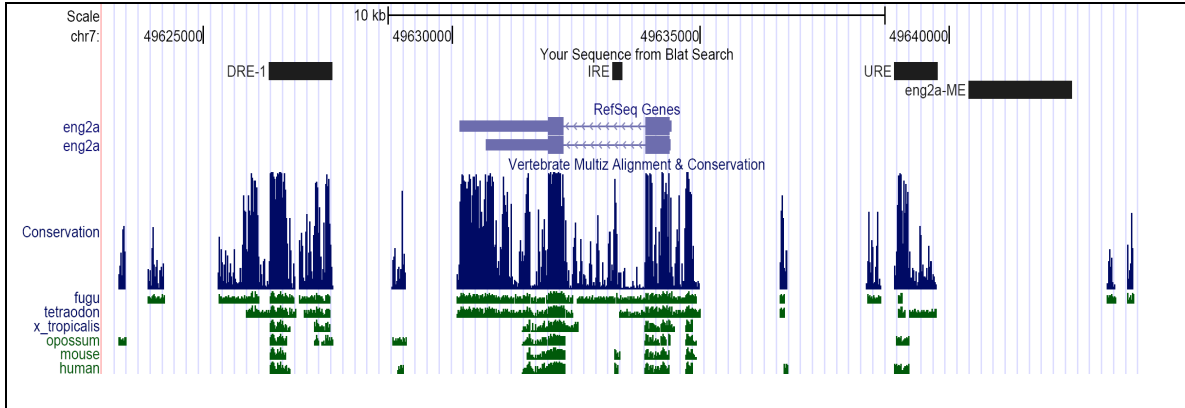
Figure 6.1: Conservation around the zebrafish *eng2a* gene

Schematic showing the zebrafish *eng2a* genomic locus and its conservation across vertebrate species. Black bars show the identified enhancer elements (URE, DRE-1 and *eng2a*-ME), the *eng2a* gene is shown in light blue blocks and runs in the opposite orientation and the level of conservation is shown by dark blue peaks. (Image was extracted from UCSC genome browser, Zv6 March 2006 assembly).

I created two stable transgenic medaka lines with this construct, both of which show expression in a medially located population of muscle cells next to the notochord, the equivalent of MP/MFFs in medaka embryos (Figure 6.2). This strongly suggested that mechanisms controlling regulation of *eng* in the myotome must be conserved in teleosts. The two lines also display strong expression around the mid-hindbrain boundary.
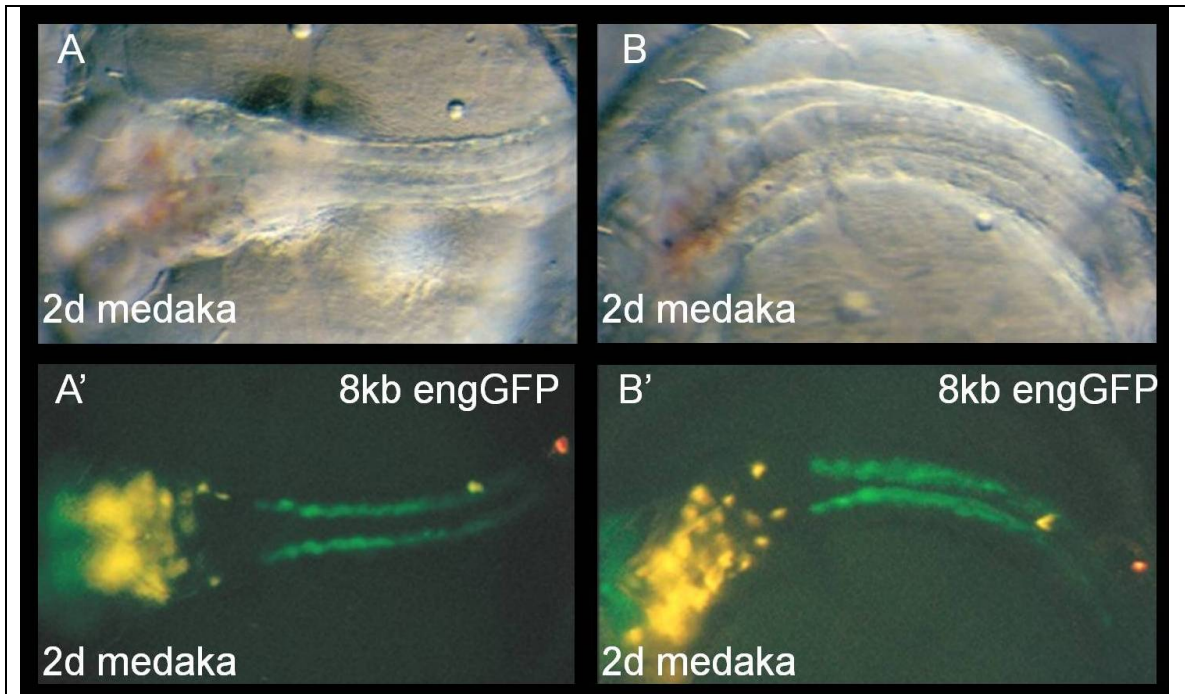
Figure 6.2: Functional conservation of the zebrafish *eng2a* ME in medaka embryos

A,A' – Brightfield and fluorescent images of a dorsally mounted 2 d medaka embryo transgenic for the zebrafish 8 kb *eng2a:eGFP* promoter construct

B,B' – Brightfield and fluorescent images of a laterally mounted 2 d medaka embryo transgenic for the zebrafish 8 kb *eng2a:eGFP* promoter construct

This functional conservation of the muscle enhancer prompted us to investigate whether the *eng2a* muscle enhancer element is conserved between Teleost species. For this, I compared -8-4 kb upstream sequence of *eng2a* to that of the medaka *eng2a* genomic locus at 50% nucleotide identity in a 50 bp sliding window, using the PipMaker program, which uses a BlastZ algorithm (Schwartz et al., 2000). Once again, the only region that displayed conservation was the previously identified UCNE, the mouse and zebrafish equivalents of which have MHB enhancer activity (Logan et al., 1993). The lack of conservation of the ME at the sequence level precluded the identification of critical trans-factor binding sites on the basis of sequence analysis, but shows that despite the re-shuffling of these binding sites their functionality is preserved.

6.2. Trans-activation screen for identifying putative regulators of the eng2a *muscle enhancer*

To identify factors controlling *eng* myotomal expression in an unbiased manner, I decided to exploit a trans-regulation screening methodology that had recently been developed and optimized by Marcel Souren in the laboratory of Joachim Wittbrodt at the European Molecular Biology Laboratory (EMBL), Heidelberg, Germany (Souren et al., 2009). I undertook this screen in the Wittbrodt laboratory with the help and guidance of Marcel Souren. A medaka cDNA library was used for this screen mainly due to the unavailability of a zebrafish full length (full coding sequences) cDNA expression library. The functional conservation of zebrafish *eng2a* muscle enhancer in medaka embryos established that medaka trans-factors can bind to this element.

Around 1200 full length medaka cDNA clones were individually screened for their ability to either suppress or enhance the activity of the *eng* muscle enhancer in BHK21 cells. The cDNA clones were selected from a medaka unigene cDNA library (Souren et al., 2009), and consisted of molecules involved in embryonic development, including secreted ligands, receptors, transducing components and transcription factors. The *eng2a-*ME:luc transgene used in the screen included -8 to -6 kb region upstream of *eng2a* coupled to a 1.5 kb *eng2a* "minimal promoter" driving luciferase.

The clones with highest regulatory potential, based on relative luciferase activity, were manually checked against the ZFIN database for availability of expression patterns. Molecules or their paralogs that displayed no expression in the zebrafish somites or clearly had nothing to do with gene expression were excluded from the list (like α-actin and other structural components of skeletal muscles). For genes that did not have expression patterns available, I checked for their expression and known roles in other organisms. Amongst the identified genes several displayed patterns that were *eng*-like in the somites, *sfrp2* and *mpp7* (*mpp3* was identified in the screen) are specifically expressed in cells resembling MP/MFFs and several others that were expressed in the myotome (Figure 6.3).
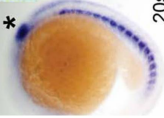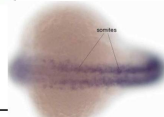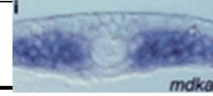
++	Mpp7	Membrane anchored kinase	Mutant: kinked vertebral column	
	Sfrp2	Secreted frizzled-related protein-2	Wnt antagonists	
	Prrx1b	Paired related homeobox 1b	Mouse mutants: loss or malformation of craniofacial, limb, and vertebral skeletal structures	Expressed in muscles in mammals
--	Smad5	MAD homolog 5 (Drosophila)	TGF-beta dependent transcription factors, ventralizing activity in vertebrate embryos	Ubiquitous
	Smyd2b	SET and MYND domain containing 2b	Trancription factors that can modify chromatin	
	Gadd45b	Growth arrest and DNA-damage-inducible, beta	Involved in somitogenesis, knockdown reduces MyoD expression in paraxial mesoderm	
	Wnt9b	Drosophila Wingless ortholog-9b, secreted ligand	In mammals, involved in development of pronephros	Not available
	Midkine-a	Secreted ligand	Involved in floor plate development	

Figure 6.3: Identified regulators of the *eng2a* ME in the tissue culture based trans-regulatory screening.

Shown are identified regulators and their expression pattern in zebrafish embryos, wherever available. Sfrp2 (Tendeng and Houart, 2006), Mpp7 (Konig et al., 1999), Smad5 (Patterson et al., 2010), Smyd2b (Sun et al., 2008), Gadd45b (Kawahara et al., 2005) and Midkine-a (Winkler et al., 2003). + + marks positive and − − marks negative regulators

One of the strongest negative regulators was *smad5*, a transcription factor that mediates BMP signaling (Graff et al., 1996; Liu, 1996; Suzuki et al., 1997; Thomsen, 1996). I chose to focus on this candidate (see Chapter 7), as it had previously been shown that ectopic expression of the secreted BMP like molecule *dorsalin-1* in the notochord of zebrafish embryos, can suppress MP differentiation without affecting slow muscle specification (Du et al., 1997). Interestingly, BMP signaling has also been implicated in negative regulation of *Engrailed* in the chick dermomyotome (Cheng et al., 2004) suggesting the mechanistic basis may be conserved between teleosts and amniotes.

Chapter 7: Results - BMP signaling inhibits Hh induced MP/MFF fate specification

7.1. Role of BMP-Smad signaling in cell fate specification in the zebrafish myotome

Smad1/5/8 as negative regulators of *eng* gene expression and of MP, MFF fate

Smad5 and the closely related *smad1* and *smad8* genes are all expressed within the zebrafish somite at the onset of *eng* expression (starting 14 ss) (Patterson et al., 2010; Thisse et al., 2004). They function similarly in mediating transcriptional effects of BMP ligands (BMP2, 4, 7, Gdf1, 3, 5, 6, 7, 10, Vg1, Dorsalin-1 among others (Satoshi and Yuji, 2005)). *Smad5* is expressed ubiquitously with elevated levels in the somites (data not shown; Patterson et al., 2010; Thisse et al., 2004). *Smad1* transcripts can be localized in the adaxial cells at the onset of somite formation and slightly later in more lateral regions of the somite, i.e. the fast fiber compartment (Dick et al., 1999). *Smad1* is ectopically expressed throughout the somites and paraxial mesoderm in response to ectopic Hh activity in the somites (Dick et al., 1999). *Smad8* transcripts accumulate in more restricted domains within the somites at these stages (Thisse et al., 2004).

7.2. Activated Smads accumulate within nuclei of Eng negative myoblasts

The BMP signal transduction starts with reception of BMP ligands by heteromeric complex of typeI and II BMP receptors. This leads to auto-phosphorylation and receptor

complex activation, which promotes recruitment of Smads (1, 5, 8) and phosphorylation of their C-terminal tails. Smads then partner with Smad4 (a common co-factor for TGF-β and for BMP specific regulatory Smads), resulting in their nuclear translocation and modulation of gene expression (Hoodless, 1996; Kretzschmar et al., 1997). Therefore, as readout for BMP signaling activity, I next analyzed the distribution of phosphorylated Smads in the zebrafish myotome.

To address the *in vivo* significance of Smad5-mediated repression of the *eng2a* muscle enhancer, I used an anti C-terminal phospho-Smad-1/5/8 antibody (pSmad, Cell Signaling) to analyze the distribution of its activated and dually phosphorylated form in the zebrafish myotome. At the onset of slow muscle specification and prior to the onset of Eng expression, high levels of pSmad accumulate in the most dorsal and ventral regions of the slow fiber compartment, marked by F59 (Figure 7.1 A-A'').

Slightly later at the time of slow muscle elongation and stacking (Devoto et al., 1996), I found that pSmad accumulates in dorso-ventrally expanding pre-migratory slow muscle nuclei but is completely absent from medially located Eng[+] nuclei, the MPs (Figure 7.1 B-B'', C-C''). This is in agreement with the notion that BMP signals acting through Smads are inhibiting *eng* gene expression and the specification of muscle pioneers.
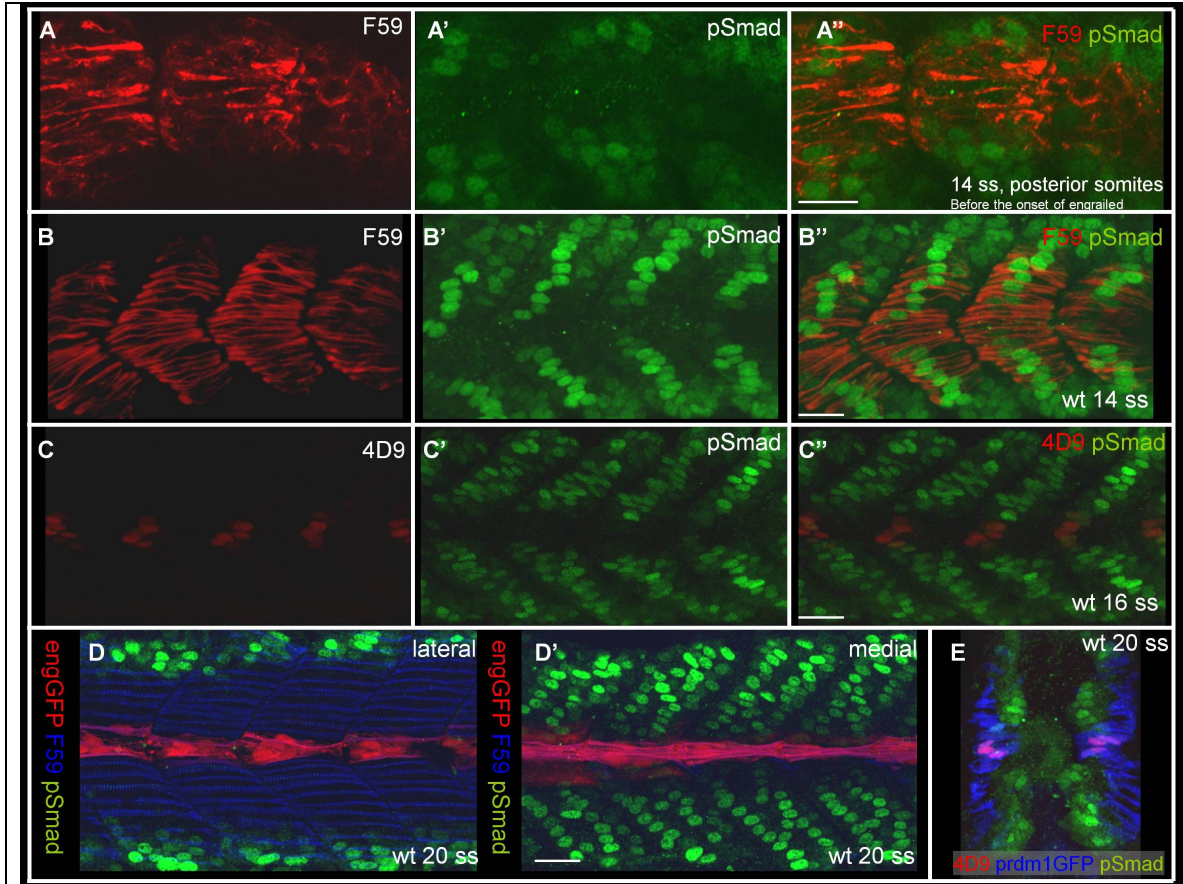
Figure 7.1: Dynamic distribution of activated Smads (phospho-Smad1/5/8) in the zebrafish embryonic myotome

A,A',A'' – Parasagittal optical sections of a 14 ss embryonic myotome showing posterior somites before the onset of Eng, displaying pSmad marking the most dorsal and ventral parts of the adaxial cells (marked by F59).

B,B',B'' – Parasagittal optical sections of a 14 ss embryonic myotome showing anterior somites, at the time when the adaxial cells have stacked, showing pSmad marking all slow fibers except for the ones in the medial locations, the MPs.

C,C',C'' – Parasagittal optical sections of a 16 ss embryonic myotome showing pSmad marks Eng negative nuclei

D,D' – Parasagittal optical sections of a 20 ss embryonic myotome showing pSmad distribution in lateral regions of the somite (D) and in the medial region (D'). At this stage slow fibers marked in blue have migrated laterally and no longer accumulate

pSmad. High levels of pSmad are now seen labeling a subset of fast fibers located medially.

E – Cross section of a 20 ss embryo showing pSmad marking a medially located population of nuclei that are distinct from the slow fibers (marked in blue). Scale bars are 25 microns.

Cross sections of the embryonic trunk reveal that pSmad marks the migratory adaxial cells specifically before the onset of their lateral migration (data not shown), when these adaxial cells are in close proximity to the neural tube on the ventral side and to the hypochord on the ventral side. Slightly later (22 h), when the adaxial cells have completed their lateral migration and formed a superficial layer of slow fibers on the surface of the myotome, they no longer show accumulation of pSmad. Instead, high levels of pSmad are detected again in cells adjacent to the neural tube and along the hypochord (Figure 7.1 D, D' and E). This later pSmad accumulation is largely specific to fast muscle progenitors, which after the lateral migration of adaxial cells are displaced next to the neural tube dorsally and to the hypochord ventrally, possible sources of BMP ligands. High levels of pSmad are also detected in broader domains at the most dorsal and ventral extremes of the somite (Figure 7.1 B-B'', D).

7.3. Ectopic, cell autonomous activation of BMP-Smad signaling potently inhibits MP/MFF fate specification

A previous study by Du et al., 1997 had shown that over-expression of chick *dorsalin-1* from the notochord repressed *eng* activation in the zebrafish myotome. I wanted to test if this was due to stabilization of pSmad, resulting in *eng* repression. To conditionally express *dorsalin-1* in the myotome, I utilized the GAL4-UAS system, driving expression under the control of the *actin:GAL4* driver line (Scheer and Campos-Ortega, 1999). The *actin:GAL4* driver targets expression of UAS transgenes to all myotomal progenitors (Figure 3.3).

Expression of *dorsalin-1* uniformly stabilized pSmad (data not shown) within the myotome and potently suppressed *eng* expression (Figure 7.2 A-A'). This suppression is seen in both the MP and MFF cells. In embryos where *dorsalin-1* was expressed (marked by a bi-cistronic *UAS:turboFP635*, tRFP) later and/or at lower levels, I observed suppression of the MFF fate but not of the MPs (Figure 7.2 B-B''). This shows that pSmad mediated suppression of *eng2a:eGFP* occurs at the time of specification and is not a dominant effect on these cell types.

I next asked whether the accumulation of pSmad is sufficient to block the activation of *eng2a* expression (and MP, MFF differentiation). For this, I used a constitutively active form of the mouse BMP receptor (caALK3) (Wieser et al., 1995) to ectopically activate Smads within the myotome. As BMP signaling underlies the establishment of the early embryonic dorso-ventral axis, I could not use routine loss- and gain-of-function experiments (using available mutants or by injecting MOs or RNA). Therefore, I again employed the GAL4-UAS system to target *caALK3* expression specifically to myotomal progenitor cells using the *actin:GAL4* line. This resulted in a clear increase in pSmad levels in cells that were expressing the transgene, marked by tRFP (Figure 7.2 E').
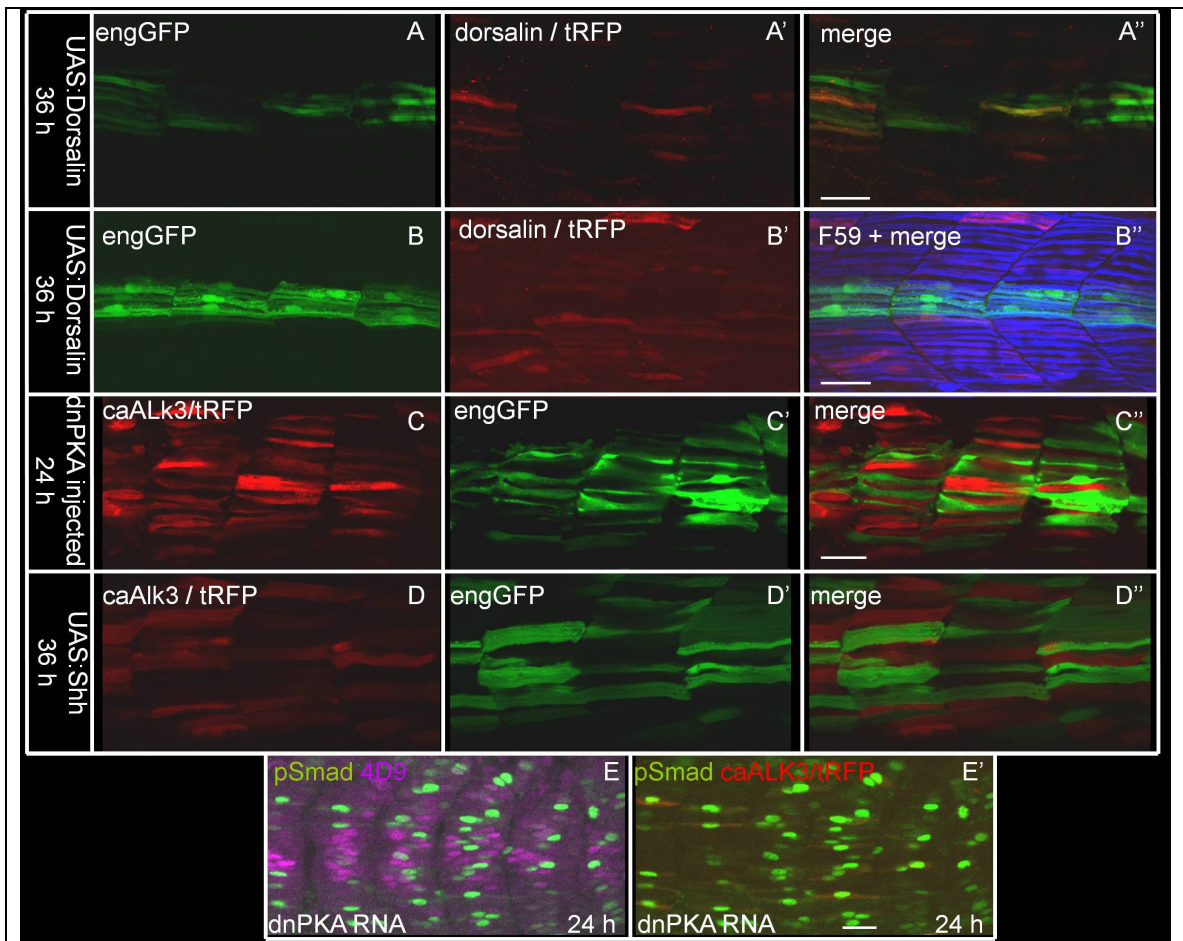
Figure 7.2: BMP signaling activity potently and cell autonomously inhibits Hh induced *eng* transcription and MP, MFF differentiation.

A,A',A'' – Parasagittal optical sections of a 36 h *Tg(eng2a:eGFP)^{i233}, Tg(actin:GAL4)* embryo, injected with *UAS:dorsalin-1*, marked by tRFP, showing loss of eGFP from the myotome.

B,B',B'' – Similarly prepared embryo with specific loss of eGFP from the fast fibers, interpreted to be expressing lower/delayed expression of *dorsalin-1*. MP as marked by mono-nucleate eGFP positive fibers are clearly visible.

C,C',C'' – Parasagittal optical sections of a 24 h *Tg(eng2a:eGFP)^{i233}, Tg(actin:GAL4)* embryo, injected with dnPKA RNA and *UAS:caALK3* (marked by tRFP), showing clear suppression of eGFP expression (MP) in tRFP expressing cells.

D,D',D'' – Parasagittal optical sections of a 36 h *Tg(eng2a:eGFP$^{)i233}$, Tg(actin:GAL4)*

embryo, injected with *UAS:Shh* and *UAS:caALK3* (marked by tRFP), showing clear suppression of eGFP expression (MFF) in tRFP expressing cells.

E,E' – Parasagittal optical sections of a 24 h *Tg(actin:GAL4)* embryo, injected with dnPKA RNA and *UAS:caALK3* (marked by tRFP), showing that the caALK3 construct cell autonomously up-regulate pSmad resulting in clear suppression of Eng expression (marked by 4D9, MP) in tRFP expressing cells. Scale bars are 25 microns.

The *caALK3* construct when seen expressed close to the horizontal myoseptum suppressed *eng2a:eGFP* expression (data not shown). To increase the probability of expressing the caALK3 in prospective MPs, I expanded the MP progenitor pool by ectopic activation of Hh signaling in the myotome by injecting dnPKA RNA at one cell stage. I then asked if these Hh induced MPs could be suppressed by cell autonomously activating BMP signaling using the *caALK3* transgene. I saw a clear separation of tRFP and *eng2a:eGFP* expressing MPs/MFFs cells, and very often the tRFP positive cells were seen in the middle of the expanded stack of MP/MFF cells (Figure 7.2 C-C''). Therefore it can be concluded that the expression of *caALK3* potently suppressed the induction of *eng* or, the activation of BMP signaling can cell autonomously inhibit *eng* expression in response to Hh signaling.

I next asked if ectopic activation of Smad could suppress induction of MFF by Shh. For this I injected *UAS:caALK3/tRFP* and *UAS:Shh* transgenes into embryos obtained from *actin:Gal4* line crossed to *Tg(eng2a:eGFP)^{i233}*. Embryos over-expressing Shh from this construct display conversion of almost the entire population of fast fibers to MFFs (Figure 4.3 D). Fibers expressing *caALK3*, marked by tRFP were unable to induce *eng* in response to Shh. In these embryos tRFP and eGFP never labeled the same cell, while being next to each other (Figure 7.2 D-D''), suggesting *caALK3* expression efficiently inhibited *eng2a:eGFP* expression. From these experiments, I conclude that Smad activity can cell autonomously suppress Hh induced *eng* expression in both the slow and fast fiber compartments.

7.4. Suppression of BMP-Smad signaling leads to ectopic, Hh-induced MP/MFF

I next wanted to investigate if relieving pSmad mediated repression would lead to ectopic *eng* or ectopic MP, MFF differentiation. To suppress BMP signaling I used the *actin:Gal4* driver line to ectopically express a dominant negative BMP receptor (dnBMPr) (Suzuki et al., 1994), which has previously been shown to antagonize BMP signaling in the early embryo. This construct even at high levels of expression of dnBMPr/tRFP did not result in ectopic *eng* expression. I next checked if the dnBMPr molecule was indeed depleting pSmad in the myotome. Transgenic lines expressing high levels of dnBMPr were unable to effectively remove pSmad staining in the myotome (data not shown), which explained the lack of ectopic *eng* in these embryos. To efficiently abolish pSmad accumulation in the myotome, I next expressed inhibitory Smads, again using the GAL4-UAS system. Inhibitory Smads antagonize the BMP pathway and are known to act both at the level of the receptor and at the level of regulatory-Smad, Smad4 complexes (Hata et al., 1998; Imamura, 1997; Nakao, 1997; Zhang et al., 2007). *Xenopus-smad7* when expressed in the myotome using the *actin:GAL4* driver line resulted in several ectopic MPs and MFFs (Figure 7.3). This construct efficiently and cell autonomously depleted pSmad levels within the myotome (Figure 7.3 C, C'). A mouse flag tagged Smad6 also displayed similar activity but was somewhat less efficient in driving ectopic *eng* expression (data not shown).
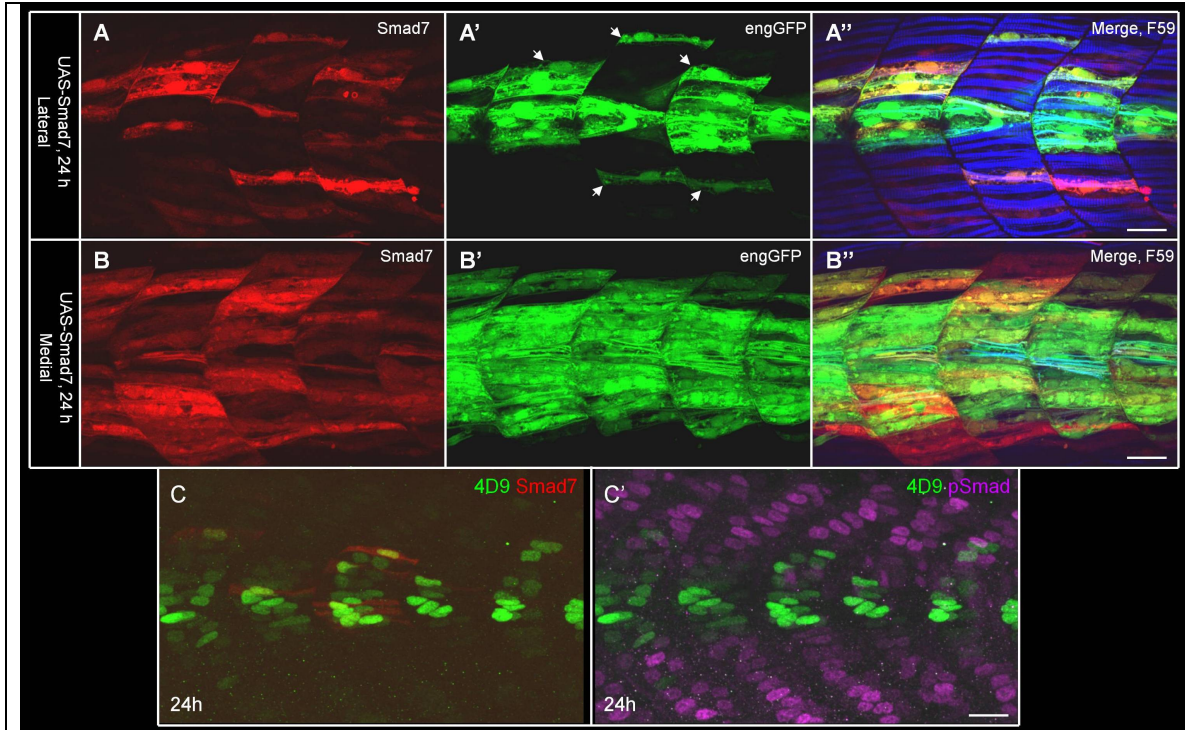
Figure 7.3: Cell autonomous inhibition of BMP signaling leads to ectopic MP/MFF differentiation.

A,A',A'' – Parasagittal optical sections of a 24 h *Tg(eng2a:eGFP)^{i233}, Tg(actin:GAL4)* embryo, injected with *UAS:xsmad7/tRFP*, showing cell autonomous, ectopic activation of eGFP (arrows) in slow fibers (blue) expressing Smad7 (red).

B,B',B'' – Same embryo displaying cell autonomous, ectopic activation of eGFP in fast fibers.

C,C' – Parasagittal optical sections of a 24 h *Tg(actin:GAL4)* embryo, injected with *UAS:xsmad7/tRFP,* showing Smad7 effectively eliminates pSmad accumulation and activates Eng in individual fibers. Scale bars are 25 microns.

Although these loss and gain of function experiments show that BMP signaling is both necessary and sufficient for inhibiting *eng* in the myotome, they are based on over-expression of cDNAs. I next attempted to inhibit endogenous BMP signaling using morpholino mediated gene knock down approach by targeting a type-I BMP receptor, *bmpr1ba,* which is expressed specifically in the myotome (Nikaido et al., 1999). Using this morpholino I was able to efficiently inhibit Smad activity within the myotome (Figure 7.4 A, B), pSmad staining in the epidermis, ventral somite and the neural tube remained unaffected (data not shown). Concomitant with this depletion in Smad activity I saw a significant increase in Eng activation in more numbers of both slow as well as fast fibers, assayed both by 4D9 and *eng2a:eGFP* staining (Figure 7.4 A-E). Quantification of the effect shows the extent of expansion of Eng[+] fibers (Figure 7.4 E). Therefore, inhibition of BMP signaling results in ectopic activation of *eng* gene expression in both the slow and fast fiber compartments.
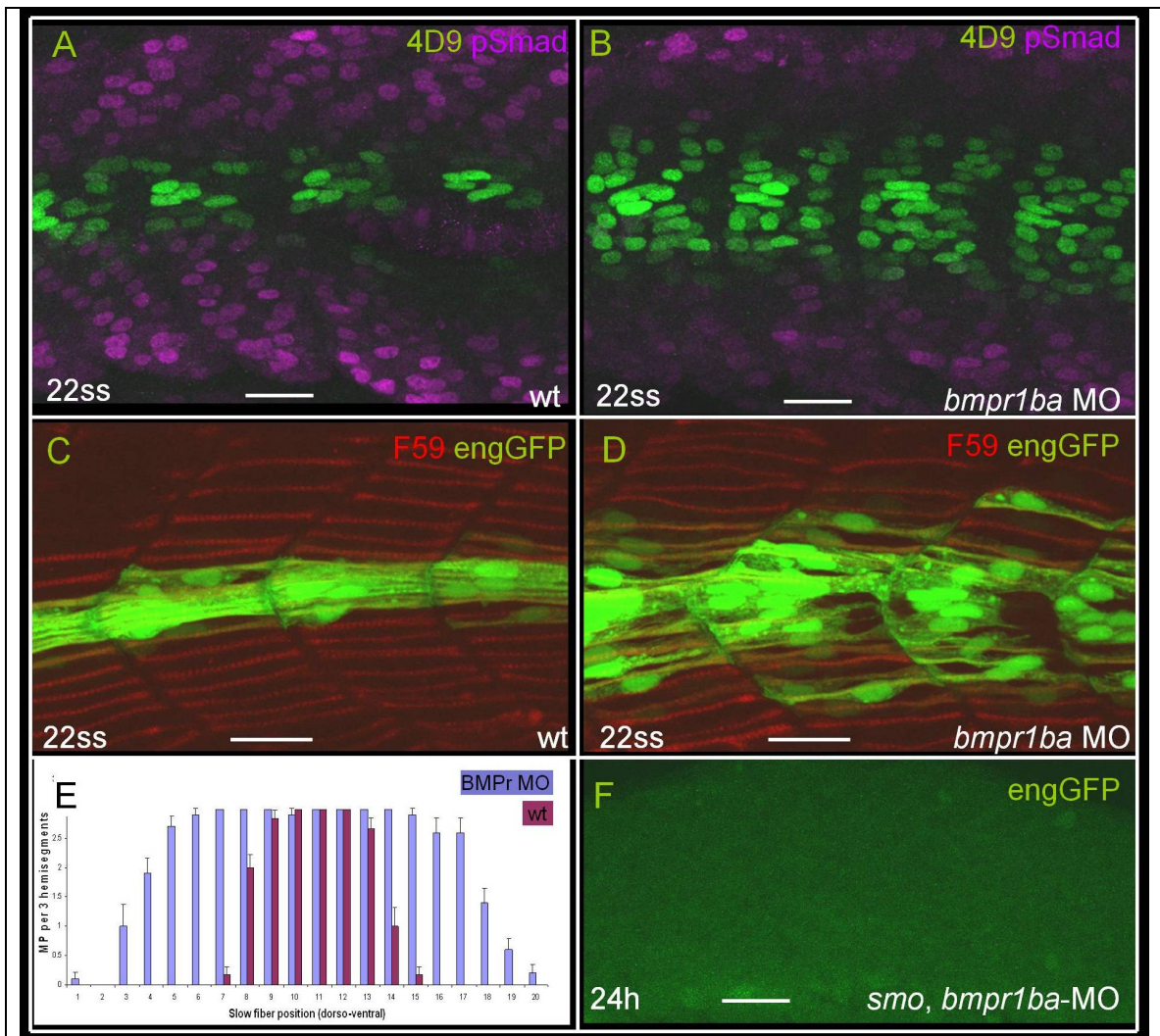
Figure 7.4: Characterization of a type-I BMP receptor function in modulating *eng* expression in the zebrafish myotome.

A – A 22 ss old zebrafish embryos showing the endogenous distribution of Eng (4D9) and pSmad.

B – A similarly staged embryo injected with bmpr1ba MO, showing severe reduction in pSmad levels and a concomitant increase in Eng expression

C – A 22 ss *Tg(eng2a:eGFP)^{i233}* showing MPs marked by eGFP and slow fibers marked by F59.

D – A similarly staged and stained embryo injected with bmpr1ba MO, showing expansion in the number of fibers expressing eGFP (MPs).

E – Quantification done on embryos similar to that shown in D,E to compare the extent of expansion between the wt and morphants.

F – A 24 h *Tg(eng2a:eGFP)^{i233}*, smo mutant embryo injected with bmpr1ba MO does not display rescue or expansion of eGFP positive fibers, showing absolute requirement of Hh pathway activity to induce Eng. Scale bars are 25 microns.

7.5. Ectopic induction of MP/MFFs by inhibition of BMP signaling critically requires Hh induced activity

I next tested if this ectopic *eng* inducing ability of Smad7 is dependent on Hh signaling. For this, embryos expressing clones of Smad7 in the myotome were exposed to 50 μM cyclopamine to block all Hh signaling. In such embryos, I found little or no expression of *eng* in the myotome, similar to embryos with no Smad7 expression. Similarly, attenuating the level of BMP signaling by *bmpr1ba* MO injection in *smo* mutant embryos did not rescue Eng activation, showing the absolute requirement of Hh in inducing *eng* (Figure 7.4 F).

Increasing the levels of hedgehog signaling either by injecting Shh or dnPKA encoding RNA leads to the conversion of the entire myotome into slow fibers (Blagden et al., 1997). This also leads to a large increase in the number of MPs but their expansion is limited to the medial location dorso-ventrally within the somite (Currie and Ingham, 1996). A significant number of slow fibers both dorsally and ventrally are resistant to conversion to MP fate. Here, I show that these dorsal and ventral regions within the somite are actively receiving BMP like signals and it is these signals that suppress *eng* gene expression and limit the expression of *eng* medially, along the dorso-ventral axis of the somite. Moreover, increasing Shh signaling in the myotome makes the myotome more competent for the reception of BMP like signals by upregulating *smad1* transcription (Dick et al., 1999), which could be one mechanism of achieving the right proportion of *eng* positive vs. other cell types within the myotome. In accordance with

this interpretation, the levels of pSmad in individual muscle nuclei of Shh RNA injected embryos was much higher compared to that in uninjected controls (data not shown).

In all instances where Hh or BMP signaling were manipulated, pSmad was never seen expressed in a MP and only rarely at very low levels seen in a MFF cell. Together these data show that in addition to Hh signaling, depletion of pSmad is both necessary and sufficient for MP and MFF differentiation in the zebrafish myotome.

Chapter 8: Results - Interaction between the Hh and BMP signaling pathways in the zebrafish myotome

8.1. Nuclear accumulation of pSmad is antagonized by Hh pathway activity

eng expression is exquisitely sensitive to the levels of Hh signaling, increasing Hh leads to large increase in the number of MP/MFFs and a slight decrease in Hh results in complete elimination of MP/MFFs (Wolff et al., 2003). As shown in the previous sections, pSmad inhibits *eng* and marks fibers abutting the *eng* expression domain, therefore I next investigated what happens to pSmad distribution and levels when cell fates in the myotome are altered by manipulating levels of Hh signaling. The Hh receptor Ptc1 and its paralog Ptc2 act as negative regulators of Hh target gene expression in absence of the ligand; hence in the absence of Ptc1 and Ptc2, Hh target genes are de-repressed and Hh-dependent cell types, including the MPs and slow fibers are expanded at the expense of later specified fast-twitch fibers (Wolff et al., 2003). I found that in *ptc1, ptc2* double mutant embryos, pSmad was depleted from a larger population of cells medially along the dorso-ventral axis, correlating precisely with the ectopic expression and expansion of *eng2a* (Figure 8.1 A, A', compare with B, D').
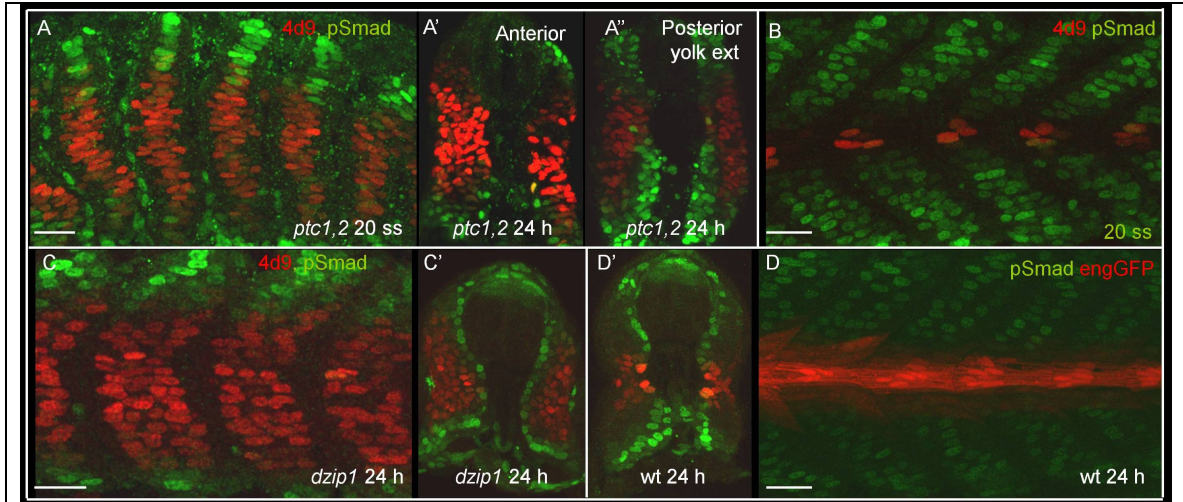
Figure 8.1: Modulation of pSmad accumulation and Eng expression by Hh pathway activity.

A-A" – Parasagittal optical section and transverse sections at different levels along the rostro-caudal axis of *ptc1*[hu1602]; *ptc2*[tj222] double homozygous mutant embryo at 20 ss and 24 h respectively showing vastly expanded MPs (revealed by 4D9, red) and a reciprocal loss of pSmad accumulation (green); compared with wild type embryo at a similar stage in B, note the expansion in the domain of pSmad accumulation dorsally and ventrally in the *ptc* mutants, especially at more caudal levels; compare to the 24 h wild type embryo shown in D.

C,C' – Parasagittal optical section and transverse section *dzip1*[lfs294e] homozygous mutant embryo at 24 h showing expanded MFFs (revealed by 4D9, red) and a reciprocal loss of pSmad accumulation (green); compare with the 24 h wild type embryo shown in D and D'. Scale bars are 25 microns.

In 24 h *dzip1* mutant embryos, the number of MFFs is vastly expanded, whereas the number of slow fibers and MPs appear normal (Wolff et al., 2004). This has been attributed to perturbations in Gli processing resulting in slight but constitutive up-regulation of the pathway (Huang and Schier, 2009). This expanded population of MFFs in *dzip1* embryos display a clear lack of pSmad accumulation, pSmad stains the nuclei of fast fibers that are next to the neural tube and the hypochord (Figure 8.1 C, C'). Cross-sections reveal that most fast fibers are converted to MFF fate except for a monolayer of pSmad positive population closest to the dorsal and the ventral midline of the somite (Figure 8.1 C, C'). In wildtype embryos, pSmad stains larger domains of cells around the neural tube and hypochord (Figure 8.1 D, D').

These results imply that hyper-activation of the Hh pathway inhibits nuclear accumulation of pSmad. To test this, I activated the pathway by microinjection of mRNA encoding either the Shh protein or a dnPKA (Currie and Ingham, 1996; Hammerschmidt et al., 1996). Shh results in activation of the pathway at the level of Smo, the transmembrane transducer of Hh activity, while dnPKA acts at the level of Gli transcription factors. In both cases, I observed a lack of pSmad accumulation in the expanded population of MPs (data not shown), although it is known that the levels of Smad1 transcript increase within the myotome upon Hh upregulation (Dick et al., 1999).

A similar phenomenon is seen in the *Drosophila* wing imaginal disc. Phospho-Mad (Smad1/5/8 ortholog) accumulates in cells exposed to the Dpp signal (BMP4 ortholog). Within the anterior compartment the levels of pMad at the point of highest Hh

concentration remain lower than expected (a symmetric pMad gradient is not seen in response to a symmetric *dpp* gradient) (Tanimoto et al., 2000). The authors then show that activation of the Hh pathway leads to reduction in pMad levels and attribute this effect to down-regulation of the Dpp receptor (*tkv*) by Hh signaling. This may not apply for the similar activity of Hh signaling towards pSmad levels within the zebrafish myotome. Clonal, ectopic expression of *UAS:dorsalin-1* (a secreted BMP like molecule from chick) within the myotome using the actin-Gal4 line leads to high levels and ubiquitous accumulation of pSmad in all myotomal nuclei. Dorsalin-1 potently suppressed MP, MFF fate specification (section 7.3; Du et al., 1997). If some cells had little or no BMP receptor levels due to high Hh (precursors of MPs and MFFs), then these would be refractory to Dorsalin-1 and accumulation of pSmad. A type I BMP receptor which is expressed in a restricted fashion in many tissue types including the somites does not show differential expression within the somite (Nikaido et al., 1999).

8.2. Suppression of BMP signaling can rescue the effects of dampened Hh signaling on Eng activation

I next asked if inhibition of BMP signaling can rescue the effects of reduced Hh signaling. For this, I injected *bmpr1ba* MO into embryos mutant for *disp1*. Disp1 is a 12 pass transmembrane protein that is required for efficient secretion of Hh ligands (Burke *et al.*, 1999; Caspary *et al.*, 2002; Kawakami *et al.*, 2002; Ma *et al.*, 2002). In zebrafish *disp1* mutants, Hh signaling is severely compromised such that slow fibers are reduced in number and MP, MFFs are almost entirely absent (Nakano et al., 2004). Inhibition of BMP signaling in the somites of *disp1* mutants resulted in robust rescue of *eng2a:eGFP*

expression in both the slow and fast fiber compartments (Figure 8.2). This shows that it is the relative levels of Hh and BMP pathway activity that control *eng* gene expression. If the activating inputs from Hh pathway are reduced, *eng* can be rescued by relieving inhibitory inputs from the BMP pathway. Another interpretation of these results is that Hh acts to alleviate BMP mediated repression of *eng*.
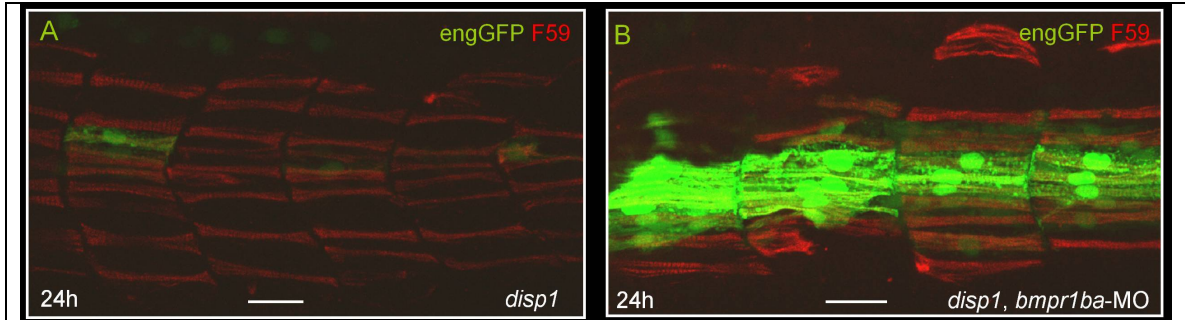
Figure 8.2: Inhibition of BMP signaling lowers the Eng inducing Hh threshold

A – Parasagittal optical cross sections of a 24 h *Tg(eng2a:eGFP)^{i233}, disp1* mutant embryo, displaying reduced number of slow fibers (compare with Figure 7.4C) and almost complete absence of MP,MFF marked by eGFP

B – A similar embryo additionally injected with the bmpr1ba MO, displaying rescue of eGFP positive MP and MFF (not visible). Note the number of slow fibers remains reduced. Scale bars are 25 microns.

8.3. Activation of Hh target genes is unable to deplete pSmad

I next tested if activation of *eng* by the Hh pathway is also coupled to pSmad depletion. For this, I expressed *gli1* in myoblasts again using the *actin:GAL4*, UAS system. Gli1 acts as a constitutive activator of Hh target genes. Expression of *gli1* in myotomal cells can ectopically and cell autonomously activate *eng2a:eGFP* in a number of pSmad negative myotomal cells (Figure 8.3 A-A'''). I was also able to find several clones of cells that displayed both high levels of Gli1 and pSmad. Only cells that displayed no pSmad displayed ectopic activation of *eng2a:eGFP* (Figure 8.3 B-B'''). This suggests that the depletion of pSmad by Hh pathway activity is not mediated by its downstream transcriptional targets.
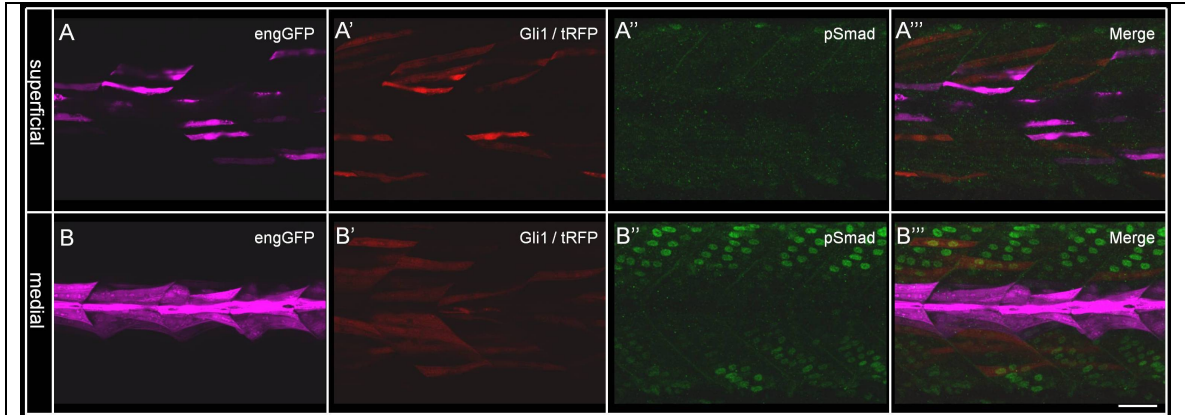
Figure 8.3: Activating Hh target genes activates *eng* in pSmad negative cells

A, A', A'', A''' – Parasagittal optical sections of the lateral regions of the myotome of a 30h *Tg(eng2a:eGFP)^{i233}* injected with *UAS:Gli1/tRFP* construct. Several tRFP marked clones display activation of eGFP.

B, B', B'', B''' – Medial regions of the same embryo displaying several cells expressing tRFP but none upregulating eGFP in response. Note - these medial regions display high levels of pSmad accumulation in their nuclei. Scale bar is 25 microns.

8.4. Hh signaling acts cell autonomously to activate eng transcription

I next asked if Hh signaling acts cell autonomously to activate *eng* transcription. For this I made clones of myotomal cells over-expressing dnPKA or membrane tethered N-terminal fragment of mouse Shh, mShhCD4 (obtained from Henk Roelink (Incardona et al., 2000)). Both of these constructs activated *eng2a:eGFP* transgene only within the over-expressing cells and not in the surrounding cells (Figure 8.4 A-A'', B-B''). I also tested these constructs in *disp1* mutant embryos, which display little or no Eng activation in the myotome. Clones of cells over-expressing dnPKA cell autonomously activated *eng2a:eGFP* in such embryos (Figure 8.4 C, C'). These results show that Hh acts cell autonomously to activate *eng* and also likely pSmad depletion.
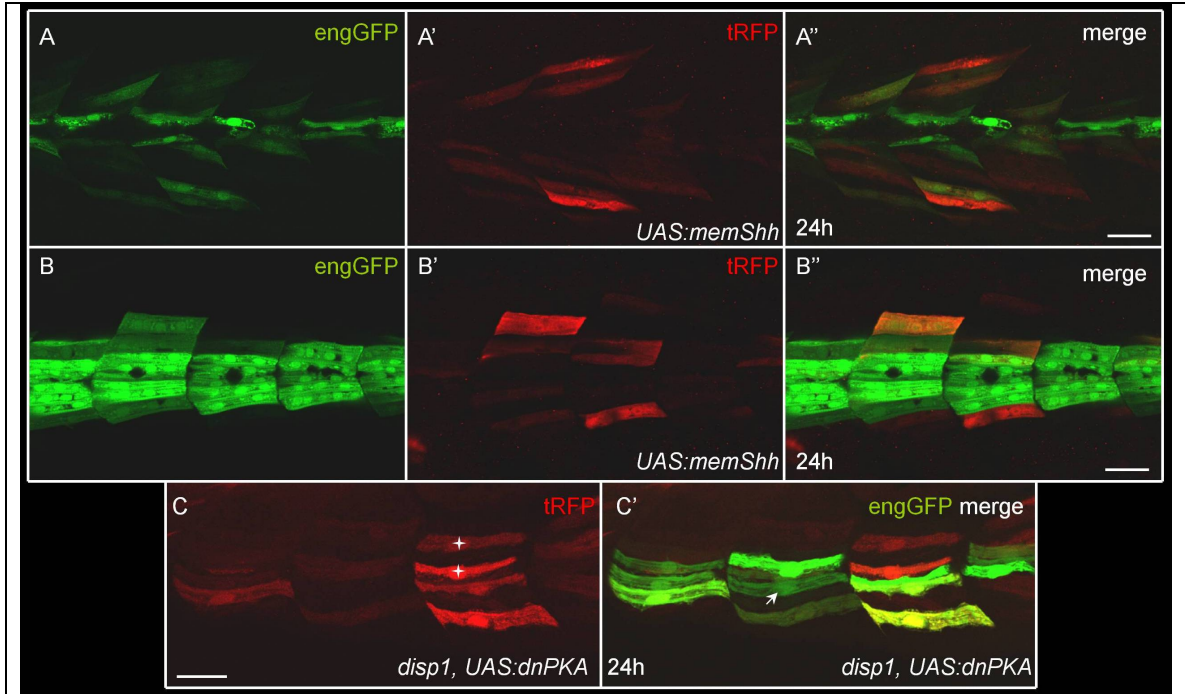
Figure 8.4: Hh signaling acts cell autonomously to activate *eng* in the myotome.

A,A',A'' – Parasagittal optical sections of a 24 h *Tg(eng2a:eGFP)^{i233}* embryo injected with *UAS:memShh/tRFP* displaying individual tRFP expressing cells ectopically activating the eGFP, Eng reporter. Sections obtained from lateral regions of the somite showing mostly slow fibers.

B,B',B'' – A similar embryo showing ectopic activation of the engGFP reporter in the fast fiber compartment, sections obtained from medial regions within the somite.

C,C' – Parasagittal optical sections of a 24 h *Tg(eng2a:eGFP)^{i233}, disp1* mutant embryo injected with *UAS:dnPKA/tRFP* construct, showing several examples of ectopic engGFP in response to dnPKA over-expression. White plus sign indicates fibers that express dnPKA but do not up-regulate eGFP, whereas the arrow indicates a fiber expressing eGFP but not over-expressing dnPKA, being likely an endogenous MP. Scale bars are 25 microns.

8.5. Depletion of Gli3, Smad1 or Bmp4 results in ectopic eng expression in both slow and fast fibers

Gli1 and Gli2a mediate the activating ability of Hh within the myotome (Wolff et al., 2003). I next asked if Gli3, which in other contexts acts predominantly as a repressor (Hui and Joyner, 1993; Litingtung and Chiang, 2000; Rallu et al., 2002; Wijgerde et al., 2002) was controlling cell fates in the zebrafish myotome. I injected a *gli3* MO into *Tg(eng2a:eGFP)^{i233}* line and observed ectopic expansion of *eng2a:eGFP* in both the slow and fast fiber compartment at around 3 days (Figure 8.5 A, A'); this suggests that in addition of Gli2a repressor activity, Gli3 repressor activity may also function within the myotome.

I next investigated if reducing the levels of *smad1* in the embryo would result in ectopic activation of *eng*. For this, I injected *smad1* MO into zebrafish embryos. MP and MFF fate was assessed using the *eng2a:eGFP* transgene. Morphant embryos displayed normal eGFP expression pattern until 2 d. On the 3rd day, several slow and fast fibers in the posterior somites displayed ectopic activation of eGFP (Figure 8.5 B, B'). Consistent with this, a *bmp4* MO also displayed a similar phenotype but was somewhat less efficient in activating this later, ectopic *eng2a:eGFP* (Figure 8.5 C, C').
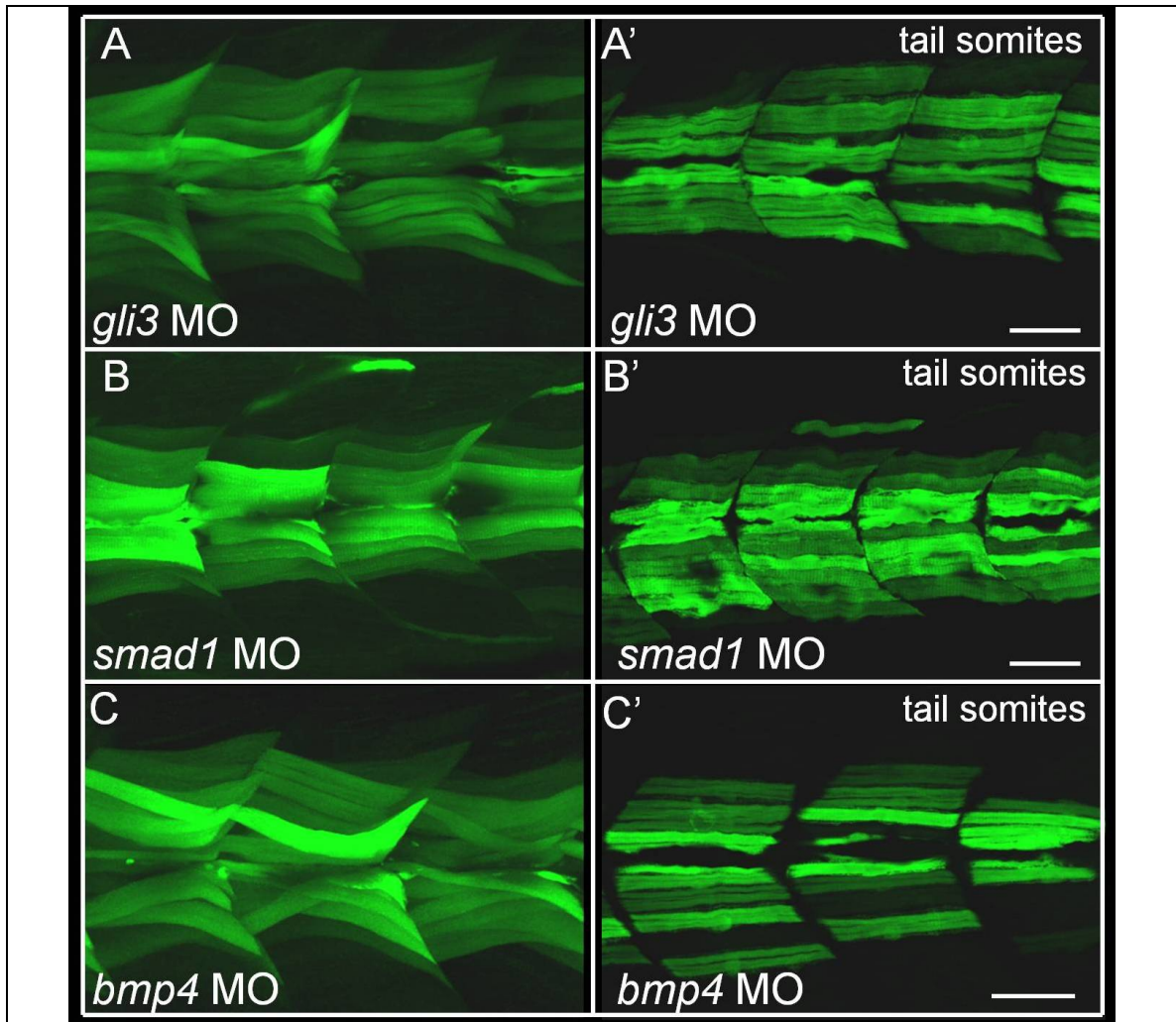
Figure 8.5: Depletion of repressor *gli3*, *smad1* and *bmp4* results in ectopic Eng in the myotome.

A,A' – Parasagittal optical section of 3 d *Tg(eng2a:eGFP)^{i233}* embryos injected with a *gli3* MO, displaying an expansion of engGFP reporter expression in the fast compartment in A and in the slow compartment in A'.

B,B' – Parasagittal optical section of 3 d *Tg(eng2a:eGFP)^{i233}* embryos injected with a *smad1* MO, displaying an expansion of engGFP reporter expression in the fast compartment in A and in the slow compartment in A'.

C,C' – Parasagittal optical section of 3 d *Tg(eng2a:eGFP)^{i233}* embryos injected with a *bmp4* MO, displaying an expansion of engGFP reporter expression in the fast compartment in A and in the slow compartment in A'. Scale bars are 25 microns.

It remains difficult to reconcile this later ectopic induction with the much earlier specification events by the Hh and BMP signaling pathways. It is possible that these phenotypes are the result of off target effects of the morpholinos used. I did observe a number of malformed embryos and these were excluded from this analysis, which could be due to the toxic nature of these MOs and so the surviving ones were those that received a much lower dose of MOs and hence a weaker knockdown resulting in the later phenotypes.

8.6. Truncated but not full length Gli2a sequesters Smad1 into myotomal nuclei

Our data imply that Hh pathway activity modulates the nuclear accumulation of pSmad and that this effect is mediated at the level of Gli proteins. Previous studies have reported that truncated, though not full length forms of Gli can be co-precipitated with Smads from tissue culture cells transfected with constructs encoding tagged forms of both proteins (Liu et al., 1998). This suggests a possible mechanistic basis for the observed modulation of pSmad accumulation by Hh signaling, whereby the truncated repressor form but not the full length forms of Gli might promote the nuclear accumulation of pSmads. To explore this possibility, I employed the Bimolecular Fluorescence Complementation (BiFC) assay (Hu et al., 2002; Saka et al., 2007) to investigate the potential of the two proteins to interact directly in an *in vivo* context (Figure 8.6). BiFC exploits the ability to reconstitute a fluorescent protein (modified non-aggregating forms of Venus) from its two halves (Vn - N terminal fragment and Vc - C Terminal fragment) neither of which fluoresces in isolation (Figure 8.6) (Hu et al., 2002; Saka et al., 2007).

Figure 8.6: Schematic representation of Bi-molecular Fluorescence complementation to study protein interactions in live cells and the transgenic strategy used to express the tagged proteins in the zebrafish myotome.
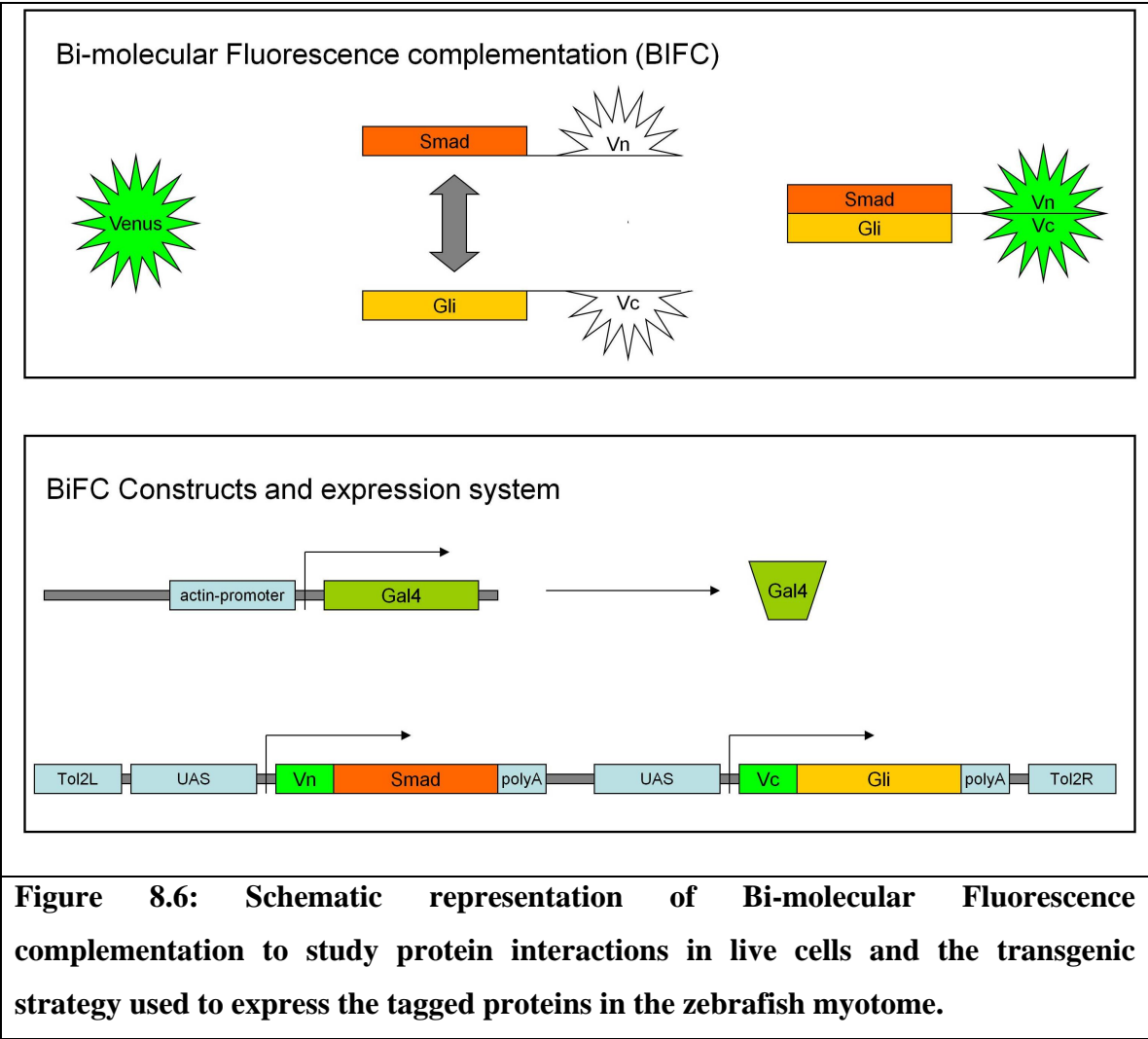
In order to test the efficacy of the BiFC system, I assayed the well characterized interaction first between Smad1 and its co-factor Smad4 and then between Glis and Sufu (Suppressor of Fused, a component of the Hh signaling pathway). I made Vn-Smad1 and obtained Vc-Smad4 from Steve Harvey and Jim Smith (Harvey and Smith, 2009) and cloned them into a bi-cistronic UAS construct, such that they are independently transcribed at the same level from the same transgene (Figure 8.6). I injected this bi-cistronic BiFC construct into *actin:GAL4* transgenic embryos and assayed for BiFC signal at 24 h in live embryos. The Smad1, Smad4 pair resulted in robust complementation of Venus in myotomal cells (Figure 8.7 A). Fluorescence was observed in and around the nuclei and on the plasma membrane in punctate pattern.

A 30h
Smad1 + Smad4

F 40h
Gli2aR + Smad4

B 24h
Gli1 + Sufu

G 24h
Gli1 + Smad1

C 24h
Gli2a-FL + Sufu

H 24h
Gli2a-FL + Smad1

D 24h
Gli2aR + Sufu

I 24h
Gli2aR + Smad1

E

J 24h
bmpr1ba-MO + Gli2aR-Vc + Vn-Smad1

K
ΔZnFn-Gli2aR + Smad1

L
ΔZnFn-Gli2aR + Sufu
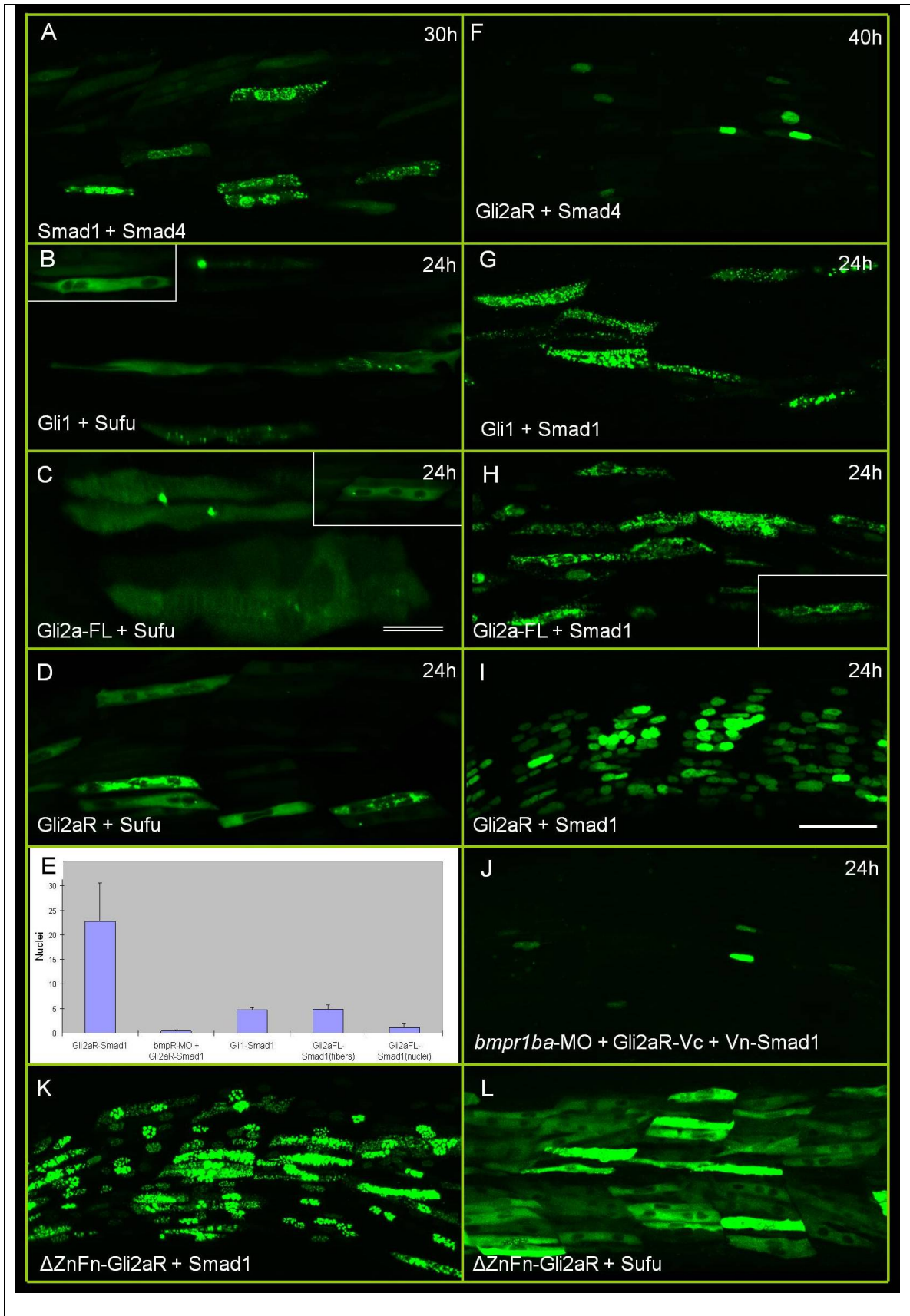
Figure 8.7: Bi-Fluorescence complementation assay for *in vivo* protein-protein interactions.

Parasagittal optical sections of live embryos injected with various constructs expressing Vn and Vc tagged proteins form the same UAS promoter and imaged at 24 h.

A - Smad1 and Smad4: note speckled appearance of signal which shows a cytoplasmic and perinuclear localization.

B – Gli1 and SuFu. Signal is localized to the cytoplasm and excluded from the nucleus (inset).

C – Full length Gli2a and SuFu. Signal is similarly localized to the cytoplasm and excluded from the nucleus (inset).

D – Truncated Gli2a and SuFu. Signal is similarly localized to the cytoplasm and excluded from the nucleus. Signal is also seen in spots inside the cell that resemble the basal body.

E – Histogram showing frequency of Venus positive fibres in embryos injected with different Gli-Smad combinations; representative examples shown in panels.

F – Truncated Gli2a and Smad4 imaged at 40 h. A few nuclei show signal.

G – Gli1 and Smad1. Note speckled appearance of signal which shows a cytoplasmic and perinuclear localization.

H – Gli2a-FL and Smad1. Note speckled appearance of signal which shows a cytoplasmic and perinuclear localization (see inset).

I – Gli2aR and Smad1. Majority of fibres in each somite are Venus positive, with signal localized exclusively to the nucleus.

J – Gli2aR and Smad1 co-injected with *bmpr1ba* morpholino: Majority of fibres in each somite are Venus negative.

K – ΔZnFn-Gli2aR and Smad1. Fluorescent signal is seen in the nucleus that appears to be large inclusion bodies, compare with I.

L – ΔZnFn-Gli2aR and Sufu. Signal is restricted to the cytoplasm as is in D.

Scale bars – 10 microns (double line), 25 microns (single line).

I next asked if the system could faithfully display the well known interaction between Gli2aR (a truncated form of Gli2a which is missing the C-terminal activating domain, but retaining the N-terminal repressor domain and Zinc-finger DNA binding domain; resembling the endogenous Gli2 repressor) and Sufu, a negative component of the Hh pathway. For this I made Vn-Gl2aR, Vc-Gli2aR, Gli2aR-Vn, Gli2aR-Vc, Vn-Sufu and Vc-Sufu fusion constructs. These were appropriately cloned into bi-cistronic UAS constructs and expressed by the *actin:GAL4* driver. The Gli2aR-Sufu BiFC pair (UAS:Gli2aR-Vc=UAS:Vn-Sufu) displayed robust complementation and the BiFC signal was observed in the cytoplasm, clearly excluded from the nuclei, in line with Sufu being a cytoplasmic tether for Gli (Figure 8.7 D) (Dunaeva et al., 2003; Humke et al., 2010; Pearse et al., 1999; Stone et al., 1999). Similar cytoplasmic distribution was observed for Gli1, Gli2a full length forms when tested for interaction with Sufu (UAS:Gli2a-Vc=UAS:Vn-Sufu and UAS:Vc-Gli1=UAS:Vn-Sufu) in this system (Figure 8.7 B, C). In addition, I observed strong localization of Gli-Sufu pairs in spots that appear to be basal bodies, this fits well with the association of Hh pathway to primary cilia and basal body.

These experiments suggested that the BiFC assay can faithfully report protein-protein interactions *in vivo* in the myotome. Co-expression of the full length forms of Gli1 or Gli2a with Smad1 also resulted in significant levels of fluorescence in some fibres; in both cases the signal was localized predominantly in the cytoplasm, though some nuclei were labeled with the Gli2a–Smad1 pair (Figure 8.7 G, H, E). By contrast, co-expression of the truncated Gli2a and Smad1 tagged pairs resulted in robust levels of fluorescence at high frequency (Figure 8.7 I, E); notably, this signal was largely abolished when the

bmpr1ba MO was simultaneously injected with the constructs (Figure 8.7 E, J), implying that the interaction was dependent upon phosphorylation of Smad1. Co-expression of truncated Gli2a and Smad4 resulted in very weak complementation both in the nuclei and cytoplasm that was detectable only by 40 h in contrast to 24 h for all the other tagged pairs (Figure 8.7 F). As the zinc-fingers (ZnFn) of Gli3 have been implicated in binding to Smads in tissue culture (Liu et al., 1998), I asked if in our BiFC assay the association between Gli2aR and Smad1 be affected if the Gli2a-ZnFn is deleted. For this, I deleted all the five ZnFn from Gli2aR and made the BiFC bi-cistronic UAS construct again. I found that the uniform BiFC distribution disappeared and changed into what appeared to be large inclusion bodies in the nucleus (Figure 8.7 K). The same Gli2aR with its ZnFn deleted displayed unchanged BIFC with SuFu (Figure 8.7 L).

8.7. Ectopic Gli2aR can suppress Eng but does not lead to obvious accumulation of pSmad

I next tested if Gli2aR (truncated form) when over-expressed can inhibit *eng* activation. For this, I expressed the Gli2aR using the GAL4, UAS system, under the control of *actin:GAL4* and marked by tRFP on the same transgene. This construct displayed a clear but mild downregulation of *eng2a:eGFP* when expressed in the Eng$^+$ domain. In order to further test this, I expanded the *eng2a:eGFP* domain by simultaneously injecting *UAS:Shh* construct along with *UAS:Gli2aR* (Figure 8.8). This led to a clear and slight downregulation of eGFP in cells marked by tRFP, while being surrounded by cells with upregulated eGFP, due to the effects of Shh (Figure 8.8).
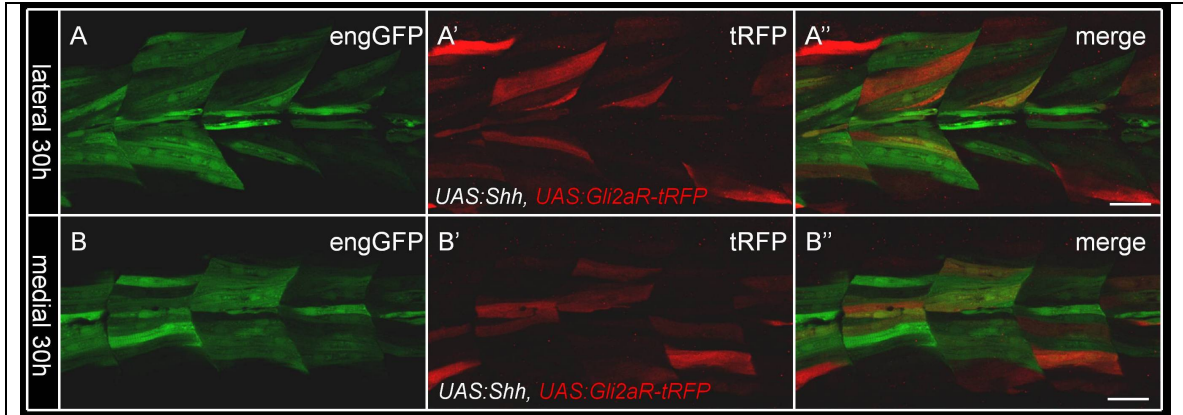
Figure 8.8: Gli2aR can attenuate *eng2a:gfp* expression, but does not lead to obvious detectable accumulation of pSmad.

A,A',A'' – Parasagittal optical sections of a 30 h *Tg(eng2a:eGFP)^{i233}*, *Tg(actin:GAL4)* embryo, injected with *UAS:Shh, UAS:Gli2aR/tRFP*, showing expansion of MP,MFF marked by eGFP. Cells marked by tRFP show a reduction in eGFP accumulation. Shown are stacks of lateral regions within the somite.

B,B',B'' – Same embryo as in A-A'', showing medial regions within the somite. Scale bars are 25 microns.

I next asked if in this context Gli2aR due to its association with Smads would ectopically accumulate pSmad. For this, I stained embryos injected with *UAS:Gli2aR* with pSmad, but was unable to detect any ectopic accumulation of pSmad (data not shown). Gli2aR by inhibiting Hh target genes likely down-regulates *smad1* transcription, thereby lowering the levels of pSmad such that they are below the detection threshold of the staining methods I have used.

8.8. Gli2-repressor (yot) differentially represses MP versus slow muscle gene expression

I next asked if the Gli repressor form encoded by the *yot* mutant allele (Karlstrom et al., 1999) has differential effects on *eng* expression compared to a lower threshold slow muscle target gene. If a single copy of the *yot* repressor allele shows a stronger repressive effect on *eng* when compared to F59, a slow muscle marker, this would give additional support to the idea that Gli^R may be controlling high threshold Hh target gene expression by controlling the activity of Smads. I injected dnPKA RNA into embryos obtained from *Tg(eng2a:eGFP)^{i233}*crossed to the *yot* heterozygotes. The *yot* heterozygotes obtained showed resistance of all fibers being converted to slow fate, supporting previous findings that it acts as a dominant negative repressor. Despite the lack of slow fiber expansion in most of the *yot* heterozygotes, I was able to find a small proportion of *yot* heterozygotes that displayed a complete conversion of all fibers to slow fate, but displayed significantly reduced *eng* expression (Figure 8.9).
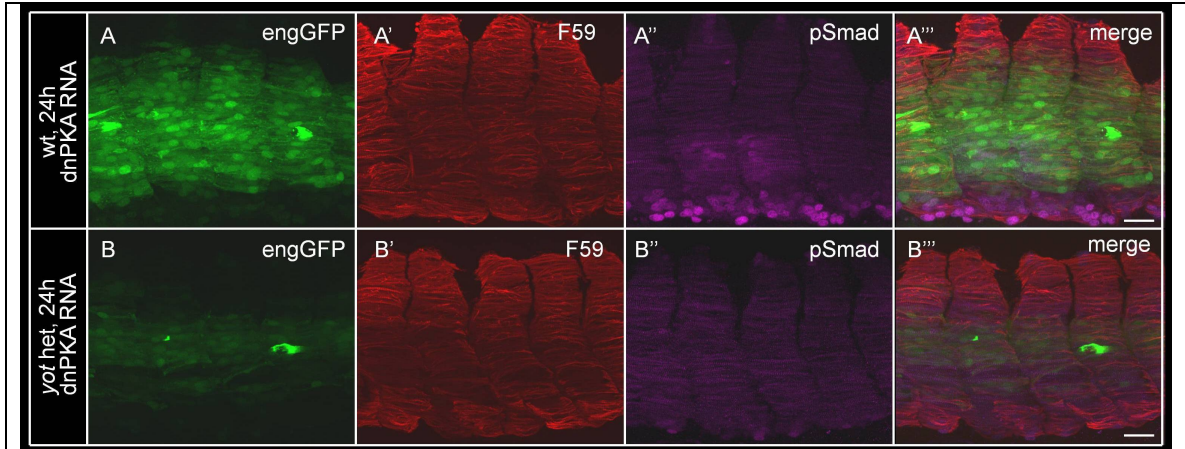
Figure 8.9: Repressor Gli2a can differentially regulate *eng* compared to lower threshold Hh targets.

A-A''' – Parasagittal optical section of a 24 h *Tg(eng2a:eGFP)^{i233}* embryo injected with a dnPKA RNA, displaying a large expansion of MP marked by eGFP in the slow compartment, F59 (red).

B-B''' – Parasagittal optical section of a 24 h *Tg(eng2a:eGFP)^{i233}, yot* mutant embryo injected with a dnPKA RNA, displaying weak expression and expansion of MP marked by eGFP in the slow compartment, F59 (red). Slow muscle marker F59 is seen expanded and is comparable to A'. Scale bars are 25 microns.

Another prediction of such a model is that if Gli2aR is additionally repressing *eng* by stabilizing pSmad, then pSmad levels should be higher in these *yot* heterozygotes compared to wt. I found to the contrary, that pSmad levels were reduced in injected *yot* heterozygotes. This I believe may be due to the reduction in *smad1* (and possibly *smad5, smad8*) transcription.

Additional indirect support for our model (whereby Gli^R stabilize pSmad) comes from experiments done by Kawakami et al., 2005, where *eng* expression can be partially restored in *yot* mutants by suppression of BMP ligands. This suggests that even in the absence of detectable pSmad, these cells perceive BMP signals and this level of signaling activity is sufficient to repress *eng* expression. Moreover, staining for pSmad in embryos with compromised Hh signaling like *disp1* mutants shows little or no pSmad accumulation (data not shown), but this level of pSmad is still sufficient to suppress *eng* in this context (Section 8.2)

8.9. eng2a *ME responds to Gli transcription factors* in vitro *in tissue culture*

I next tested if the *eng* ME responds to Gli trans-activation in BHK21 cells. For this, I transfected increasing amounts of *gli1*, *gli2*, *gli3* full length clones along with the ME-luciferase transgene. Gli1 and Gli2 which have major activating roles in many tissue types displayed concentration dependent activation of the ME, whereas Gli3 which functions largely as repressor did not activate the ME (Figure 8.10).
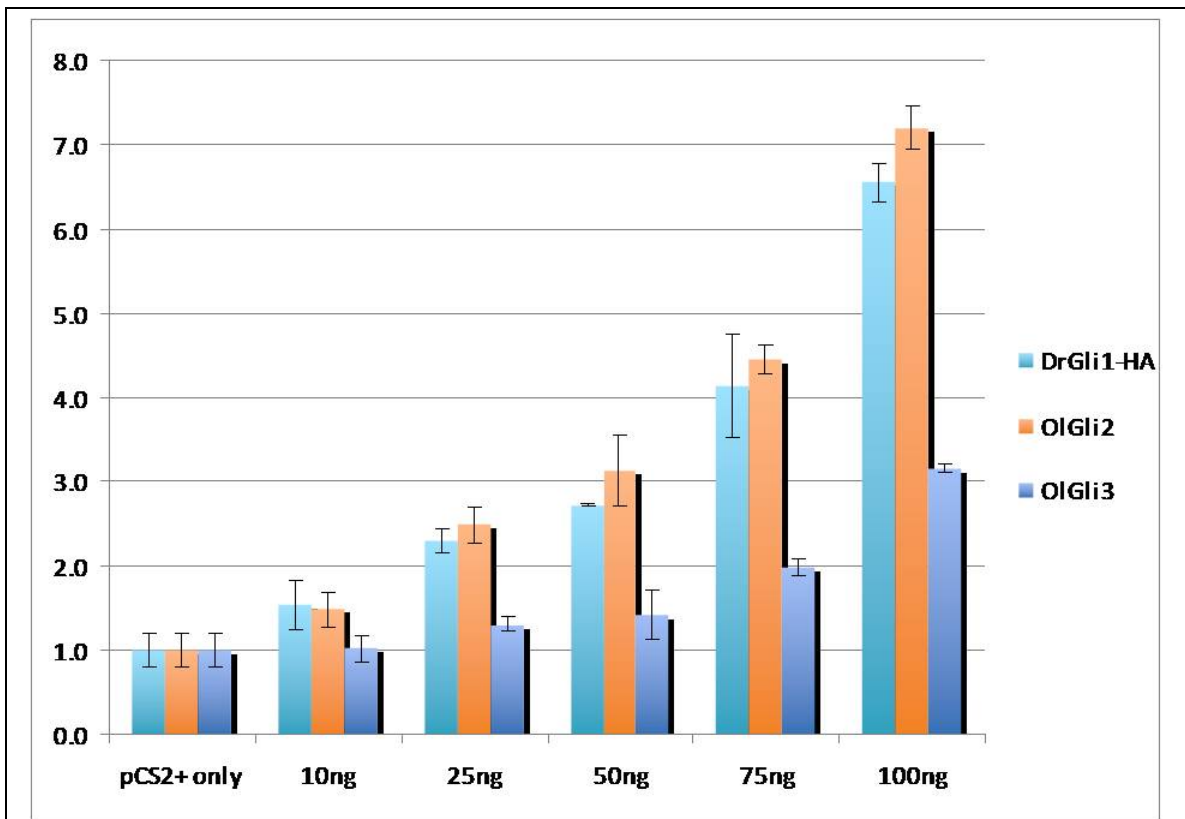
Figure 8.10: Dose dependent activation of *eng2a* ME in response to activating Gli transcription factors in BHK21 tissue culture cells.

8.10. Activated Gli2a and Smads bind to eng2a *ME and deletion of Smad sites results in ectopic activation of the ME*

Given the response of *eng2a* ME to Gli levels in tissue culture assay and *in vivo* in the zebrafish myotome, we next asked if Gli2a associates with the ME *in vivo* using chromatin immuno-precipitation (ChIP) from zebrafish embryos with a Gli2a antibody followed by quantitative PCR detection of the *eng2a* ME and flanking regions. ChIP was done according to von Hofsten et al., 2008 with minor modifications (Maurya et al., 2011). We found that Gli2a did show significant and preferential association with the ME (Maurya et al., 2011), although the association did not uncover sharp peaks, but pointed to a lower affinity association within the entire central region of the ME, which would fit with *eng2a* being a high threshold Hh target gene. The Gli2a antibody was characterized by Wang Xingang and myself, whereas the ME association was uncovered by Tan Haihan, colleagues in the Ingham laboratory, IMCB.

We next asked if the regulation of the *eng2a* muscle enhancers by Smad proteins is direct. This was again done by ChIP using the pSmad antibody on zebrafish embryos followed by quantitative PCR for detecting fragments around the *eng2a* ME. We found robust enrichment of the identified *eng2a* muscle enhancer in the ChIPed material, in comparison to the adjacent exonic regions of the *eng2a* gene. Marcel Souren uncovered the pSmad association with the ME and Tan Haihan repeated and confirmed these initial findings, both working in the Ingham laboratory (Maurya et al., 2011).

Deletion analysis of the ME had shown that some of the smaller fragments displayed ectopic activity (section 4.1 and 4.2); I next asked if this ectopic activation reflected the loss of Smad mediated repression. For this, I searched the ME for Smad consensus binding sites and found two such sites, one (distal to *eng2a*) of which differed the consensus at one nucleotide and another (proximal to *eng2a*) differed the consensus at two nucleotides (Figure 8.11). From the deletion analysis of the ME, I have shown that fragments that do not contain the proximal Smad site display ectopic activation of the transgene (Figure 8.11 A, B, C). Site directed mutations of the distal Smad site resulted in disruption of enhancer activity, possibly reflecting overlap with activating sites (data not shown).

Figure 8.11: Functional architecture of the *eng2a* ME

A – ME deletion constructs assayed for activity in stable transgenic lines. Fragment lengths boxed in orange indicate those that show ectopic expression. The dotted orange box indicates a putative repressor element reveled by this analysis.

B – Nucleotide sequence of the *eng2a* minimal ME showing the two putative Smad binding sites (highlighted).

C – Examples of ectopic eGFP expression in 24 h embryos from transgenic lines *Tg(eng2a:eGFP)[i247]* (I) and *Tg(eng2a:eGFP)[i249]* (III) and normal expression in lines *Tg(eng2a:eGFP)[i248]* (II) and *Tg(eng2a:eGFP)[i250]* (IV). Scale bar is 25 microns.

8.11. Smad1 is limiting in Eng⁺ cells and is stabilized by its activation through BMP ligands

I next expressed an N-terminally mCherry tagged Smad1 in the myotome using the GAL4-UAS system. mCherry positive clones found in the Eng$^+$ fibers showed a moderate but clear suppression of *eng2a:eGFP* expression (data not shown). To test and confirm this further, I increased the numbers of Eng$^+$ fibers by injecting *UAS:Shh* along with UAS:mCherry-Smad1. The mCherry positive clones displayed a clear down-regulation of *eng2a:eGFP* expression (data not shown). These experiments show that Smads are limiting in Eng$^+$ myotomal cells and this limitation can be partly relieved by its ectopic expression.

I next asked if BMP signaling activity is required for Eng repression by ectopic Smad1. For this, I injected the *bmpr1ba* MO along with *UAS:mCherry-smad1* fusion construct into *actin:GAL4* embryos. In these embryos, I was unable to detect any mCherry$^+$ clones, although the injection of *UAS:mCherry-smad1* construct alone in *actin:GAL4* embryos resulted in large numbers of mCherry$^+$ fibers. From these experiments I conclude that inactive Smads undergo quick turnover within myotomal cells and their activation by BMP signaling protects them from degradation, possibly through its interaction with Gli2aR.

8.12. Conservation of regulatory mechanisms in somites of medaka embryos

Having established that the zebrafish *eng2a* ME remains functional in medaka embryos (see section 6.1), I next asked if somites in medaka embryos sense BMPs and if BMPs were acting to inhibit *eng* expression. For this, I used the pSmad and 4D9 antibodies to label somites of medaka embryos (2-3 d). The pattern and distribution of Eng (4D9) and pSmad positive nuclei in medaka somites is very similar to that in zebrafish. The antibodies label cells in a mutually exclusive manner with Eng$^+$ nuclei located medially and their dorsal and ventral neighbors marked by pSmad (Figure 8.12). Taken together these results show that despite the lack of conservation at the DNA sequence level (section 6.1), mechanisms controlling *eng* gene expression have been well conserved between zebrafish and medaka, which diverged 110 million years ago from a common ancestor (Wittbrodt et al., 2002).

Figure 8.12: Activity of zebrafish *eng2a* enhancers in medaka embryos.

A-A'' – Parasagittal optical sections of a 3 d medaka embryo showing distribution of active Smads (pSmad1/5/8) and Eng (4D9) in the myotome.

Chapter 9: Results - Regulatory potential of other identified factors

9.1. Positive regulatory inputs into eng2a *transcription, myogenic factors,* myoD*, myf5, and* mef2

Simultaneous knockdown of the myogenic regulatory factors (MRFs - Myf5 and MyoD) results in abrogation of the skeletal myogenic program in zebrafish and the concomitant disruption of Eng activation in the somites. Induction of Eng in the myotome has also been shown to depend upon Mef2c and Mef2d (Hinits and Hughes, 2007), which are thought to lie further downstream of MRF-induced myogenic program. The ME is highly enriched for predicted binding sites for myogenic factors like, MyoD, Myf5, Mef2 and others. Therefore, I investigated whether expression of the *eng2a:eGFP* transgene is affected by Mef2 depletion. Injection of *mef2c,d* MO into *eng2a:eGFP* embryos resulted in severe inhibition of eGFP (Figure 9.1), as was reported for *eng2a* transcripts (Hinits and Hughes, 2007).
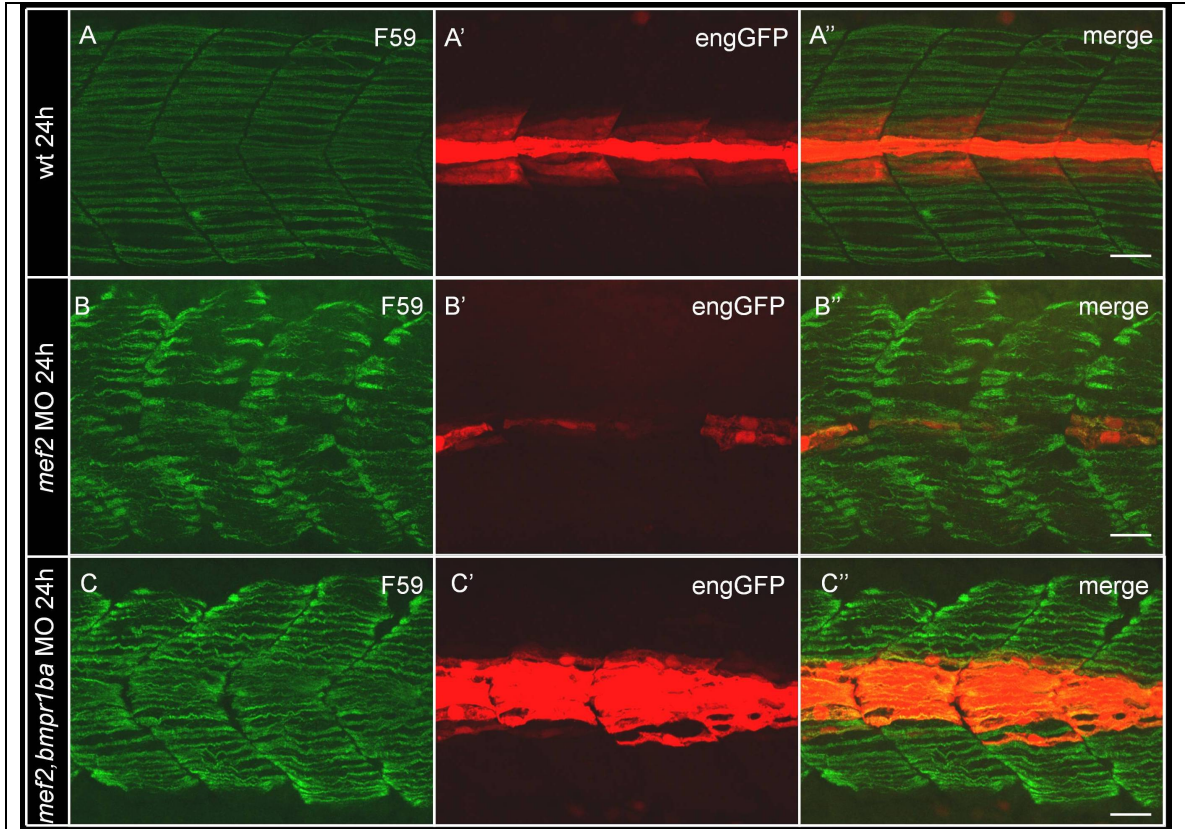
Figure 9.1: Mef2 is a permissive factor regulating *eng2a* gene expression.

A,A',A'' – Parasagittal optical section of a 24 h *Tg(eng2a:eGFP)^{i233}* embryo showing the normal distribution of slow fibers (green), MP and MFFs (in red).

B,B',B'' – Parasagittal optical section of a 24 h *Tg(eng2a:eGFP)^{i233}* embryo injected with *mef2* MO, showing poorly differentiated slow fibers and severely reduced engGFP expression.

C,C',C'' – Parasagittal optical section of a 24 h *Tg(eng2a:eGFP)^{i233}* embryo injected with *mef2* and *bmpr1ba* MO, showing recovery and also ectopic engGFP expression. Slow fiber differentiation also seems somewhat recovered. Scale bars are 25 microns.

I next asked if these myogenic factors are epistatic to Smad mediated repression of *eng*. For this, I co-injected the *mef2* and *bmpr1ba* MO into the *eng2a:eGFP* line. The *bmpr1ba* MO did significantly de-repress *eng2a:eGFP* in a lot more fibers compared to the *mef2* morphants alone (Figure 9.1), suggesting that pSmad mediated repression happens in parallel with *mef2* mediated activation of *eng*.

9.2. Analysis of other candidate regulators of eng2a *from the* trans-regulation screen

Secreted Frizzled Related Protein 2 (Sfrp2) - was identified as a positive regulator in the trans-regulatory screen; it is a secreted molecule that binds Wnt ligands and competes with their receptors (Frizzled) to modulate ligand availability. It is also known to modulate the spread of Wnt signaling and in this case has been shown to act as a positive regulator by increasing the range of Wnt ligands (Mii and Taira, 2009). Sfrp2 is also known to regulate both Wnt and BMP signaling levels when tested in mesenchymal stem cell culture (Alfaro et al., 2010).

I used a MO to knock down *sfrp2* gene function. MO injections did not result in any significant changes in either the number or pattern of Eng^{+ve} cells within the myotome. At higher doses the fibers looked malformed, which I assume is due to the toxicity of the MO. To test the effect of over-expressing *sfrp2*, I made a *UAS:sfrp2-UAS:tRFP* transgene and drove it in the myoblasts using the *actin:GAL4* driver line. The transient transgenic embryos did not show any discernible effect on the patterning and levels of *eng* expression in the myotome.

Midkine-a – Midkines are secreted heparin binding growth factors with neurotrophic activity in tissue culture assays and have been implicated in a number of developmental events like, neuronal survival, angiogenesis, wound healing and cancer (for review see Kadomatsu and Muramatsu, 2004). In zebrafish, *mdka* is expressed prior to MP, MFF fate specification in the paraxial mesoderm and sets apart MFP fate from the notochord after the initial induction in the organizer (Schafer et al., 2005). In order to distinguish between its effects on the specification of the notochord and its role in MP, MFF fate specification, I over expressed *mdka* using the *actin:GAL4*, UAS system. *mdka* even at high levels of ectopic expression did not result in any obvious effects on *eng2a:eGFP* expression in the myotome.

Chapter 10: Discussion

10.1. Proposed model for the cross talk between the Hh and BMP signaling pathway in the teleost myotome.

I set out to understand the differential response of cells to Hh signaling by studying the *cis*-regulation of a putative high threshold Hh target gene *eng2a* in the zebrafish myotome. Using transgenic analysis, I dissected the *eng2a* promoter and identified a minimal enhancer element that is sufficient to recapitulate the endogenous pattern of *eng2a* expression in the myotome. I then employed a tissue culture based screen to identify a number of candidate trans-regulators of the enhancer and discovered Smad5 to be a potent repressor of this element. Using a number of loss- and gain-of-function approaches to manipulate BMP and Hh signaling, I found that BMP signaling restricts the expression of Hh-induced Eng *in vivo*. In addition, I uncovered modulation of pSmad distribution in myotomal nuclei in response to Hh pathway activity. Based on various indirect lines of evidence, I conclude that this interaction between the two pathways is cell autonomous and postulate that it occurs at the level of Gli and Smad factors. To begin to test this model, I used an *in vivo* protein-protein interaction assay to investigate whether Gli and Smad proteins can in principle physically interact in embryonic myotomal cells. My data confirm and extending previous findings (Liu et al., 1998), showing that truncated repressor-like forms but not full-length forms of Gli2a can interact with active Smads to sequester them specifically in the nuclei. There remains a possibility that these experiments display over-expression artifacts, therefore stronger evidence for

such a mechanism would come from co-immuno-precipitation of endogenous Gli2 and Smad proteins.

The spatial distribution of active Smads within the myotome suggests the source of BMP ligands to be at the most dorsal and ventral regions of the somite (Figure 10.1 A). The *radar* gene, which encodes a member of the BMP family, is expressed at the right time and place to modulate Smad activation in the myotome (Kawakami et al., 2005; Rissi et al., 1995). In this view, a cell that is located more dorsally or ventrally in the developing myotome would receive higher levels of BMP and lower levels of Hh, resulting in it accumulating high levels of pSmad, whose activity will be potentiated by higher levels of Gli^R generated in cells that are distant from the Hh source, thereby inhibiting *eng* transcription (Figure 10.1). On the other hand, a cell located medially close to the Shh-secreting notochord, would be expected to have reduced levels of Gli^R insufficient to stabilize the low levels of pSmad generated at the low point of the BMP gradient, resulting in activation of Eng by Gli^A (Figure 10.1). In this way, Shh signaling would convert the graded distribution of BMP signals into a step function of Smad activity, thereby generating a sharp boundary of eng expression.

According to this model, Hh acts in two ways to control Eng in the myotome: (1) - It directly activates the *eng* enhancer, and (2) - it removes Gli^R resulting in destabilized pSmad (Figure 10.1 B). The finding that in *disp1* mutant embryos the removal of pSmad or the inactivation of PKA can both cell autonomously rescue Eng activation, supports the notion that Hh signaling functions primarily by removing pSmad mediated repression

of *eng*. The importance of the balance between pSmad and Gli activities for the correct regulation of *eng* expression is further underscored by the *dzip1* mutant phenotype. In this case, the effects of lowered Gli^A activity postulated to occur due to disruption of the primary cilium, are offset by the loss of nuclear pSmad accumulation in fast twitch myoblasts, a loss that we propose reflects a failure of processing Gli to its repressor form (Haycraft et al., 2005; Kim et al., 2010). Taken together, it follows that it is not the absolute level of Gli^A activity but rather the relative levels of Gli^A and pSmad present within the nucleus that is critical for the correct activation of the *eng* gene (Figure 10.1 B).
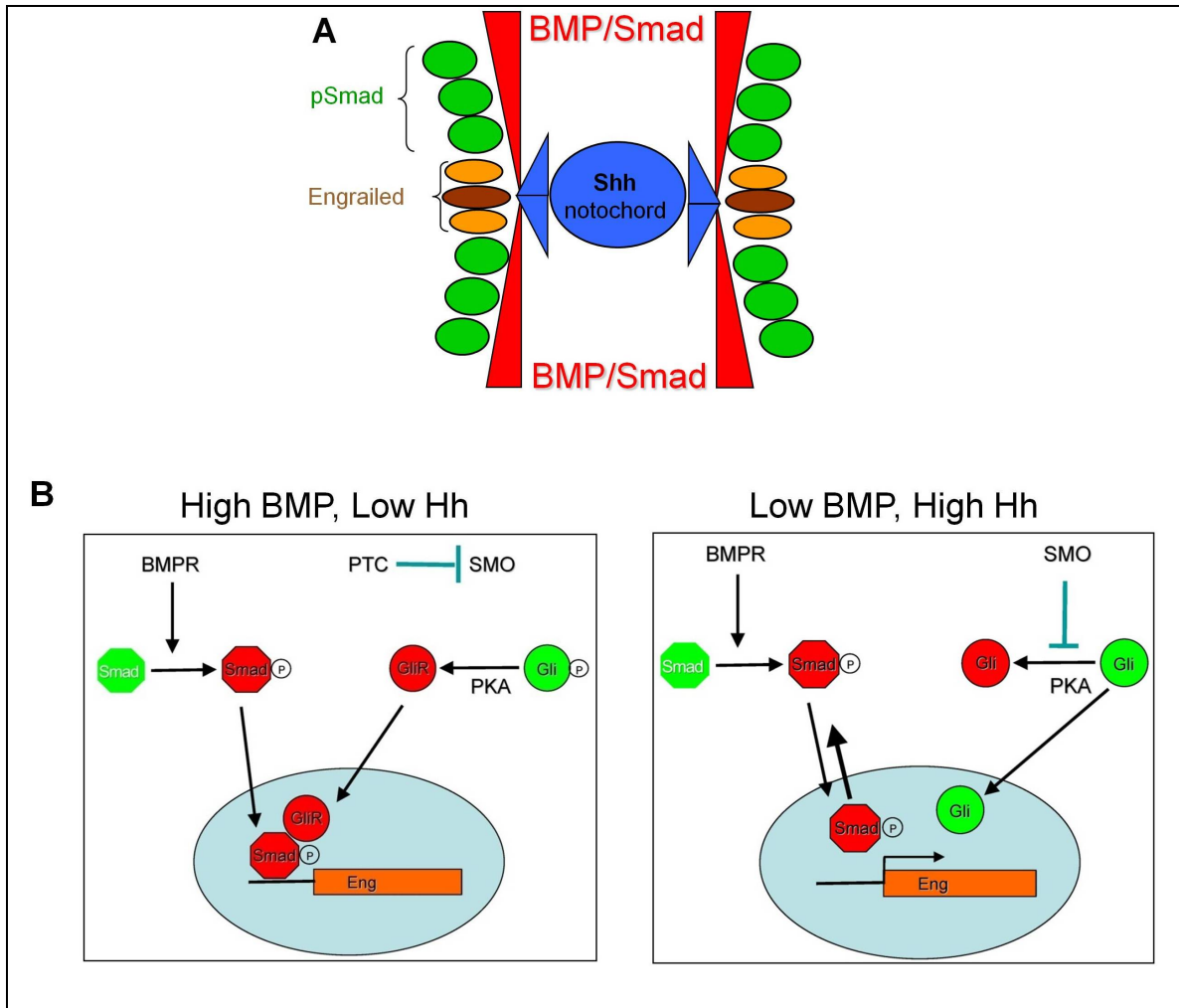
Figure 10.1: Patterning of the zebrafish myotome by antagonistic gradients of Shh and BMP and the model for cross-talk between the two pathways.

(A) - Schematic representation of a transverse section of the developing embryo showing the inferred distributions of Shh and BMP activities and their effects on myoblast identity. The most medially located myoblasts are postulated to respond to BMP activity emanating from dorsal and ventral regions of the somite by accumulating pSmad in their nuclei, with the exception of those closest to the source of Shh, the notochord. These cells activate *eng* expression in response to Gli^A activity and depletion of nuclear pSmad, both of which are promoted by high levels of Shh.

(B) - A model for the modulation of pSmad accumulation and regulation of the *eng2a* ME by Shh activity. In cells receiving relatively low levels of Shh and relatively high levels of BMP, accumulation of pSmad in the nucleus is promoted by the repressor forms

of the Gli proteins (red) that are generated in response to phosphorylation of the full length Glis. Accumulated pSmad binds to the *eng2a* ME, repressing transcription of the gene. In cells that see high levels of Shh and relatively low levels of BMP, the processing of the Glis is blocked: this results in depletion of pSmad from the nucleus and hence form the ME, favouring Gli[A] (green) binding and activation of transcription (Maurya et al., 2011).

As the levels of Smads in the myotome are limiting (section 8.10) and Hh positively regulates *smad* transcription, we can conclude that Hh makes the myotome more responsive to BMP ligands. So upregulation of Hh pathway activity will also induce an increase in BMP mediated *eng* repression. This could be one mechanism for countering the effects of excessive Hh signaling. Similarly when Hh pathway is slightly down-regulated this BMP mediated repression maybe slightly reduced. Such a mechanism would buffer the effects of mild perturbations in Hh pathway activity.

My findings also suggest that these mechanisms are likely to be conserved between zebrafish and the distantly related medaka. The distributions of Eng and pSmad in the somites of medaka embryos imply the same inhibitory and inverse relationship between Eng expression and BMP signaling operates in this species. Consistent with this, I found that the zebrafish *eng2a* ME is functional in medaka embryos, implying that the trans regulatory mechanism is conserved, despite the lack of sequence conservation of this element between the two species .

The expression and regulation of *eng* genes in the somites of zebrafish shows interesting parallels with their amniote orthologs. Within the chick and mouse somite, *eng* is expressed in restricted domains in the dermomyotome (Cheng et al., 2004; Davis et al., 1991). In the chick, *eng* expression is localized to cells that form the epaxial and hypaxial boundary, a structure possibly homologous to the fish horizontal myoseptum, which in zebrafish embryos is constituted of Eng[+ve] MP. Shh soaked beads can replace notochord and floor plate in their ability to maintain *eng* expression in chick somites, whereas Bmp4

soaked beads potently suppressed the dermomyotomal *eng* expression (Cheng et al., 2004). Therefore, despite the obvious differences in the organization of the teleost and amniote somite some aspects of cell specification seem to be conserved. Towards this end, in collaboration with Ray Dunn (Institute of Medical Biology, Singapore), I tested the activity of the 10 kb *eng2a* promoter fragment in mouse embryos in transient transgenics. We obtained one embryo that displayed expression in the MHB at embryonic day 12.5, but did not show detectable expression within the somites (data not shown).

In the course of this study, I have generated a number of transgenic lines and DNA constructs that will be useful for assaying and perturbing both Hh and BMP signaling pathways. The *Tg(eng2a:eGFP)^{i233}* reports the activity of both pathways and will also report defects in the formation of primary cilia, as is shown for *eng* transcription in *iguana* and maternal zygotic *polaris* mutants (Glazer et al., 2010; Huang and Schier, 2009; Kim et al., 2010; Sekimizu et al., 2004; Tay et al., 2010; Wolff et al., 2004), both of which show defects in the formation of cilia and expansion of *eng* expression in the fast fibers. Therefore this line could be used in forward genetic screens to isolate mutants with defects in Hh, BMP signaling pathways and also for defects in genes involved in primary cilia formation. Similarly, the *ptc* reporter lines will be useful to assay Hh signaling at single cell resolution not only in embryos but also in adults during homeostasis and during repair. Most of the lines generated for the UAS constructs became silenced in the next generation, which may be attributable to the large number of repeats (14 in each case) in the UAS sequences (Akitake et al., 2011; Goll et al., 2009). Despite the silencing of these UAS transgenes, the constructs can be adapted for

perturbing Hh and BMP pathway activity in other tissue types in a mosaic and transient manner.

10.2. Regulatory potential of myogenic factors

Mef2, a downstream factor in the myogenic program, has been implicated in controlling genes required for thick filament assembly in zebrafish embryonic muscle fibers (Hinits and Hughes, 2007). I have shown that the *eng2a* ME recapitulates the response of *eng* upon Mef2 depletion. Epistasis analysis between Mef2 and pSmad uncovered a permissive role for Mef2 in *eng* regulation, where the suppression of *eng* transcription upon Mef2 depletion can be rescued by simultaneous depletion of pSmad. Several open questions remain with regards to the role of Mef2 in regulating *eng*. Is Mef2 controlling the levels of BMP signaling? Is Mef2 a factor that modifies chromatin around the *eng2a*-ME to prime transcription (which would fit with its role as a permissive factor)? If so, then how in its absence, the inhibition of pSmad is still able to de-repress *eng*? Does Mef2 mediate the response of cells to Hh signaling and can hyper-activation of the Hh pathway circumvent the requirement for Mef2 in activating *eng*?

10.3. Future directions

The interplay between the Hh and BMP pathway in the myotome raises the possibility of a similar antagonism and interaction of the two pathways in the neural tube. Some evidence for such an interaction comes from studies in chick, where the induction of floor plate requires both Shh and a BMP inhibitor in the absence of the notochord (Patten and Placzek, 2002). Analysis of zebrafish mutants with defects in floor plate specification

also suggests contributions from another pathway (Odenthal et al., 2000). Do differing levels of Hh modulate the distribution of pSmad within the neural tube? If so, does it also occur at the level of Gli and Smad proteins?

The restricted expression of *eng* and its precise regulation by two important signaling pathways raises the question of its function within the myotome. Is it controlling boundary formation by regulating the expression of adhesion molecules? Or does it act as a signaling center controlling axon guidance and/or neural crest migration. These Eng^{+} cells act as choice points for primary motor neurons (Melancon et al., 1997) and for correct patterning of melanocytes (Svetic et al., 2007). What are the roles of BMP signaling within the zebrafish myotome, does it delay differentiation as is the case in the amniote myotome (Reshef et al., 1998) or does it control secondary slow fiber differentiation (Barresi et al., 2001) at the most dorsal and ventral regions of the somite, where the levels of BMP signaling are highest? MPs indeed do differentiate prior to the migrating slow fibers.

References

Agren, M., Kogerman, P., Kleman, M. I., Wessling, M. and Toftgard, R. (2004). Expression of the PTCH1 tumor suppressor gene is regulated by alternative promoters and a single functional Gli-binding site. *Gene* **330**, 101-14.

Akitake, C. M., Macurak, M., Halpern, M. E. and Goll, M. G. (2011). Transgenerational analysis of transcriptional silencing in zebrafish. *Dev Biol* **352**, 191-201.

Alcedo, J., Ayzenzon, M., Von Ohlen, T., Noll, M. and Hooper, J. E. (1996). The Drosophila smoothened gene encodes a seven-pass membrane protein, a putative receptor for the hedgehog signal. *Cell* **86**, 221-32.

Alexandre, C. (2008). Cuticle preparation of Drosophila embryos and larvae. *Methods Mol Biol* **420**, 197-205.

Alexandre, C., Jacinto, A. and Ingham, P. W. (1996). Transcriptional activation of *hedgehog* target genes in *Drosophila* is mediated directly by the cubitus interruptus protein, a member of the GLI family of zinc finger DNA-binding proteins. *Genes Dev* **10**, 2003-13.

Alfaro, M. P., Vincent, A., Saraswati, S., Thorne, C. A., Hong, C. C., Lee, E. and Young, P. P. (2010). sFRP2 suppression of bone morphogenic protein (BMP) and Wnt signaling mediates mesenchymal stem cell (MSC) self-renewal promoting engraftment and myocardial repair. *J Biol Chem* **285**, 35645-53.

Alves, G., Limbourg-Bouchon, B., Tricoire, H., Brissard-Zahraoui, J., Lamour-Isnard, C. and Busson, D. (1998). Modulation of Hedgehog target gene expression by the Fused serine-threonine kinase in wing imaginal discs. *Mech Dev* **78**, 17-31.

Aparicio, S., Morrison, A., Gould, A., Gilthorpe, J., Chaudhuri, C., Rigby, P., Krumlauf, R. and Brenner, S. (1995). Detecting conserved regulatory elements with the model genome of the Japanese puffer fish, Fugu rubripes. *Proc Natl Acad Sci U S A* **92**, 1684-8.

Aza-Blanc, P., Lin, H. Y., Ruiz i Altaba, A. and Kornberg, T. B. (2000). Expression of the vertebrate Gli proteins in Drosophila reveals a distribution of activator and repressor activities. *Development* **127**, 4293-301.

Aza-Blanc, P., Ramirez-Weber, F. A., Laget, M. P., Schwartz, C. and Kornberg, T. B. (1997). Proteolysis that is inhibited by *hedgehog* targets Cubitus interruptus protein to the nucleus and converts it to a repressor. *Cell* **89**, 1043-53.

Balciunas, D., Wangensteen, K. J., Wilber, A., Bell, J., Geurts, A., Sivasubbu, S., Wang, X., Hackett, P. B., Largaespada, D. A., McIvor, R. S. et al. (2006). Harnessing a High Cargo-Capacity Transposon for Genetic Applications in Vertebrates. *PLoS Genet* **2**, e169.

Barresi, M. J., D'Angelo, J. A., Hernandez, L. P. and Devoto, S. H. (2001). Distinct mechanisms regulate slow-muscle development. *Curr Biol* **11**, 1432-8.

Barth, K. A., Kishimoto, Y., Rohr, K. B., Seydler, C., Schulte-Merker, S. and Wilson, S. W. (1999). Bmp activity establishes a gradient of positional information throughout the entire neural plate. *Development* **126**, 4977-4987.

Basler, K., Edlund, T., Jessell, T. M. and Yamada, T. (1993). Control of cell pattern in the neural tube: Regulation of cell differentiation by dorsalin-1, a novel TGFβ family member. *Cell* **73**, 687-702.

Baxendale, S., Davison, C., Muxworthy, C., Wolff, C., Ingham, P. W. and Roy, S. (2004). The B-cell maturation factor Blimp-1 specifies vertebrate slow-twitch muscle fiber identity in response to Hedgehog signaling. *Nat Genet* **36**, 88-93.

Beaster-Jones, L., Schubert, M. and Holland, L. Z. (2007). Cis-regulation of the amphioxus *engrailed* gene: insights into evolution of a muscle-specific enhancer. *Mech Dev* **124**, 532-42.

Bejerano, G., Lowe, C. B., Ahituv, N., King, B., Siepel, A., Salama, S. R., Rubin, E. M., Kent, W. J. and Haussler, D. (2006). A distal enhancer and an ultraconserved exon are derived from a novel retroposon. *Nature* **441**, 87-90.

Blagden, C. S., Currie, P. D., Ingham, P. W. and Hughes, S. M. (1997). Notochord induction of zebrafish slow muscle mediated by Sonic hedgehog. *Genes Dev* **11**, 2163-75.

Brand, M., Heisenberg, C. P., Warga, R. M., Pelegri, F., Karlstrom, R. O., Beuchle, D., Picker, A., Jiang, Y. J., Furutani-Seiki, M., van Eeden, F. J. et al. (1996). Mutations affecting development of the midline and general body shape during zebrafish embryogenesis. *Development* **123**, 129-42.

Briscoe, J., Chen, Y., Jessell, T. M. and Struhl, G. (2001). A hedgehog-insensitive form of patched provides evidence for direct long-range morphogen activity of sonic hedgehog in the neural tube. *Mol Cell* **7**, 1279-91.

Briscoe, J. and Ericson, J. (1999). The specification of neuronal identity by graded Sonic Hedgehog signalling. *Semin Cell Dev Biol* **10**, 353-62.

Briscoe, J., Pierani, A., Jessell, T. M. and Ericson, J. (2000). A homeodomain protein code specifies progenitor cell identity and neuronal fate in the ventral neural tube. *Cell* **101**, 435-45.

Brockes, J. (1991). Developmental biology. We may not have a morphogen. *Nature* **350**, 15.

Bumcrot, D. A., Takada, R. and McMahon, A. P. (1995). Proteolytic processing yields two secreted forms of sonic hedgehog. *Mol Cell Biol* **15**, 2294-303.

Burke, R., Nellen, D., Bellotto, M., Hafen, E., Senti, K. A., Dickson, B. J. and Basler, K. (1999). Dispatched, a novel sterol-sensing domain protein dedicated to the release of cholesterol-modified hedgehog from signaling cells. *Cell* **99**, 803-15.

Carpenter, D. (1998). Characterization of two patched receptors for the vertebrate hedgehog protein family. *Proc. Natl Acad. Sci. USA* **95**, 13630.

Caspary, T., Garcia-Garcia, M. J., Huangfu, D., Eggenschwiler, J. T., Wyler, M. R., Rakeman, A. S., Alcorn, H. L. and Anderson, K. V. (2002). Mouse Dispatched homolog1 is required for long-range, but not juxtacrine, Hh signaling. *Curr Biol* **12**, 1628-32.

Chamoun, Z., Mann, R. K., Nellen, D., von Kessler, D. P., Bellotto, M., Beachy, P. A. and Basler, K. (2001). Skinny hedgehog, an acyltransferase required for palmitoylation and activity of the hedgehog signal. *Science* **293**, 2080-4.

Chandrasekhar, A., Schauerte, H. E., Haffter, P. and Kuwada, J. Y. (1999). The zebrafish detour gene is essential for cranial but not spinal motor neuron induction. *Development* **126**, 2727-37.

Chen, W., Burgess, S. and Hopkins, N. (2001). Analysis of the zebrafish smoothened mutant reveals conserved and divergent functions of hedgehog activity. *Development* **128**, 2385-96.

Chen, Y. and Struhl, G. (1996). Dual roles for patched in sequestering and transducing Hedgehog. *Cell* **87**, 553-63.

Cheng, L., Alvares, L. E., Ahmed, M. U., El-Hanfy, A. S. and Dietrich, S. (2004). The epaxial-hypaxial subdivision of the avian somite. *Dev Biol* **274**, 348-69.

Cheung, H. O., Zhang, X., Ribeiro, A., Mo, R., Makino, S., Puviindran, V., Law, K. K., Briscoe, J. and Hui, C. C. (2009). The kinesin protein Kif7 is a critical regulator of Gli transcription factors in mammalian hedgehog signaling. *Sci Signal* **2**, ra29.

Chiang, C., Litingtung, Y., Lee, E., Young, K. E., Corden, J. L., Westphal, H. and Beachy, P. A. (1996). Cyclopia and defective axial patterning in mice lacking Sonic hedgehog gene function. *Nature* **383**, 407-13.

Concordet, J. P., Lewis, K. E., Moore, J. W., Goodrich, L. V., Johnson, R. L., Scott, M. P. and Ingham, P. W. (1996). Spatial regulation of a zebrafish *patched* homologue reflects the roles of *sonic hedgehog* and protein kinase A in neural tube and somite patterning. *Development* **122**, 2835-46.

Corbit, K. C., Aanstad, P., Singla, V., Norman, A. R., Stainier, D. Y. and Reiter, J. F. (2005). Vertebrate Smoothened functions at the primary cilium. *Nature* **437**, 1018-21.

Corish, P. and Tyler-Smith, C. (1999). Attenuation of green fluorescent protein half-life in mammalian cells. *Protein Eng* **12**, 1035-40.

Currie, P. D. and Ingham, P. W. (1996). Induction of a specific muscle cell type by a hedgehog-like protein in zebrafish. *Nature* **382**, 452-5.

Dai, P., Akimaru, H., Tanaka, Y., Maekawa, T., Nakafuku, M. and Ishii, S. (1999). Sonic Hedgehog-induced activation of the Gli1 promoter is mediated by GLI3. *J Biol Chem* **274**, 8143-52.

Davis, C. A., Holmyard, D. P., Millen, K. J. and Joyner, A. L. (1991). Examining pattern formation in mouse, chicken and frog embryos with an En-specific antiserum. *Development* **111**, 287-298.

Denef, N., Neubuser, D., Perez, L. and Cohen, S. M. (2000). Hedgehog induces opposite changes in turnover and subcellular localization of patched and smoothened. *Cell* **102**, 521-31.

Devoto, S. H., Melancon, E., Eisen, J. S. and Westerfield, M. (1996). Identification of separate slow and fast muscle precursor cells *in-vivo*, prior to somite formation. *Development* **122**, 3371-80.

di Magliano, M. P. and Hebrok, M. (2003). Hedgehog signalling in cancer formation and maintenance. *Nat Rev Cancer* **3**, 903.

Dick, A., Andrea, M. and Matthias, H. (1999). Smad1 and Smad5 have distinct roles during dorsoventral patterning of the zebrafish embryo. *Developmental Dynamics* **216**, 285-298.

Echelard, Y., Epstein, D. J., St-Jacques, B., Shen, L., Mohler, J., McMahon, J. A. and McMahon, A. P. (1993). Sonic hedgehog, a member of a family of putative signaling molecules, is implicated in the regulation of CNS polarity. *Cell* **75**, 1417-30.

Eggenschwiler, J. T. and Anderson, K. V. (2007). Cilia and developmental signaling. *Annu Rev Cell Dev Biol* **23**, 345-73.

Ekker, M., Wegner, J., Akimenko, M. A. and Westerfield, M. (1992). Coordinate embryonic expression of three zebrafish engrailed genes. *Development* **116**, 1001-10.

Endoh-Yamagami, S., Evangelista, M., Wilson, D., Wen, X., Theunissen, J. W., Phamluong, K., Davis, M., Scales, S. J., Solloway, M. J., de Sauvage, F. J. et al. (2009). The mammalian Cos2 homolog Kif7 plays an essential role in modulating Hh signal transduction during development. *Curr Biol* **19**, 1320-6.

Ericson, J., Briscoe, J., Rashbass, P., van Heyningen, V. and Jessell, T. M. (1997). Graded sonic hedgehog signaling and the specification of cell fate in the ventral neural tube. *Cold Spring Harb Symp Quant Biol* **62**, 451-66.

Fietz, M. J., Concordet, J. P., Barbosa, R., Johnson, R., Krauss, S., McMahon, A. P., Tabin, C. and Ingham, P. W. (1994). The hedgehog gene family in Drosophila and vertebrate development. *Dev Suppl*, 43-51.

Fischer, J. A., Giniger, E., Maniatis, T. and Ptashne, M. (1988). GAL4 activates transcription in Drosophila. *Nature* **332**, 853.

Forbes, A. J., Nakano, Y., Taylor, A. M. and Ingham, P. W. (1993). Genetic analysis of hedgehog signalling in the Drosophila embryo. *Dev Suppl*, 115-24.

Garcia-Bellido, A., Ripoll, P. and Morata, G. (1976). Developmental compartmentalization in the dorsal mesothoracic disc of Drosophila. *Dev Biol* **48**, 132-47.

Glasgow, E. and Tomarev, S. I. (1998). Restricted expression of the homeobox gene prox 1 in developing zebrafish. *Mech Dev* **76**, 175-8.

Glazer, A. M., Wilkinson, A. W., Backer, C. B., Lapan, S. W., Gutzman, J. H., Cheeseman, I. M. and Reddien, P. W. (2010). The Zn Finger protein Iguana impacts Hedgehog signaling by promoting ciliogenesis. *Developmental Biology* **337**, 148-156.

Goll, M. G., Anderson, R., Stainier, D. Y., Spradling, A. C. and Halpern, M. E. (2009). Transcriptional silencing and reactivation in transgenic zebrafish. *Genetics* **182**, 747-55.

Goodrich, L. V., Johnson, R. L., Milenkovic, L., McMahon, J. A. and Scott, M. P. (1996). Conservation of the hedgehog/patched signaling pathway from flies to mice: induction of a mouse patched gene by Hedgehog. *Genes Dev* **10**, 301-12.

Goodrich, L. V., Milenkovic, L., Higgins, K. M. and Scott, M. P. (1997). Altered neural cell fates and medulloblastoma in mouse patched mutants. *Science* **277**, 1109.

Graff, J. M., Bansal, A. and Melton, D. A. (1996). Xenopus Mad proteins transduce distinct subsets of signals for the TGF-β superfamily. *Cell* **85**, 479-487.

Gritli-Linde, A., Lewis, P., McMahon, A. P. and Linde, A. (2001). The whereabouts of a morphogen: direct evidence for short- and graded long-range activity of hedgehog signaling peptides. *Dev Biol* **236**, 364-86.

Gustafsson, M. K., Pan, H., Pinney, D. F., Liu, Y., Lewandowski, A., Epstein, D. J. and Emerson, C. P., Jr. (2002). *Myf5* is a direct target of long-range Shh signaling and Gli regulation for muscle specification. *Genes Dev* **16**, 114-26.

Hammerschmidt, M., Bitgood, M. J. and McMahon, A. P. (1996). Protein kinase A is a common negative regulator of Hedgehog signaling in the vertebrate embryo. *Genes Dev* **10**, 647-58.

Harvey, S. A. and Smith, J. C. (2009). Visualisation and Quantification of Morphogen Gradient Formation in the Zebrafish. *PLoS Biol* **7**, e1000101.

Hatta, K., Bremiller, R., Westerfield, M. and Kimmel, C. B. (1991). Diversity of expression of engrailed-like antigens in zebrafish. *Development* **112**, 821-32.

Hatta, K., Tsujii, H. and Omura, T. (2006). Cell tracking using a photoconvertible fluorescent protein. *Nat. Protocols* **1**, 960.

Haycraft, C. J., Banizs, B., Aydin-Son, Y., Zhang, Q., Michaud, E. J. and Yoder, B. K. (2005). Gli2 and Gli3 localize to cilia and require the intraflagellar transport protein polaris for processing and function. *PLoS Genet* **1**, e53.

Henry, C. A. and Amacher, S. L. (2004). Zebrafish slow muscle cell migration induces a wave of fast muscle morphogenesis. *Dev Cell* **7**, 917-23.

Hepker, J., Wang, Q. T., Motzny, C. K., Holmgren, R. and Orenic, T. V. (1997). Drosophila cubitus interruptus forms a negative feedback loop with patched and regulates expression of Hedgehog target genes. *Development* **124**, 549-58.

Hinits, Y. and Hughes, S. M. (2007). Mef2s are required for thick filament formation in nascent muscle fibres. *Development* **134**, 2511-9.

Hirsinger, E., Stellabotte, F., Devoto, S. H. and Westerfield, M. (2004). Hedgehog signaling is required for commitment but not initial induction of slow muscle precursors. *Dev Biol* **275**, 143-57.

Hollway, G. E., Maule, J., Gautier, P., Evans, T. M., Keenan, D. G., Lohs, C., Fischer, D., Wicking, C. and Currie, P. D. (2006). Scube2 mediates Hedgehog signalling in the zebrafish embryo. *Dev Biol* **294**, 104-18.

Hoodless, P. A. (1996). MADR1, a MAD-related protein that functions in BMP2 signaling pathways. *Cell* **85**, 489-500.

Hooper, J. E. and Scott, M. P. (1989). The Drosophila patched gene encodes a putative membrane protein required for segmental patterning. *Cell* **59**, 751-65.

Hooper, J. E. and Scott, M. P. (2005). Communicating with Hedgehogs. *Nat Rev Mol Cell Biol* **6**, 306-17.

Hu, C. D., Chinenov, Y. and Kerppola, T. K. (2002). Visualization of interactions among bZIP and Rel family proteins in living cells using bimolecular fluorescence complementation. *Mol Cell* **9**, 789-98.

Huang, P. and Schier, A. F. (2009). Dampened Hedgehog signaling but normal Wnt signaling in zebrafish without cilia. *Development* **136**, 3089-3098.

Huangfu, D., Liu, A., Rakeman, A. S., Murcia, N. S., Niswander, L. and Anderson, K. V. (2003). Hedgehog signalling in the mouse requires intraflagellar transport proteins. *Nature* **426**, 83-7.

Hui, C. C. and Joyner, A. L. (1993). A mouse model of greig cephalopolysyndactyly syndrome: the extra-toesJ mutation contains an intragenic deletion of the Gli3 gene. *Nat Genet* **3**, 241-6.

Hynes, M., Stone, D. M., Dowd, M., Pitts-Meek, S., Goddard, A., Gurney, A. and Rosenthal, A. (1997). Control of cell pattern in the neural tube by the zinc finger transcription factor and oncogene Gli-1. *Neuron* **19**, 15-26.

Hynes, M., Ye, W., Wang, K., Stone, D., Murone, M., Sauvage, F. and Rosenthal, A. (2000). The seven-transmembrane receptor smoothened cell-autonomously induces multiple ventral cell types. *Nat Neurosci* **3**, 41-6.

Imamura, T. (1997). Smad6 is an inhibitor in the TGF-β superfamily signalling. *Nature* **389**, 622-626.

Incardona, J. P., Lee, J. H., Robertson, C. P., Enga, K., Kapur, R. P. and Roelink, H. (2000). Receptor-mediated endocytosis of soluble and membrane-tethered Sonic hedgehog by Patched-1. *Proc Natl Acad Sci U S A* **97**, 12044-9.

Ingham, P. W. (1991). Segment polarity genes and cell patterning within the Drosophila body segment. *Curr Opin Genet Dev* **1**, 261-7.

Ingham, P. W. and Fietz, M. J. (1995). Quantitative effects of hedgehog and decapentaplegic activity on the patterning of the Drosophila wing. *Curr Biol* **5**, 432-40.

Ingham, P. W. and Kim, H. R. (2005). Hedgehog signalling and the specification of muscle cell identity in the zebrafish embryo. *Exp Cell Res* **306**, 336-42.

Ingham, P. W. and McMahon, A. P. (2001). Hedgehog signaling in animal development: paradigms and principles. *Genes Dev* **15**, 3059-87.

Ingham, P. W. and McMahon, A. P. (2009). Hedgehog signalling: Kif7 is not that fishy after all. *Curr Biol* **19**, R729-31.

Ingham, P. W., Taylor, A. M. and Nakano, Y. (1991). Role of the Drosophila patched gene in positional signalling. *Nature* **353**, 184-7.

James, L. F., Panter, K. E., Gaffield, W. and Molyneux, R. J. (2004). Biomedical applications of poisonous plant research. *J Agric Food Chem* **52**, 3211-30.

Johnson, R. L., Milenkovic, L. and Scott, M. P. (2000). In vivo functions of the patched protein: requirement of the C terminus for target gene inactivation but not Hedgehog sequestration. *Mol Cell* **6**, 467-78.

Kadomatsu, K. and Muramatsu, T. (2004). Midkine and pleiotrophin in neural development and cancer. *Cancer Lett* **204**, 127-43.

Karlstrom, R. O., Talbot, W. S. and Schier, A. F. (1999). Comparative synteny cloning of zebrafish you-too: mutations in the Hedgehog target gli2 affect ventral forebrain patterning. *Genes Dev* **13**, 388-93.

Karlstrom, R. O., Tyurina, O. V., Kawakami, A., Nishioka, N., Talbot, W. S., Sasaki, H. and Schier, A. F. (2003). Genetic analysis of zebrafish *gli1* and *gli2* reveals divergent requirements for *gli* genes in vertebrate development. *Development* **130**, 1549-64.

Kawahara, A., Che, Y. S., Hanaoka, R., Takeda, H. and Dawid, I. B. (2005). Zebrafish GADD45beta genes are involved in somite segmentation. *Proc Natl Acad Sci U S A* **102**, 361-6.

Kawakami, A., Nojima, Y., Toyoda, A., Takahoko, M., Satoh, M., Tanaka, H., Wada, H., Masai, I., Terasaki, H., Sakaki, Y. et al. (2005). The zebrafish-secreted matrix protein you/scube2 is implicated in long-range regulation of hedgehog signaling. *Curr Biol* **15**, 480-8.

Kawakami, T., Kawcak, T., Li, Y. J., Zhang, W., Hu, Y. and Chuang, P. T. (2002). Mouse *dispatched* mutants fail to distribute hedgehog proteins and are defective in hedgehog signaling. *Development* **129**, 5753-65.

Ke, Z., Emelyanov, A., Lim, S. E., Korzh, V. and Gong, Z. (2005). Expression of a novel zebrafish zinc finger gene, gli2b, is affected in Hedgehog and Notch signaling related mutants during embryonic development. *Dev Dyn* **232**, 479-86.

Khaliullina, H., Panakova, D., Eugster, C., Riedel, F., Carvalho, M. and Eaton, S. (2009). Patched regulates Smoothened trafficking using lipoprotein-derived lipids. *Development* **136**, 4111-21.

Kim, H., Richardson, J., van Eeden, F. and Ingham, P. (2010). Gli2a protein localization reveals a role for Iguana/DZIP1 in primary ciliogenesis and a dependence of Hedgehog signal transduction on primary cilia in the zebrafish. *BMC Biology* **8**, 65.

Konig, C., Yan, Y. L., Postlethwait, J., Wendler, S. and Campos-Ortega, J. A. (1999). A recessive mutation leading to vertebral ankylosis in zebrafish is associated with amino acid alterations in the homologue of the human membrane-associated guanylate kinase DLG3. *Mech Dev* **86**, 17-28.

Koudijs, M. J., den Broeder, M. J., Groot, E. and van Eeden, F. J. (2008). Genetic analysis of the two zebrafish *patched* homologues identifies novel roles for the hedgehog signaling pathway. *BMC Dev Biol* **8**, 15.

Koudijs, M. J., den Broeder, M. J., Keijser, A., Wienholds, E., Houwing, S., van Rooijen, E. M., Geisler, R. and van Eeden, F. J. (2005). The zebrafish mutants *dre*, *uki*, and *lep* encode negative regulators of the hedgehog signaling pathway. *PLoS Genet* **1**, e19.

Krauss, S., Concordet, J. P. and Ingham, P. W. (1993). A functionally conserved homolog of the Drosophila segment polarity gene *hh* is expressed in tissues with polarizing activity in zebrafish embryos. *Cell* **75**, 1431-44.

Kretzschmar, M., Liu, F., Hata, A., Doody, J. and Massague, J. (1997). The TGF-β family mediator Smad1 is phosphorylated directly and activated functionally by the BMP receptor kinase. *Genes Dev.* **11**, 984-995.

Laner-Plamberger, S., Kaser, A., Paulischta, M., Hauser-Kronberger, C., Eichberger, T. and Frischauf, A. M. (2009). Cooperation between GLI and JUN enhances transcription of JUN and selected GLI target genes. *Oncogene* **28**, 1639-51.

Lee, E. C., Yu, D., Martinez de Velasco, J., Tessarollo, L., Swing, D. A., Court, D. L., Jenkins, N. A. and Copeland, N. G. (2001). A highly efficient Escherichia coli-based chromosome engineering system adapted for recombinogenic targeting and subcloning of BAC DNA. *Genomics* **73**, 56-65.

Lee, J., Platt, K. A., Censullo, P. and Ruiz i Altaba, A. (1997). Gli1 is a target of Sonic hedgehog that induces ventral neural tube development. *Development* **124**, 2537-52.

Lee, J. J., Ekker, S. C., von Kessler, D. P., Porter, J. A., Sun, B. I. and Beachy, P. A. (1994). Autoproteolysis in hedgehog protein biogenesis. *Science* **266**, 1528-37.

Lee, J. J., von Kessler, D. P., Parks, S. and Beachy, P. A. (1992). Secretion and localized transcription suggest a role in positional signaling for products of the segmentation gene hedgehog. *Cell* **71**, 33-50.

Lee, K. J., Dietrich, P. and Jessell, T. M. (2000). Genetic ablation reveals that the roof plate is essential for dorsal interneuron specification. *Nature* **403**, 734-40.

Lee, K. J., Mendelsohn, M. and Jessell, T. M. (1998). Neuronal patterning by BMPs: a requirement for GDF7 in the generation of a discrete class of commissural interneurons in the mouse spinal cord. *Genes Dev* **12**, 3394-407.

Lettre, G., Jackson, A. U., Gieger, C., Schumacher, F. R., Berndt, S. I., Sanna, S., Eyheramendy, S., Voight, B. F., Butler, J. L., Guiducci, C. et al. (2008). Identification of ten loci associated with height highlights new biological pathways in human growth. *Nat Genet* **40**, 584-91.

Leung, A. Y., Mendenhall, E. M., Kwan, T. T., Liang, R., Eckfeldt, C., Chen, E., Hammerschmidt, M., Grindley, S., Ekker, S. C. and Verfaillie, C. M. (2005). Characterization of expanded intermediate cell mass in zebrafish chordin morphant embryos. *Dev Biol* **277**, 235-54.

Lewis, K. E., Concordet, J. P. and Ingham, P. W. (1999a). Characterisation of a second patched gene in the zebrafish Danio rerio and the differential response of patched genes to Hedgehog signalling. *Dev Biol* **208**, 14-29.

Lewis, K. E., Currie, P. D., Roy, S., Schauerte, H., Haffter, P. and Ingham, P. W. (1999b). Control of muscle cell-type specification in the zebrafish embryo by Hedgehog signalling. *Dev Biol* **216**, 469-80.

Liem, K. F., Jr., He, M., Ocbina, P. J. and Anderson, K. V. (2009). Mouse Kif7/Costal2 is a cilia-associated protein that regulates Sonic hedgehog signaling. *Proc Natl Acad Sci U S A* **106**, 13377-82.

Liem, K. F., Jr., Jessell, T. M. and Briscoe, J. (2000). Regulation of the neural patterning activity of sonic hedgehog by secreted BMP inhibitors expressed by notochord and somites. *Development* **127**, 4855-66.

Liem, K. F., Jr., Tremml, G. and Jessell, T. M. (1997). A role for the roof plate and its resident TGFbeta-related proteins in neuronal patterning in the dorsal spinal cord. *Cell* **91**, 127-38.

Liem, K. F., Jr., Tremml, G., Roelink, H. and Jessell, T. M. (1995). Dorsal differentiation of neural plate cells induced by BMP-mediated signals from epidermal ectoderm. *Cell* **82**, 969-79.

Litingtung, Y. and Chiang, C. (2000). Specification of ventral neuron types is mediated by an antagonistic interaction between Shh and Gli3. *Nat Neurosci* **3**, 979-85.

Liu, F. (1996). A human Mad protein acting as a BMP-regulated transcriptional activator. *Nature* **381**, 620-623.

Liu, F., Massague, J. and Ruiz i Altaba, A. (1998). Carboxy-terminally truncated Gli3 proteins associate with Smads. *Nat Genet* **20**, 325-6.

Logan, C., Khoo, W. K., Cado, D. and Joyner, A. L. (1993). Two enhancer regions in the mouse En-2 locus direct expression to the mid/hindbrain region and mandibular myoblasts. *Development* **117**, 905-16.

Ma, Y., Erkner, A., Gong, R., Yao, S., Taipale, J., Basler, K. and Beachy, P. A. (2002). Hedgehog-mediated patterning of the mammalian embryo requires transporter-like function of dispatched. *Cell* **111**, 63-75.

Marigo, V., Johnson, R. L., Vortkamp, A. and Tabin, C. J. (1996a). Sonic hedgehog differentially regulates expression of GLI and GLI3 during limb development. *Dev Biol* **180**, 273-83.

Marigo, V., Scott, M. P., Johnson, R. L., Goodrich, L. V. and Tabin, C. J. (1996b). Conservation in hedgehog signaling: induction of a chicken patched homolog by Sonic hedgehog in the developing limb. *Development* **122**, 1225-33.

Marigo, V. and Tabin, C. J. (1996). Regulation of patched by sonic hedgehog in the developing neural tube. *Proc Natl Acad Sci U S A* **93**, 9346-51.

Marti, E., Bumcrot, D. A., Takada, R. and McMahon, A. P. (1995). Requirement of 19K form of Sonic hedgehog for induction of distinct ventral cell types in CNS explants. *Nature* **375**, 322-5.

Maurya, A. K., Tan, H., Souren, M., Wang, X., Wittbrodt, J. and Ingham, P. W. (2011). Integration of Hedgehog and BMP signalling by the engrailed2a gene in the zebrafish myotome. *Development* **138**, 755-765.

McMahon, J. A., Takada, S., Zimmerman, L. B., Fan, C. M., Harland, R. M. and McMahon, A. P. (1998). Noggin-mediated antagonism of BMP signaling is required for growth and patterning of the neural tube and somite. *Genes Dev* **12**, 1438-52.

McReynolds, L. J., Gupta, S., Figueroa, M. E., Mullins, M. C. and Evans, T. (2007). Smad1 and Smad5 differentially regulate embryonic hematopoiesis. *Blood* **110**, 3881-90.

Mekki-Dauriac, S., Agius, E., Kan, P. and Cochard, P. (2002). Bone morphogenetic proteins negatively control oligodendrocyte precursor specification in the chick spinal cord. *Development* **129**, 5117-30.

Melancon, E., Liu, D. W., Westerfield, M. and Eisen, J. S. (1997). Pathfinding by identified zebrafish motoneurons in the absence of muscle pioneers. *J Neurosci* **17**, 7796-804.

Methot, N. and Basler, K. (1999). Hedgehog controls limb development by regulating the activities of distinct transcriptional activator and repressor forms of Cubitus interruptus. *Cell* **96**, 819-31.

Methot, N. and Basler, K. (2000). Suppressor of fused opposes hedgehog signal transduction by impeding nuclear accumulation of the activator form of Cubitus interruptus. *Development* **127**, 4001-10.

Mii, Y. and Taira, M. (2009). Secreted Frizzled-related proteins enhance the diffusion of Wnt ligands and expand their signalling range. *Development* **136**, 4083-8.

Mohler, J. and Vani, K. (1992). Molecular organization and embryonic expression of the hedgehog gene involved in cell-cell communication in segmental patterning of Drosophila. *Development* **115**, 957-71.

Motoyama, J., Takabatake, T., Takeshima, K. and Hui, C. (1998). Ptch2, a second mouse Patched gene is co-expressed with Sonic hedgehog. *Nat Genet* **18**, 104-6.

Muller, B. and Basler, K. (2000). The repressor and activator forms of Cubitus interruptus control Hedgehog target genes through common generic gli-binding sites. *Development* **127**, 2999-3007.

Mullor, J. L., Calleja, M., Capdevila, J. and Guerrero, I. (1997). Hedgehog activity, independent of decapentaplegic, participates in wing disc patterning. *Development* **124**, 1227-37.

Mullor, J. L., Dahmane, N., Sun, T. and Ruiz i Altaba, A. (2001). Wnt signals are targets and mediators of Gli function. *Curr. Biol.* **11**, 769.

Nakano, Y., Guerrero, I., Hidalgo, A., Taylor, A., Whittle, J. R. and Ingham, P. W. (1989). A protein with several possible membrane-spanning domains encoded by the Drosophila segment polarity gene patched. *Nature* **341**, 508-13.

Nakano, Y., Kim, H. R., Kawakami, A., Roy, S., Schier, A. F. and Ingham, P. W. (2004). Inactivation of *dispatched 1* by the *chameleon* mutation disrupts Hedgehog signalling in the zebrafish embryo. *Dev Biol* **269**, 381-92.

Nieuwenhuis, E., Motoyama, J., Barnfield, P. C., Yoshikawa, Y., Zhang, X., Mo, R., Crackower, M. A. and Hui, C. C. (2006). Mice with a targeted mutation of patched2 are viable but develop alopecia and epidermal hyperplasia. *Mol Cell Biol* **26**, 6609-22.

Nikaido, M., Tada, M. and Ueno, N. (1999). Restricted expression of the receptor serine/threonine kinase BMPR-IB in zebrafish. *Mech Dev* **82**, 219-22.

Nobrega, M. A., Ovcharenko, I., Afzal, V. and Rubin, E. M. (2003). Scanning human gene deserts for long-range enhancers. *Science* **302**, 413.

Nusslein-Volhard, C. and Wieschaus, E. (1980). Mutations affecting segment number and polarity in Drosophila. *Nature* **287**, 795.

Odenthal, J., van Eeden, F. J., Haffter, P., Ingham, P. W. and Nusslein-Volhard, C. (2000). Two distinct cell populations in the floor plate of the zebrafish are induced by different pathways. *Dev Biol* **219**, 350-63.

Ohlig, S., Farshi, P., Pickhinke, U., van den Boom, J., Hoing, S., Jakuschev, S., Hoffmann, D., Dreier, R., Scholer, H. R., Dierker, T. et al. (2011). Sonic hedgehog shedding results in functional activation of the solubilized protein. *Dev Cell* **20**, 764-74.

Park, H. L., Bai, C., Platt, K. A., Matise, M. P., Beeghly, A., Hui, C. C., Nakashima, M. and Joyner, A. L. (2000). Mouse Gli1 mutants are viable but have defects in SHH signaling in combination with a Gli2 mutation. *Development* **127**, 1593-605.

Patel, N. H., Martin-Blanco, E., Coleman, K. G., Poole, S. J., Ellis, M. C., Kornberg, T. B. and Goodman, C. S. (1989). Expression of engrailed proteins in arthropods, annelids, and chordates. *Cell* **58**, 955-968.

Patten, I. and Placzek, M. (2002). Opponent activities of Shh and BMP signaling during floor plate induction in vivo. *Curr Biol* **12**, 47-52.

Patterson, S. E., Bird, N. C. and Devoto, S. H. (2010). BMP regulation of myogenesis in zebrafish. *Dev Dyn* **239**, 806-17.

Persson, M., Stamataki, D., te Welscher, P., Andersson, E., Bose, J., Ruther, U., Ericson, J. and Briscoe, J. (2002). Dorsal-ventral patterning of the spinal cord requires Gli3 transcriptional repressor activity. *Genes Dev* **16**, 2865-78.

Philipp, M., Fralish, G. B., Meloni, A. R., Chen, W., MacInnes, A. W., Barak, L. S. and Caron, M. G. (2008). Smoothened signaling in vertebrates is facilitated by a G protein-coupled receptor kinase. *Mol Biol Cell* **19**, 5478-89.

Porter, J. A., von Kessler, D. P., Ekker, S. C., Young, K. E., Lee, J. J., Moses, K. and Beachy, P. A. (1995). The product of hedgehog autoproteolytic cleavage active in local and long-range signalling. *Nature* **374**, 363-6.

Porter, J. A., Young, K. E. and Beachy, P. A. (1996). Cholesterol modification of hedgehog signaling proteins in animal development. *Science* **274**, 255-9.

Preat, T. (1992). Characterization of Suppressor of fused, a complete suppressor of the fused segment polarity gene of Drosophila melanogaster. *Genetics* **132**, 725-36.

Price, M. A. and Kalderon, D. (1999). Proteolysis of cubitus interruptus in Drosophila requires phosphorylation by protein kinase A. *Development* **126**, 4331-9.

Rallu, M., Machold, R., Gaiano, N., Corbin, J. G., McMahon, A. P. and Fishell, G. (2002). Dorsoventral patterning is established in the telencephalon of mutants lacking both Gli3 and Hedgehog signaling. *Development* **129**, 4963-4974.

Regl, G., Neill, G. W., Eichberger, T., Kasper, M., Ikram, M. S., Koller, J., Hintner, H., Quinn, A. G., Frischauf, A. M. and Aberger, F. (2002). Human GLI2 and GLI1 are part of a positive feedback mechanism in Basal Cell Carcinoma. *Oncogene* **21**, 5529-39.

Reshef, R., Maroto, M. and Lassar, A. B. (1998). Regulation of dorsal somitic cell fates: BMPs and Noggin control the timing and pattern of myogenic regulator expression. *Genes Dev* **12**, 290-303.

Riddle, R. D., Johnson, R. L., Laufer, E. and Tabin, C. (1993). Sonic hedgehog mediates the polarizing activity of the ZPA. *Cell* **75**, 1401-16.

Rios, I., Alvarez-Rodriguez, R., Marti, E. and Pons, S. (2004). Bmp2 antagonizes sonic hedgehog-mediated proliferation of cerebellar granule neurones through Smad5 signalling. *Development* **131**, 3159-68.

Rissi, M., Wittbrodt, J., Délot, E., Naegeli, M. and Rosa, F. M. (1995). Zebrafish Radar: A new member of the TGF-[beta] superfamily defines dorsal regions of the neural plate and the embryonic retina. *Mechanisms of Development* **49**, 223-234.

Robbins, D. J., Nybakken, K. E., Kobayashi, R., Sisson, J. C., Bishop, J. M. and Therond, P. P. (1997). Hedgehog elicits signal transduction by means of a large complex containing the kinesin-related protein costal2. *Cell* **90**, 225-34.

Roelink, H., Augsburger, A., Heemskerk, J., Korzh, V., Norlin, S., Ruiz i Altaba, A., Tanabe, Y., Placzek, M., Edlund, T., Jessell, T. M. et al. (1994). Floor plate and motor neuron induction by *vhh-1*, a vertebrate homolog of *hedgehog* expressed by the notochord. *Cell* **76**, 761-75.

Roelink, H., Porter, J. A., Chiang, C., Tanabe, Y., Chang, D. T., Beachy, P. A. and Jessell, T. M. (1995). Floor plate and motor neuron induction by different concentrations of the amino-terminal cleavage product of sonic hedgehog autoproteolysis. *Cell* **81**, 445-55.

Rohatgi, R., Milenkovic, L. and Scott, M. P. (2007). Patched1 regulates hedgehog signaling at the primary cilium. *Science* **317**, 372-6.

Roy, S., Wolff, C. and Ingham, P. W. (2001). The *u-boot* mutation identifies a Hedgehog-regulated myogenic switch for fiber-type diversification in the zebrafish embryo. *Genes Dev* **15**, 1563-76.

Rudin, C. M., Hann, C. L., Laterra, J., Yauch, R. L., Callahan, C. A., Fu, L., Holcomb, T., Stinson, J., Gould, S. E., Coleman, B. et al. (2009). Treatment of Medulloblastoma with Hedgehog Pathway Inhibitor GDC-0449. *N Engl J Med* **361**, 1173-1178.

Ruiz i Altaba, A. (1998). Combinatorial Gli gene function in floor plate and neuronal inductions by Sonic hedgehog. *Development* **125**, 2203-12.

Ruiz i Altaba, A. (1999). Gli proteins encode context-dependent positive and negative functions: implications for development and disease. *Development* **126**, 3205-16.

Ruiz i Altaba, A. and Jessell, T. M. (1993). Midline cells and the organization of the vertebrate neuraxis. *Curr Opin Genet Dev* **3**, 633-40.

Saka, Y., Hagemann, A. I., Piepenburg, O. and Smith, J. C. (2007). Nuclear accumulation of Smad complexes occurs only after the midblastula transition in Xenopus. *Development* **134**, 4209-18.

Sasaki, H., Hui, C., Nakafuku, M. and Kondoh, H. (1997). A binding site for Gli proteins is essential for *HNF-3beta* floor plate enhancer activity in transgenics and can respond to Shh in vitro. *Development* **124**, 1313-22.

Satoshi, K. and Yuji, M. (2005). BMP signaling and early embryonic patterning. *Cytokine & growth factor reviews* **16**, 265.

Schafer, M., Rembold, M., Wittbrodt, J., Schartl, M. and Winkler, C. (2005). Medial floor plate formation in zebrafish consists of two phases and requires trunk-derived Midkine-a. *Genes Dev* **19**, 897-902.

Schauerte, H. E., van Eeden, F. J., Fricke, C., Odenthal, J., Strahle, U. and Haffter, P. (1998). Sonic hedgehog is not required for the induction of medial floor plate cells in the zebrafish. *Development* **125**, 2983-93.

Scheer, N. and Campos-Ortega, J. A. (1999). Use of the Gal4-UAS technique for targeted gene expression in the zebrafish. *Mechanisms of Development* **80**, 153-158.

Schwartz, S., Zhang, Z., Frazer, K. A., Smit, A., Riemer, C., Bouck, J., Gibbs, R., Hardison, R. and Miller, W. (2000). PipMaker--a web server for aligning two genomic DNA sequences. *Genome Res* **10**, 577-86.

Sekimizu, K., Nishioka, N., Sasaki, H., Takeda, H., Karlstrom, R. O. and Kawakami, A. (2004). The zebrafish iguana locus encodes Dzip1, a novel zinc-finger protein required for proper regulation of Hedgehog signaling. *Development* **131**, 2521-32.

Sisson, J. C., Ho, K. S., Suyama, K. and Scott, M. P. (1997). Costal2, a novel kinesin-related protein in the Hedgehog signaling pathway. *Cell* **90**, 235-45.

Souren, M., Martinez-Morales, J., Makri, P., Wittbrodt, B. and Wittbrodt, J. (2009). A global survey identifies novel upstream components of the Ath5 neurogenic network. *Genome Biology* **10**, R92.

Stamataki, D., Ulloa, F., Tsoni, S. V., Mynett, A. and Briscoe, J. (2005). A gradient of Gli activity mediates graded Sonic Hedgehog signaling in the neural tube. *Genes Dev* **19**, 626-41.

Stone, D. M., Hynes, M., Armanini, M., Swanson, T. A., Gu, Q., Johnson, R. L., Scott, M. P., Pennica, D., Goddard, A., Phillips, H. et al. (1996). The tumour-suppressor gene patched encodes a candidate receptor for Sonic hedgehog. *Nature* **384**, 129-34.

Strigini, M. and Cohen, S. M. (1997). A Hedgehog activity gradient contributes to AP axial patterning of the Drosophila wing. *Development* **124**, 4697-705.

Sun, X. J., Xu, P. F., Zhou, T., Hu, M., Fu, C. T., Zhang, Y., Jin, Y., Chen, Y., Chen, S. J., Huang, Q. H. et al. (2008). Genome-wide survey and developmental expression mapping of zebrafish SET domain-containing genes. *PLoS ONE* **3**, e1499.

Suzuki, A., Chang, C., Yingling, J. M., Wang, X. F. and Hemmati-Brivvanlous, A. (1997). Smad5 induces ventral fates in *Xenopus* embryo. *Dev. Biol.* **184**, 402-405.

Suzuki, A., Thies, R. S., Yamaji, N., Song, J. J., Wozney, J. M., Murakami, K. and Ueno, N. (1994). A truncated bone morphogenetic protein receptor affects dorsal-ventral patterning in the early Xenopus embryo. *Proc Natl Acad Sci U S A* **91**, 10255-9.

Svetic, V., Hollway, G. E., Elworthy, S., Chipperfield, T. R., Davison, C., Adams, R. J., Eisen, J. S., Ingham, P. W., Currie, P. D. and Kelsh, R. N. (2007). Sdf1a patterns zebrafish melanophores and links the somite and melanophore pattern defects in choker mutants. *Development* **134**, 1011-22.

Tabata, T., Eaton, S. and Kornberg, T. B. (1992). The Drosophila hedgehog gene is expressed specifically in posterior compartment cells and is a target of engrailed regulation. *Genes Dev* **6**, 2635-45.

Taipale, J., Cooper, M. K., Maiti, T. and Beachy, P. A. (2002). Patched acts catalytically to suppress the activity of Smoothened. *Nature* **418**, 892-7.

Tanimoto, H., Itoh, S., ten Dijke, P. and Tabata, T. (2000). Hedgehog creates a gradient of DPP activity in *Drosophila* wing imaginal discs. *Mol Cell* **5**, 59-71.

Tay, S. Y., Ingham, P. W. and Roy, S. (2005). A homologue of the Drosophila kinesin-like protein Costal2 regulates Hedgehog signal transduction in the vertebrate embryo. *Development* **132**, 625-34.

Tay, S. Y., Yu, X., Wong, K. N., Panse, P., Ng, C. P. and Roy, S. (2010). The iguana/DZIP1 protein is a novel component of the ciliogenic pathway essential for axonemal biogenesis. *Developmental Dynamics* **239**, 527-534.

Tehrani, Z. and Lin, S. (2011). Antagonistic interactions of hedgehog, Bmp and retinoic acid signals control zebrafish endocrine pancreas development. *Development* **138**, 631-40.

Tendeng, C. and Houart, C. (2006). Cloning and embryonic expression of five distinct sfrp genes in the zebrafish Danio rerio. *Gene Expr Patterns* **6**, 761-71.

Therond, P. P., Limbourg Bouchon, B., Gallet, A., Dussilol, F., Pietri, T., van den Heuvel, M. and Tricoire, H. (1999). Differential requirements of the fused kinase for hedgehog signalling in the Drosophila embryo. *Development* **126**, 4039-51.

Thisse, B., Heyer, V., Lux, A., Alunni, V., Degrave, A., Seiliez, I., Kirchner, J., Parkhill, J. P. and Thisse, C. (2004). Spatial and temporal expression of the zebrafish genome by large-scale in situ hybridization screening. *Methods Cell Biol* **77**, 505-19.

Thisse, B., Pflumio, S., Fürthauer, M., Loppin, B., Heyer, V., Degrave, A., Woehl, R., Lux, A., Steffan, T., Charbonnier, X. Q. et al. (2001). Expression of the zebrafish genome during embryogenesis (NIH R01 RR15402). ZFIN Direct Data Submission (http://zfin.org). (ed.

Thomsen, G. H. (1996). Xenopus mothers against decapentaplegic is an embryonic ventralizing agent that acts downstream of the BMP-2/4 receptor. *Development* **122**, 2359-2366.

Tyurina, O. V., Guner, B., Popova, E., Feng, J., Schier, A. F., Kohtz, J. D. and Karlstrom, R. O. (2005). Zebrafish Gli3 functions as both an activator and a repressor in Hedgehog signaling. *Dev Biol* **277**, 537-56.

Urasaki, A., Morvan, G. and Kawakami, K. (2006). Functional dissection of the Tol2 transposable element identified the minimal cis-sequence and a highly repetitive sequence in the subterminal region essential for transposition. *Genetics* **174**, 639-49.

van den Heuvel, M. and Ingham, P. W. (1996). smoothened encodes a receptor-like serpentine protein required for hedgehog signalling. *Nature* **382**, 547-51.

van Eeden, F. J., Granato, M., Schach, U., Brand, M., Furutani-Seiki, M., Haffter, P., Hammerschmidt, M., Heisenberg, C. P., Jiang, Y. J., Kane, D. A. et al. (1996a). Mutations affecting somite formation and patterning in the zebrafish, Danio rerio. *Development* **123**, 153-64.

van Eeden, F. J., Granato, M., Schach, U., Brand, M., Furutani-Seiki, M., Haffter, P., Hammerschmidt, M., Heisenberg, C. P., Jiang, Y. J., Kane, D. A. et al. (1996b). Mutations affecting somite formation and patterning in the zebrafish, *Danio rerio*. *Development* **123**, 153-164.

Varga, Z. M., Amores, A., Lewis, K. E., Yan, Y. L., Postlethwait, J. H., Eisen, J. S. and Westerfield, M. (2001). Zebrafish *smoothened* functions in ventral neural tube specification and axon tract formation. *Development* **128**, 3497-509.

Vokes, S. A., Ji, H., McCuine, S., Tenzen, T., Giles, S., Zhong, S., Longabaugh, W. J., Davidson, E. H., Wong, W. H. and McMahon, A. P. (2007). Genomic characterization of Gli-activator targets in sonic hedgehog-mediated neural patterning. *Development* **134**, 1977-89.

Vokes, S. A., Ji, H., Wong, W. H. and McMahon, A. P. (2008). A genome-scale analysis of the cis-regulatory circuitry underlying sonic hedgehog-mediated patterning of the mammalian limb. *Genes Dev* **22**, 2651-63.

Von Hoff, D. D., LoRusso, P. M., Rudin, C. M., Reddy, J. C., Yauch, R. L., Tibes, R., Weiss, G. J., Borad, M. J., Hann, C. L., Brahmer, J. R. et al. (2009). Inhibition of the Hedgehog Pathway in Advanced Basal-Cell Carcinoma. *N Engl J Med* **361**, 1164-1172.

Wang, B., Fallon, J. F. and Beachy, P. A. (2000a). Hedgehog-regulated processing of Gli3 produces an anterior/posterior repressor gradient in the developing vertebrate limb. *Cell* **100**, 423-34.

Wang, G., Amanai, K., Wang, B. and Jiang, J. (2000b). Interactions with Costal2 and suppressor of fused regulate nuclear translocation and activity of cubitus interruptus. *Genes Dev* **14**, 2893-905.

Warming, S., Costantino, N., Court, D. L., Jenkins, N. A. and Copeland, N. G. (2005). Simple and highly efficient BAC recombineering using galK selection. *Nucleic Acids Res* **33**, e36.

Weedon, M. N., Lango, H., Lindgren, C. M., Wallace, C., Evans, D. M., Mangino, M., Freathy, R. M., Perry, J. R., Stevens, S., Hall, A. S. et al. (2008). Genome-wide association analysis identifies 20 loci that influence adult height. *Nat Genet* **40**, 575-83.

Weinberg, E. S., Allende, M. L., Kelly, C. S., Abdelhamid, A., Murakami, T., Andermann, P., Doerre, O. G., Grunwald, D. J. and Riggleman, B. (1996). Developmental regulation of zebrafish MyoD in wild-type, no tail and spadetail embryos. *Development* **122**, 271-80.

Wieser, R., Wrana, J. L. and Massague, J. (1995). GS domain mutations that constitutively activate TβR-I, the downstream signaling component in the TGF-β receptor complex. *EMBO J.* **14**, 2199-2208.

Wijgerde, M., McMahon, J. A., Rule, M. and McMahon, A. P. (2002). A direct requirement for Hedgehog signaling for normal specification of all ventral progenitor domains in the presumptive mammalian spinal cord. *Genes Dev* **16**, 2849-64.

Wilkie, A. O. and Morriss-Kay, G. M. (2001). Genetics of craniofacial development and malformation. *Nat Rev Genet* **2**, 458-68.

Wilkinson, R. N., Pouget, C., Gering, M., Russell, A. J., Davies, S. G., Kimelman, D. and Patient, R. (2009). Hedgehog and Bmp polarize hematopoietic stem cell emergence in the zebrafish dorsal aorta. *Dev Cell* **16**, 909-16.

Winkler, C., Schafer, M., Duschl, J., Schartl, M. and Volff, J. N. (2003). Functional divergence of two zebrafish midkine growth factors following fish-specific gene duplication. *Genome Res* **13**, 1067-81.

Winklmayr, M., Schmid, C., Laner-Plamberger, S., Kaser, A., Aberger, F., Eichberger, T. and Frischauf, A. M. (2010). Non-consensus GLI binding sites in Hedgehog target gene regulation. *BMC Mol Biol* **11**, 2.

Wittbrodt, J., Shima, A. and Schartl, M. (2002). Medaka--a model organism from the far East. *Nat Rev Genet* **3**, 53-64.

Wolff, C., Roy, S. and Ingham, P. W. (2003). Multiple muscle cell identities induced by distinct levels and timing of hedgehog activity in the zebrafish embryo. *Curr Biol* **13**, 1169-81.

Wolff, C., Roy, S., Lewis, K. E., Schauerte, H., Joerg-Rauch, G., Kirn, A., Weiler, C., Geisler, R., Haffter, P. and Ingham, P. W. (2004). *iguana* encodes a novel zinc-finger protein with coiled-coil domains essential for Hedgehog signal transduction in the zebrafish embryo. *Genes Dev* **18**, 1565-76.

Woods, I. G. and Talbot, W. S. (2005). The you gene encodes an EGF-CUB protein essential for Hedgehog signaling in zebrafish. *PLoS Biol* **3**, e66.

Woolfe, A., Goodson, M., Goode, D. K., Snell, P., McEwen, G. K., Vavouri, T., Smith, S. F., North, P., Callaway, H., Kelly, K. et al. (2005). Highly conserved non-coding sequences are associated with vertebrate development. *PLoS Biol* **3**, e7.

Yao, S., Lum, L. and Beachy, P. (2006). The ihog cell-surface proteins bind Hedgehog and mediate pathway activation. *Cell* **125**, 343-57.

Yauch, R. L., Dijkgraaf, G. J. P., Alicke, B., Januario, T., Ahn, C. P., Holcomb, T., Pujara, K., Stinson, J., Callahan, C. A., Tang, T. et al. (2009). Smoothened Mutation Confers Resistance to a Hedgehog Pathway Inhibitor in Medulloblastoma. *Science* **326**, 572-574.

Yavari, A., Nagaraj, R., Owusu-Ansah, E., Folick, A., Ngo, K., Hillman, T., Call, G., Rohatgi, R., Scott, M. P. and Banerjee, U. (2010). Role of lipid metabolism in smoothened derepression in hedgehog signaling. *Dev Cell* **19**, 54-65.

Zhang, W., Zhao, Y., Tong, C., Wang, G., Wang, B., Jia, J. and Jiang, J. (2005). Hedgehog-regulated Costal2-kinase complexes control phosphorylation and proteolytic processing of Cubitus interruptus. *Dev Cell* **8**, 267-78.

Zhao, Y., Tong, C. and Jiang, J. (2007). Hedgehog regulates smoothened activity by inducing a conformational switch. *Nature* **450**, 252-8.

Zhu, G., Mehler, M. F., Zhao, J., Yu Yung, S. and Kessler, J. A. (1999). Sonic Hedgehog and BMP2 Exert Opposing Actions on Proliferation and Differentiation of Embryonic Neural Progenitor Cells. *Developmental Biology* **215**, 118.